

University of Windsor

## Scholarship at UWindor

---

Electronic Theses and Dissertations

Theses, Dissertations, and Major Papers

---

1-1-1981

### The mineralogy, geochemistry and petrogenesis of the Mount Poser gabbroic pluton, southern California.

Paul Chi-Tak Cheung  
*University of Windsor*

Follow this and additional works at: <https://scholar.uwindsor.ca/etd>

---

#### Recommended Citation

Cheung, Paul Chi-Tak, "The mineralogy, geochemistry and petrogenesis of the Mount Poser gabbroic pluton, southern California." (1981). *Electronic Theses and Dissertations*. 6755.  
<https://scholar.uwindsor.ca/etd/6755>

This online database contains the full-text of PhD dissertations and Masters' theses of University of Windsor students from 1954 forward. These documents are made available for personal study and research purposes only, in accordance with the Canadian Copyright Act and the Creative Commons license—CC BY-NC-ND (Attribution, Non-Commercial, No Derivative Works). Under this license, works must always be attributed to the copyright holder (original author), cannot be used for any commercial purposes, and may not be altered. Any other use would require the permission of the copyright holder. Students may inquire about withdrawing their dissertation and/or thesis from this database. For additional inquiries, please contact the repository administrator via email ([scholarship@uwindsor.ca](mailto:scholarship@uwindsor.ca)) or by telephone at 519-253-3000ext. 3208.

THE MINERALOGY, GEOCHEMISTRY  
AND  
PETROGENESIS OF THE MOUNT POSER  
GABBROIC PLUTON,  
SOUTHERN CALIFORNIA

BY  
PAUL CHI-TAK CHEUNG

A THESIS  
SUBMITTED TO THE FACULTY OF GRADUATE STUDIES  
THROUGH THE DEPARTMENT OF  
GEOLOGY IN PARTIAL FULFILLMENT  
OF THE REQUIREMENTS FOR THE DEGREE  
OF MASTER OF SCIENCE AT  
The University of Windsor

Windsor, Ontario, Canada

1981

UMI Number: EC54738

## INFORMATION TO USERS

The quality of this reproduction is dependent upon the quality of the copy submitted. Broken or indistinct print, colored or poor quality illustrations and photographs, print bleed-through, substandard margins, and improper alignment can adversely affect reproduction.

In the unlikely event that the author did not send a complete manuscript and there are missing pages, these will be noted. Also, if unauthorized copyright material had to be removed, a note will indicate the deletion.



---

UMI Microform EC54738  
Copyright 2010 by ProQuest LLC  
All rights reserved. This microform edition is protected against  
unauthorized copying under Title 17, United States Code.

---

ProQuest LLC  
789 East Eisenhower Parkway  
P.O. Box 1346  
Ann Arbor, MI 48106-1346

ACP 1626

Copyright 1981 © by P. C. T. Cheung

757196

# TABLE OF CONTENTS

	PAGE
LIST OF TABLES.....	v
LIST OF FIGURES.....	vii
ABSTRACT.....	viii
DEDICATION.....	xi
ACKNOWLEDGEMENTS.....	xii

## CHAPTER

I. INTRODUCTION.....	1
II. REGIONAL GEOLOGICAL SETTING.....	6
III. THE PETROGRAPHY AND GEOCHEMISTRY OF THE MOUNT POSER GABBROIC PLUTON.....	13
(1). AMPHIBOLE-OLIVINE-NORITE.....	16
(2). LEUCOCRATIC-AMPHIBOLE-TROCTOLITE.....	21
(3). ORTHOPYROXENE-AMPHIBOLE-OLIVINE-GABBRO.....	25
(4). AMPHIBOLE-GABBRONORITE.....	28
(5). DYKE ROCK UNITS.....	30
(6). INCLUSIONS FROM THE INTRUSION BRECCIA.....	32
IV. EXPERIMENTAL TECHNIQUES AND BASIC THEORY.....	35
(A). ANALYTICAL TECHNIQUES.....	35
(B). PREPARATION OF PLAGIOCLASE FELDSPARS.....	35
(C). MINERAL SEPARATION.....	36
i PROCEDURE.....	38
ii SEPARATION OF PLAGIOCLASE FELDSPARS.....	39
iii SEPARATION OF OLIVINE.....	39
iv SEPARATION OF AMPHIBOLE.....	40
v PURIFICATION OF AMPHIBOLE.....	41
vi SEPARATION OF ORTHOPYROXENE AND	

CHAPTER	PAGE
CLINOPYROXENE.....	41
(D). PREPARATION OF SAMPLES FOR X-RAY FLUORESCENCE ANALYSES.....	42
i PREPARATION OF MINERAL-POWDER PELLETS.....	42
ii PREPARATION OF GLASS DISCS.....	42
iii PREPARATION OF PLAGIOCLASE.....	43
(E). TECHNIQUES OF THE X-RAY DIFFRACTION.....	43
(F). THE THEORY OF X-RAY FLUORESCENCE SPECTROSCOPY.....	45
V. THE GEOCHEMISTRY OF MINERALS OF THE MOUNT POSER GABBROIC PLUTON.....	54
(A). INTRODUCTION.....	54
(B). GEOCHEMISTRY.....	59
1 PLAGIOCLASE.....	59
2 OLIVINE.....	66
3 CLINOPYROXENE.....	72
4 ORTHOPYROXENE.....	77
5 AMPHIBOLE.....	81
(C). MULTIPLE INTRUSION AND IN SITU FRACTIONATION.	86
(D). PARENT MAGMA TYPE.....	90
(E). CALCULATED COMPOSITION OF THE RESIDUAL MELTS.	94
VI. PETROGENESIS OF THE GABBROS AND THEIR RELATIONSHIPS TO THE GRANITOIDS OF THE PENINSULAR RANGES BATHOLITH.....	101
VII. CONCLUSION.....	110
APPENDIX I PLAGIOCLASE ANALYSES.....	113
APPENDIX II OLIVINE ANALYSES.....	116
APPENDIX III CLINOPYROXENE ANALYSES.....	118
APPENDIX IV ORTHOPYROXENE ANALYSES.....	122
APPENDIX V AMPHIBOLE ANALYSES.....	125
REFERENCES.....	129
VITAE AUCTORIS.....	136

# LIST OF TABLES

TABLE		PAGE
1	Mineralogies of each unit of the Mount Poser Pluton.....	17
2	Modal mineralogy of the Mount Poser Pluton.....	18
3	Range and mean value for the analyzed elements in the various rock units of the Mount Poser Pluton.....	22
4	The procedure for the separation of minerals...	37
5	An % in plagioclase feldspars determined by XRD	46
6	Precision of XRF analyses.....	51
7	Analytical conditions for determination of major elements.....	52
8	Analytical conditions for determination of trace elements.....	53
9	Number of mineral samples separated of each rock unit.....	56
10	Major element (wt%) compositions of plagioclase feldspars from the different rock types in the pluton.....	60
11	Trace element (ppm) compositions of plagioclase feldspars from the different rock types in the pluton.....	63
12	Major element (wt%) compositions of olivines from the different rock types in the pluton....	67
13	Trace element (ppm) compositions of olivines from the different rock types in the pluton....	68
14	Major element (wt%) compositions of clinopyroxenes from the different rock types in the pluton.....	73
15	Trace element (ppm) compositions of clinopyroxenes from the different rock types in the pluton.....	75

TABLE		PAGE
16	Major element (wt%) compositions of orthopyroxenes from the different rock types in the pluton.....	79
17	Trace element (ppm) compositions of orthopyroxenes from the different rock types in the pluton.....	80
18	Major element (wt%) compositions of amphiboles from the different rock types in the pluton....	82
19	Trace element (ppm) compositions of amphiboles from the different rock types in the pluton....	83
20	A comparison of the compositions of the cumulate mineral assemblages of the Mount Poser pluton and some well described complexes.....	91
21	Calculation of liquid composition using analyzed plagioclase results from the A01N, LAT, OA01G and AGN unit and reported coefficients.....	96
22	Calculation of liquid composition using analyzed olivine results from the A01N, LAT, OA01G and A01G unit and reported coefficients..	97
23	Calculation of liquid composition using analyzed clinopyroxene results from the OA01G and AGN unit and reported coefficients.....	98
24	Calculation of liquid composition using analyzed orthopyroxene results from the LAT and AGN unit and reported coefficients.....	99
25	Calculation of liquid composition using analyzed amphibole results from the AGN unit and reported coefficients.....	100



## FIGURES

FIGURE		PAGE
1	Location of the Mount Poser Pluton.....	2
2	The plutonic sub-belts in the Peninsular Ranges batholith of Southern California, and Northern Baja California.....	7
3	Geologic map showing the lithologic units within the Mount Poser Pluton.....	14
4	Mineralogical distribution within the Mount Poser Pluton.....	19
5	Schematic view of X-ray powder diffractometer...	44
6	Schematic view of X-ray powder fluorescence.....	47
7	Location of samples used in the geochemical analyses.....	57
8	Variation in composition for clinopyroxene and orthopyroxene.....	74

## ABSTRACT

The Mount Poser gabbro is a layered gabbroic pluton, which consists of two rock series -- the plagioclase-olivine series (A01N, LAT, OA01G, A01G) and the plagioclase-pyroxene series (AGN, AG). The olivine-bearing series consists of cumulate plagioclase, olivine, spinel and clinopyroxene, whereas the non-olivine bearing series consists of cumulate plagioclase, orthopyroxene, clinopyroxene, amphibole and opaque minerals.

X.R.F. analyses of forty-six coexisting plagioclases, olivines, clinopyroxenes, orthopyroxenes and amphiboles, representing all the rock units (7), have been made from the Mount Poser gabbroic pluton.

The plagioclase is unzoned with a composition ranging from  $An_{97}$  to  $An_{87}$  in the olivine-bearing series and from  $An_{85}$  to  $An_{65}$  in the pyroxene-bearing series. Olivine, which only occurs in the olivine-bearing series, ranges in composition from  $Fo_{78.2}$  to  $Fo_{72.5}$ . The clinopyroxene belongs to the diopside-salite series and occupies the compositional range between  $Ca_{41}Mg_{46}Fe_{13}$  and  $Ca_{39}Mg_{49}Fe_{12}$ . The orthopyroxene belongs to the bronzite-hypersthene series and has the composition of hypersthene ( $Ca_2Mg_{71}Fe_{27}$ ) in the LAT unit. Subsilicic amphibole ranges from tschermakite to pargasite in the plagioclase-olivine series and it ranges from magnesio-hornblende to ferroan pargasite in the plagioclase-

olivine series and it ranges from magnesio-hornblende to ferroan pargasite in the plagioclase-pyroxene series.

The chemical compositions of the minerals indicate that the pluton was derived from a high  $Al_2O_3$  (olivine) basalt. This is supported by the comparison of the compositions of the cumulate mineral assemblages of the pluton with the compositions of the cumulate minerals of other well described complexes and volcanoes.

Calculation of trace element concentrations in the minerals has been done to trace the evolution of the pluton. This showed that the cumulate rock units in the plagioclase-olivine series were derived from a melt of high-alumina tholeiitic basalt and the cumulate rock units in the plagioclase-pyroxene series were derived from a high-alumina basaltic andesite parental magma of tholeiitic affinity and they are supported by the fractionation sequence (plagioclase, olivine, clinopyroxene, orthopyroxene and amphibole).

Petrographic, geochemical, modal abundance and structural characteristics of the pluton indicate that the pluton was formed by multiple intrusion of mafic magmas and these diagnostic features also indicate that the pluton was formed under in situ differentiation.

A simple calculation was done to determine whether the granitoid rocks of the Peninsular Ranges batholith are cogenetic with the gabbros. In order to produce the granitic

rocks with an average  $\text{SiO}_2$  of 70%, it requires at least 75% of the basaltic melt must be crystallized. But the small volume of mafic cumulates associated with the batholith indicate that the granitoid rocks can not possibly be derived from the gabbros by fractional crystallization, i.e. the granitoid rocks are not cogenetic with the gabbros.

Dedicated to my parents, Lily and Tennyson.

## ACKNOWLEDGEMENTS

The author would like to express his deepest thanks and appreciation to Dr. T. E. Smith, for his help, guidance, and encouragement throughout this work.

The author also wishes to thank Dr. John Huang for his technical guidance and helpful discussion.

## CHAPTER I

### INTRODUCTION

The Mount Poser Gabbro is a layered gabbroic pluton, located approximately 50 km east of San Diego, California, and about 10 km south of Cuyamaca Peak (Fig. 1)

The pluton underlies an area of 22 km<sup>2</sup>, and is crescentic in outcrop pattern, with its long axis trending almost east-west. The exposed complex ranges in relief from 1036 m above sea level at its base to 1194 m at the summit of the highest of its twin peaks.

Mount Poser lies within the Cuyamaca Peak Quadrangle (Fig. 1), which is approximately in the centre of the north-west-trending Peninsular Ranges (Everhart, 1951). The topography of the quadrangle is rather rugged, and shows a variety of land forms distributed irregularly. These include broad tablelands, with both rugged steep-sided bouldery peaks, and broad-based cone-shaped mountains rising above. Deep gorges and youthful canyons locally cut below the extensive upland surfaces, but in places the major streams flow through broad mature valleys. The three major streams and tributaries that drain the area flow southwest into the Pacific Ocean.

The climate of the quadrangle varies markedly according to elevation. The higher elevations have generally lower

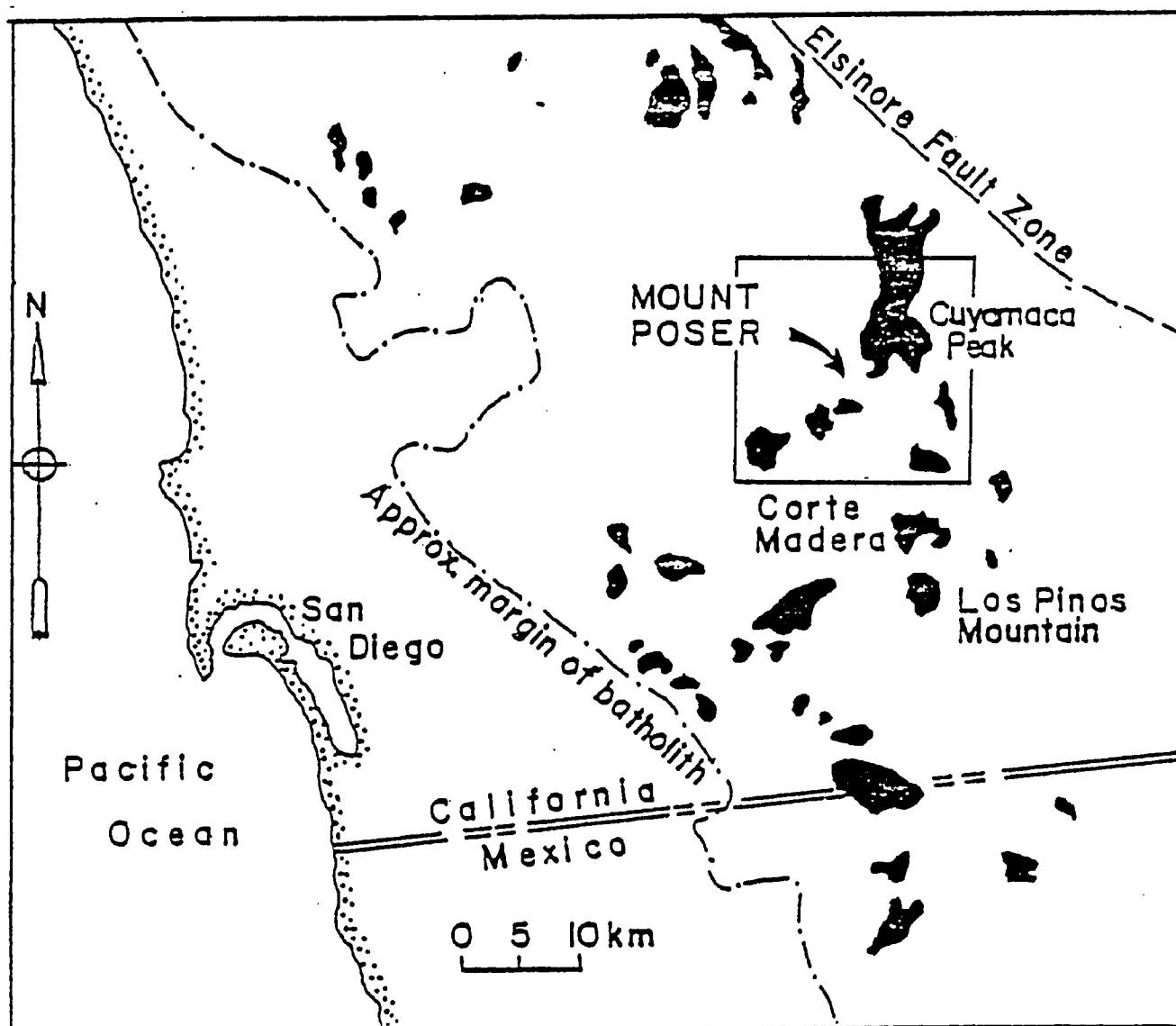


FIG.1 LOCATION OF THE MOUNT POSER PLUTON



temperatures (averaging about 41<sup>0</sup>F in winter and 63.7<sup>0</sup>F in summer), and greater precipitation than the lower valley lands along the west edge of the area. In the valleys the winters are mild, and there are few killing frosts. Snow is unknown in the valleys, but some snow does fall on the higher mountains. Mostly the summers are hot and dry over the whole region, and thunderstorms are not common.

The vegetation of the quadrangle consists of a variety of conifers, deciduous trees, bushes, shrubs, and grasses. Mount Poser has a variety of brush species, the most common of which are the manzanita and yucca plants, but sage and mesquite are also found.

Rock exposures are poor near the base of Mount Poser, and improve both in number and in size near the summit.

Previous geologic work in the Cuyamaca Peak Quadrangles dates back to early Annual Reports of the State Mineralogist, (1890). The first geological mapping in the district was done by Hudson, (1922). This study was followed by Miller (1935, 1946), Larsen (1948), Everhart (1951), and more recently Nishimori (1976), Walawender(1976), Walawender et al. (1979), Wheeler (1979), and Walawender and Smith (1980).

Broad agreement exists on the interpretation of the field relations which suggest the following sequence of events. Deposition and metamorphism of sediments to form schists, gneisses, and quartzites was followed by the emplacement of igneous rocks to form the Peninsular Ranges

batholith. Most of the contacts in the batholith are quite sharp, and show that the intrusive sequence is gabbro-tonalite- granodiorite- granite. According to Larsen (1948), the batholith comprises 7% gabbro, 68% tonalite, 28% granodiorite, and 2% granite. At some localities within the Peninsular Ranges batholith, volcanism has accompanied the emplacement of the plutonic igneous rocks.

There are several theories concerning the origin and the evolution of the plutonic rocks of this batholith. Larsen (1948) proposed that the whole series of plutonic rocks was derived from a gabbroic magma by crystal differentiation. Albarede (1976) made the alternative suggestion that all of the rock types differentiated from a tonalitic parental magma. Walawender et al.(1977, 1979), Wilson (1978), Wheeler(1979), and Walawender and Smith (1980) suggested that the gabbroic rocks are not co-genetic with the granitoid rocks.

These differences in interpretation have an important bearing on a major controversy in current petrological theory (Leake et al., 1980). The Larsen hypothesis implies that granitoid rocks are derived directly from the earth's mantle, while the interpretations of Albarede and of Walawender and co-workers, suggest that they have a crustal origin.

This study was undertaken to evaluate the suggestion that the gabbroic and granitoid rocks of the Peninsular Ranges batholith are not co-genetic. For this purpose, the

constituent minerals of all of the principal rock types of a well described gabbroic pluton, the Mount Poser pluton, were separated and analysed. The major element analyses were used to confirm the mineral compositions determined by flat stage optical and X-ray diffraction methods. Comparisons of the compositions with those of the minerals of a wide variety of well described rock suites were used to identify the magma type from which the rocks of the Mount Poser pluton formed. The contents of selected trace elements in the melts, with which the various minerals were in equilibrium, were calculated from the mineral analyses using known distribution coefficients. This information was used to confirm the magma type deduced from the major element compositions. Major element and trace element variations in the minerals and the melts were examined to see if they were the result of crystal fractionation, and to decide if such fractionation could lead to the development of the granitoid rocks of the batholith.

## CHAPTER II

### REGIONAL GEOLOGICAL SETTING

The Mount Poser gabbroic pluton is part of a large geological province, known as the Peninsular Ranges, which consists mainly of regionally metamorphosed rocks and plutonic intrusives (Fig. 2). This petrographic province, which is more than 1000 km long, and has an average width of 100 km, extends from the Transverse Ranges (latitude  $34^{\circ}\text{N}$ ), in the north, to latitude  $28^{\circ}\text{N}$  in Baja California in the south. The Pacific borderland defines the western limit of the province, and the San Andreas Fault marks its margin in the east. Much of the area is occupied by the Peninsular Ranges batholith. Mapping (Miller, 1937; Larsen, 1948; Everhart, 1951;) has demonstrated that the batholith comprises a large number of coalescent plutons which have been intruded separately. The plutons range in composition from gabbros to granites. The batholith intrudes metasedimentary rocks, known as the Julian Schist of Triassic or Jurassic age (Schwarz, 1969), and weakly metamorphosed Jurassic basalt-andesite-dacite volcanic rocks (Larsen, 1948).

Gastil (1975) has shown that the metamorphic and plutonic rocks within the Peninsular Ranges Province, can be divided into three structural and petrographic zones (A, B,

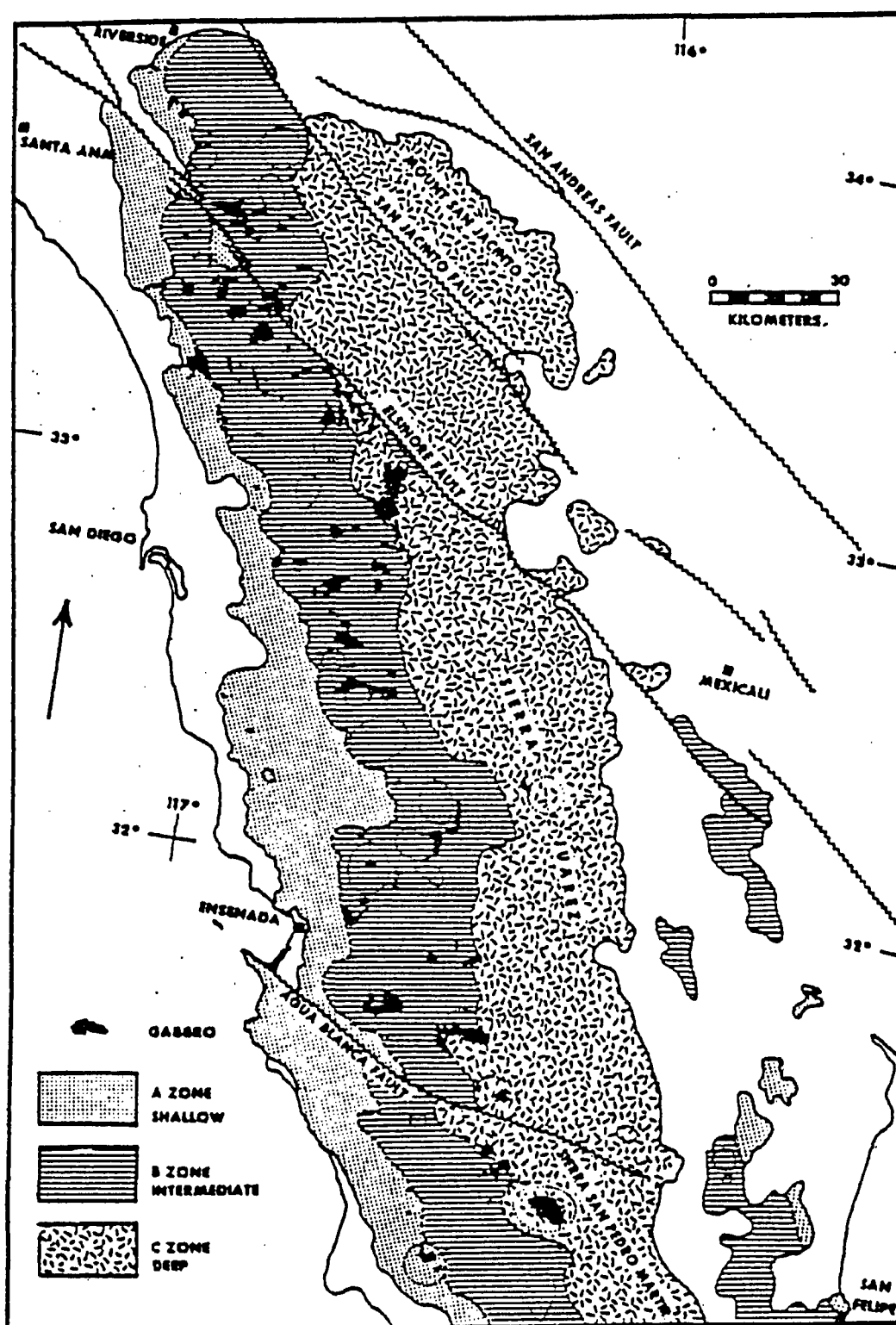


Fig. 2 The plutonic sub belts in the Peninsular Ranges batholith of southern California, and northern Baja California according to Gastil, (1975).

and C), parallel with, and symmetrical to the axis of the batholith (Fig. 2). This sub-division is based on metamorphic mineral content, texture, deformation style.

The A zone outcrops in the west and is characterized by fine-grained hornfels, slates and phyllites, in which the original textures and fossils are commonly preserved. The B zone is characterized by plastically deformed, schistose host rocks, and fewer relict structures and textures are found in this area. It occurs on both sides of the C zone. The C zone is made up of coarse-grained sillimanite-bearing schists and gneisses, and foliated amphibolites. The original textures and structures of the rocks have all been destroyed by the metamorphism.

These features are interpreted as resulting from metamorphism of the host rocks at different depths (Gastil, 1975). The characteristics of the A zone infer recrystallization at shallow depths, those of the B zone suggest that metamorphism took place at an intermediate depth, and those of the C zone imply that the rocks formed at a relatively deep level.

The intrusive rocks of the batholith may be divided into a series of petrographic sub-belts which unlike the metamorphic zones are asymmetric in their distribution (Gastil et al., 1974). These workers have recognized a gabbro sub-belt which coincides with the western side of the B zone, a tonalite sub-belt occurring in the east of the B-zone, and an adamellite sub-belt located in the C zone on

the east side of the Peninsular Ranges' Province.

In the gabbro sub-belt plutons of gabbroic rocks make up more than 20% of the total area, tonalite and granodiorite plutons make up the remainder of the area. Leucocratic hornblende-biotite tonalite, containing large sphene crystals is the dominant rock type in the tonalite sub-belt. Locally it grades into granodiorite, a few small gabbro plutons are present but no true granite has been mapped. In the adamellite sub-belt, tonalites and granodiorites are exposed over about 50% of the area, and gabbroic rocks are absent. Adamellite and granite intrusions make up the remainder of the plutonic rocks.

This asymmetry in the distribution of the plutonic rock types within the batholith is mirrored by a chemical polarity (Baird et al., 1974). These authors have shown that Na, K and Si contents of the rocks increase systematically from west to east and the Ca, Mg, and Fe contents of the rocks decrease systematically from west to east. In addition, the plutonic rocks of the western side of the batholith are in general older than those exposed further to the east. Stratigraphic evidence shows that the oldest plutonic rocks in the western part of the batholithic belt are older than upper Jurassic, and that the youngest are pre-Turonian. No stratigraphic limits can be placed on the age of intrusion in the tonalite belt. In the adamellite belt the plutonic rocks appear to have intruded middle or possibly upper Cretaceous rocks. Krummenacher et

al., (1975) using Rb/Sr and U/Pb ages, which are in agreement with the stratigraphic limits, have shown that the rocks were emplaced between 145 m.y. and 95 m.y. B.P. in the western half of the belt, and are as young as 80 m.y. in the eastern part of the belt.

The petrographic, and geochemical patterns exhibited by the rocks of the Peninsular Ranges batholith are similar to those seen in many active island arc systems, and also to those seen in several Cordilleran batholiths (Smith et al., 1979; Bateman and Dodge, 1970; Cobbing and Pitcher, 1972). The batholith has therefore been attributed to magmatism at a subduction zone (Gastil, 1975; Silver et al., 1975). Walawender and Smith (1980) commented specifically on the restriction of the basic plutons to the western margin of the Peninsular Ranges batholith, with regard to this comparison.

The majority of the gabbroic plutons, including the Mount Poser pluton, are exposed in the gabbro sub-belt of the batholith (Fig. 2). In the gabbro sub-belt, field evidence suggests that the gabbroic rocks, including the Mount Poser pluton, were emplaced first, followed by the tonalites, and then the granodiorites (Miller, 1935, 1946; Larsen, 1948; Everhart, 1951; Nishimori, 1976; Walawender, 1976). These plutonic rocks have been intruded into a metamorphosed assemblage of psammitic and pelitic rocks known locally as the Julian Schist (Hudson, 1922).

Local names have been applied by Miller (1937) to the



plutonic rocks according to their petrographic, textural and structural features. The rocks of the gabbroic plutons have all been grouped together and are referred to as the San Marcos Gabbros. Rocks having the characteristic features of the Bonsall Tonalite and the Green Valley Tonalite (both described below) have been recognized outcropping to the west and east of the Mount Poser gabbro respectively. All three rock units are cut locally by dykes of the Woodson Mountain Granodiorite and a small screen of Julian Schist is included in the Green Valley Tonalite near the western margin of the Mount Poser Complex.

The Julian Schist is made up mainly of quartz-mica schist and a small amount of quartzite. The former is generally a brownish-grey, fine-grained rock, made up of subhedral grains of plagioclase ( $An_{10-30}$ ), quartz, and small shreds of interstitial mica. The latter is a grey to white, fine-grained rock, comprising a homogeneous aggregate of interlocking sub-angular grains of clear quartz and feldspar together with minor constituents.

The gabbroic plutons, including the Mount Poser Pluton, are commonly layered. They vary in composition from peridotite to anorthosite, and include norite, gabbronorite, troctolite and gabbro. Hornblende is a common mafic component of all of the plutons.

The Bonsall tonalite is a light-grey, coarse grained (.5 mm) biotite-hornblende tonalite. It is characterized by abundant streaked inclusions which have also been described

as 'pancake-shaped' discs by Larsen (1948), and Everhart (1951).

The Green Valley tonalite is a grey, medium grained (1-5 mm), and relatively uniform, pyroxene-biotite-hornblende tonalite. It is similar to Bonsall tonalite, but it lacks the abundant streaked inclusions.

The Woodson Mountain granodiorite is a light colored granitic rock which intrudes the north-eastern and south-eastern part of the gabbroic pluton, and is also found along the north-western border of the gabbroic pluton. It is a fine to medium-grained (1-5 mm) hornblende-biotite granodiorite. Dykes, both radiating outward from, and cutting the larger granodiorite plutons, range in composition from granodiorite to granite, with the latter containing both aplitic and pegmatitic phases.

CHAPTER III

THE  
PETROGRAPHY AND GEOCHEMISTRY  
OF THE ROCKS OF THE  
MOUNT POSER GABBROIC PLUTON

Wheeler (1979) has shown that the Mount Poser Gabbroic Pluton is a heterogeneous body, and consists of four main rock types, (Fig. 3). The principal characteristics of these rock types, as described by Wheeler (1979), and supplemented by additional observations, are given below.

1. Amphibole-olivine-norite (A01N)\*, underlies approximately  $1.5 \text{ km}^2$ , or 7% of the pluton. It is exposed mainly on the southeast side of the complex, and at two other localities near the centre of the pluton, and one located near the southwest edge of the pluton.
2. Leucocratic-amphibole-troctolite (LAT), underlies approximately  $3.5 \text{ km}^2$ , or 16% of the pluton. It is exposed mainly at the eastern end of the complex, and in one small area on the southwest edge of the pluton.
3. Orthopyroxene-amphibole-olivine-gabbro (OA01G), under-

---

\*All rock names are after Streckeisen, (1973).

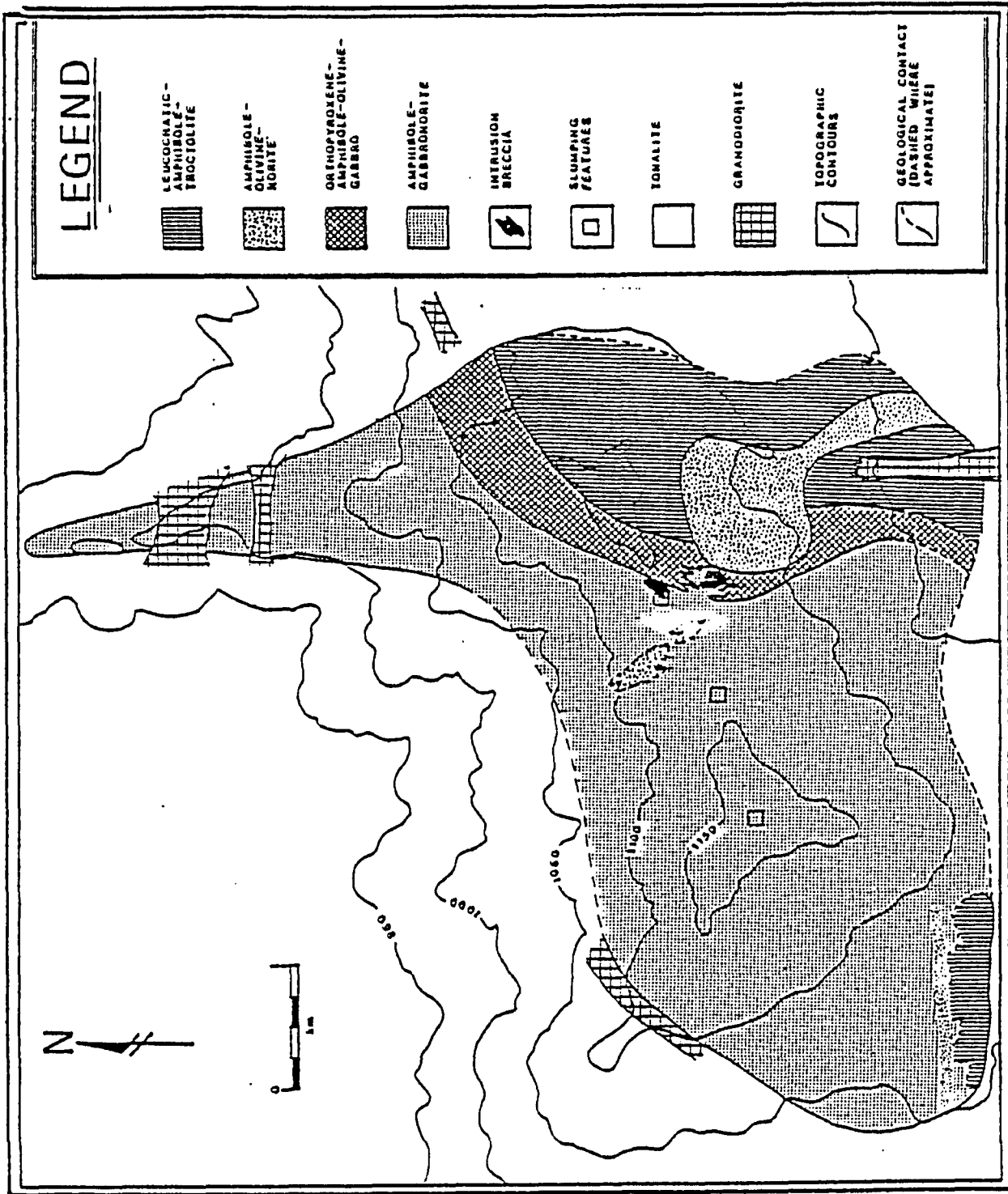


Fig. 3 GEOLOGIC MAP SHOWING THE LITHOLOGIC UNITS.

lies approximately  $1.8 \text{ km}^2$ , or 8% of the pluton. It is exposed in the central and northeast parts of the complex.

4. Amphibole-gabbro-norite (AGN) underlies approximately  $14.6 \text{ km}^2$ , or 66% of the total pluton. It underlies an area extending from the western end to the central area of the complex.

In addition, to these four main rock types, two suites of dykes penetrate the rocks of the pluton. These are a dark grey, foliated suite, and a lighter grey, non-foliated suite.

An intrusion breccia is exposed near the OA01G/AGN boundary. The inclusions reach a maximum of  $15 \times 40 \text{ cm}$  in diameter and resemble the OA01G unit in petrography. They are embedded in a groundmass of AGN.

The boundaries between the complex and the country rocks, and between the different rock units of the pluton, are not generally exposed. Hence, the time of emplacement complex as a whole, and the order of emplacement of each rock unit is uncertain. However, granodiorite dykes penetrate the complex and in the absence of evidence to the contrary it is presumed to have been emplaced prior to the granitoid rocks, in keeping with the generally observed relationships.

Within the complex, Wheeler (1979) has recognized two

series of rocks, a plagioclase-olivine series, consisting of the A01N, LAT, OA01G and the light coloured dykes (A01G), and a plagioclase-pyroxene group made up of the AGN and the dark coloured foliated dykes, (AG), (Table 1 and Fig. 4).

Field relationships suggest that the plagioclase-olivine series was largely intruded first, and was disrupted in part by the later emplacement of the plagioclase-pyroxene group. However, both sets of dykes post-date all of the main units of the complex. The dark dykes post-date the light dykes mirroring the relationships shown by the larger units. Wheeler (1979, p. 14-19) has discussed the field relationships in detail and concluded that the complex was probably formed by multiple intrusion. Walawender (1976) and Lillis (1978) have also shown that the nearby Los Pinos and Corte Madera gabbroic plutons were formed by multiple intrusion.

Table 2 summarizes the modal mineralogy of the various rock units found within the Mount Poser Complex. Wheeler (1979) used the mineralogical, textural, structural and chemical characteristics of the A01N, LAT, OA01G, and AGN to show that they are cumulate rocks. These characteristics are summarized below, the cumulus and intercumulus minerals of the various types are tabulated and illustrated in Table 1 and Fig. 4 respectively.

#### 1. Amphibole-Olivine-Norite (A01N)

The norite is the coarsest grained, (grain size 4 to

Table 1. Mineralogies of each unit of the Mount Poser Pluton.

ROCK UNIT	CUMULUS OR PRIMARY PHASE	INTERSTITIAL PHASE
A01N	Pl + Ol + Sp	Opx + Amph
LAT	(Same as A01N, smaller grain size & mafic content decreases)	Opx + Amph
OA01G	Pl + Ol + Sp	Opx + Amph + Opaq (Minor)
	Pl + Ol + Sp (Minor) + Cpx	Opaq + Amph
A01G	Pl + Ol + Sp + Cpx	Opaq + Amph
AGN	Pl + Opx + Cpx	Opaq + Amph
AG	Pl + Amph + Opaq	Opaq

	<u>LAT</u>			<u>AO1N</u>			<u>OA01G</u>	
	C-36	MP-18	MP-87	MP-22	C-16	MP-86	C-34	MP-59
Plagioclase	62	65	50	46	22	50	53	61
Olivine	9	17	5	38	42	32	12	18
Spinel	2	1	—	2	10	2	—	2
Reaction Corona	8	12	2	7	—	3	—	—
Orthopyroxene	1	1	3	1	6	5	2	4
Clinopyroxene	—	—	—	—	—	3	26	1
Amphibole	9	3	35	6	20	8	6	13
Opaques	9	1	5	—	—	—	1	1

	<u>AO1G</u>			<u>AGN</u>		<u>AG</u>	<u>INCLUSIONS</u>	
	MP-31	C-44	C-9-A	C-53	C-48-B	C-57	C-39	C-45
Plagioclase	43	44	52	60	63	36	60	61
Olivine	3	8	14	—	—	—	—	—
Spinel	—	—	1	—	—	—	—	—
Reaction Corona	—	—	—	—	—	—	—	—
Orthopyroxene	4	9	3	12	14	—	—	—
Clinopyroxene	6	6	13	10	8	—	27	28
Amphibole	31	18	16	12	7	46	3	2
Opaques	13	15	1	6	8	18	10	9

Table.2 Modal mineralogy of the Mount Pecer pluton  
Abbreviations as per text.



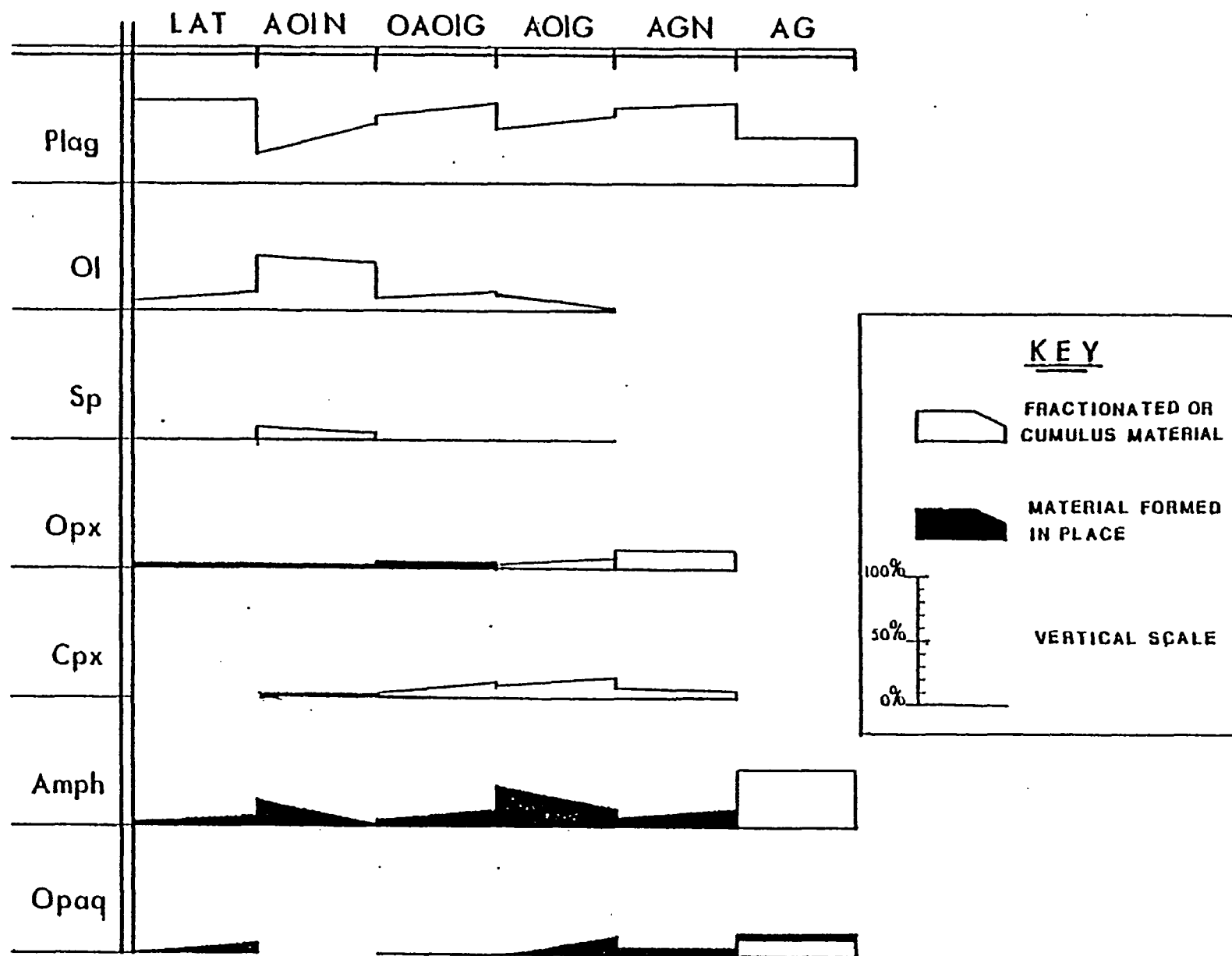


Fig. 4 MINERALOGICAL DISTRIBUTION WITHIN THE MOUNT POSER PLUTON.

8 mm) of all of Mount Poser rock units. It consists of from 35 to 40% plagioclase, 35 to 40% olivine, 3% orthopyroxene, 3% clinopyroxene, 15% amphibole and 10% spinel (maximum), (Table 2). No planar or linear structures occur in this rock type.

The plagioclase occurs as subhedral to euhedral crystals, averaging 3 mm in diameter, and is unzoned. Flat stage optical determinations, and X-ray diffraction measurements, show that the composition of the plagioclase feldspars in this unit varies from  $An_{94}$  to  $An_{85}$ .

Olivine occurs as subhedral to euhedral, rounded crystals, up to 2 to 3 mm in diameter, and commonly forms irregular clumps, up to a maximum of 1 cm in diameter. It alters extensively along cracks to iddingsite and magnetite.

The interstitial orthopyroxene occurs as subhedral crystals, up to 3 mm in diameter and has very fine exsolution lamellae of clinopyroxene parallel to (100).

The clinopyroxene occurs as subhedral crystals, up to 1 mm in diameter. It is only found in one of the samples in the southwest corner of the pluton.

Spinel occurs as anhedral to subhedral crystals, up to 1 mm in diameter, which are usually found in the poikilitic amphibole, and as small vermicular blebs within the reaction corona between olivine and plagioclase.

The amphibole occurs poikilitically enclosing olivine and plagioclase crystals. It shows green-brown to green

pleochroism, and patchy color zoning. A few samples show spotty alteration to a fibrous tremolitic amphibole.

The contacts between plagioclase and olivine are characterized by reaction coronas of olivine  $\pm$  orthopyroxene + amphibole  $\pm$  (amphibole + spinel) + plagioclase. More detailed descriptions are presented in Wheeler (1979).

Olivine, plagioclase, and spinel are interpreted as cumulus minerals, commonly making up more than 80% of the rock. The intercumulus material comprises mainly amphibole, with small quantities of orthopyroxene, and clinopyroxene. The MgO, and Ni contents of the rocks are high and CaO,  $Al_2O_3$  and Sr contents are comparatively low (Table 3) reflecting the higher percentage of olivine and lower percentage of plagioclase present.

## 2. Leucocratic-Amphibole-Troctolite (LAT)

The troctolite is a medium to coarse-grained rock, (grain size 2 to 5 mm) and consists of up to 65% plagioclase, 15% olivine, 2% orthopyroxene, 10% amphibole, and 3% spinel. Opaque minerals make up the remainder of the rock, (Table 2). Two planar structures have been identified in this rock type. The rock has a banded structure near the eastern boundary of the pluton with the tonalite. The banding is the result of variations in proportions in the mafic and felsic minerals and is sub-parallel to the boundary. The structure trends N-S and has a near vertical dip. Towards the eastern summit of the hill the banding is

ELEMENT(%)	LAT	AO1N	AO1G	OA01G
SiO <sub>2</sub>	41.30-45.02(43.39)	39.25-43.10(41.48)	40.05-42.16(40.80)	42.40-47.66(44.60)
Al <sub>2</sub> O <sub>3</sub>	17.46-25.09(22.32)	11.79-19.98(16.63)	14.97-19.05(17.37)	18.05-21.08(19.75)
TiO <sub>2</sub>	0.05- 0.16( 0.09)	0.03- 0.21( 0.09)	0.11- 1.40( 0.85)	0.06- 0.26( 0.18)
Fe <sub>2</sub> O <sub>3</sub>	5.63- 9.90( 7.54)	8.72-14.83(12.17)	11.00-13.75(12.18)	6.51-11.94( 8.83)
MnO	0.07- 0.13( 0.10)	0.13- 0.20( 0.16)	0.15- 0.21( 0.19)	0.10- 0.16( 0.13)
MgO	8.07-16.29(11.34)	13.10-26.52(19.02)	10.08-19.69(13.56)	9.43-13.15(11.43)
CaO	11.85-16.40(14.45)	7.08-12.11( 9.92)	13.33-15.15(14.23)	11.84-17.04(14.31)
Na <sub>2</sub> O	0.59- 0.97( 0.73)	0.30- 0.63( 0.48)	0.52- 1.06( 0.75)	0.56- 0.82( 0.69)
K <sub>2</sub> O	0.02- 0.10( 0.04)	0.02- 0.06( 0.03)	0.04- 0.07( 0.05)	0.02- 0.03( 0.03)
P <sub>2</sub> O <sub>5</sub>	0.004- 0.01( 0.01)	0.004- 0.02( 0.01)	0.01- 0.04( 0.02)	0.004- 0.01( 0.01)

ELEMENT(ppm)				
V	9- 90( 30)	6-125( 31)	77-356(268)	26-133( 83)
Cr	16-146( 58)	14-121( 40)	25- 71( 41)	45-119( 85)
Co	14- 28( 20)	25- 43( 34)	32- 35( 34)	17- 33( 23)
Ni	34-110( 62)	89-321(102)	8- 35( 19)	14-126( 70)
Zn	19- 44( 30)	51- 79( 65)	62- 83( 74)	23-164( 41)
Rb	1- 2( 1)	1- 5( 2)	N/D- 1( 1)	3- 4( 4)
Sr	261-398(345)	161-333(253)	281-308(297)	242-353(300)
Y	N/D- 2( 1)	N/D (N/D)	4- 23( 9)	N/D- 5( 2)
Hf	1- 3( 2)	3- 12( 8)	N/D- 2( 1)	N/D- 9( 5)
Ba	8- 21( 11)	5- 20( 10)	N/D- 61( 26)	4- 15( 10)

Table 3 Range and mean value (in parenthesis) for the analysed elements in the rock units of the Mount Poser pluton. (Wholer, 1979, P. 59-60)

ELEMENT(*)	AGN	AO	INCLUSIONS
SiO <sub>2</sub>	41.05-49.75(46.84)	39.87-43.77(41.09)	43.74-47.56(46.00)
Al <sub>2</sub> O <sub>3</sub>	16.37-20.76(18.05)	15.61-17.54(16.63)	10.12-19.34(10.63)
TiO <sub>2</sub>	0.23- 1.07( 0.63)	1.17- 1.65( 1.47)	0.90- 1.34( 1.06)
Fe <sub>2</sub> O <sub>3</sub>	7.70-12.70(10.01)	13.05-15.61(14.36)	11.09-13.55(12.00)
MnO	0.16- 0.24( 0.10)	0.17- 0.21( 0.19)	0.20- 0.22( 0.21)
MgO	6.39-12.57( 9.62)	9.07-13.02(11.36)	6.28- 7.54( 6.69)
CaO	11.30-14.46(12.35)	13.25-14.27(13.61)	11.61-12.69(12.11)
Na <sub>2</sub> O	0.77- 2.44( 1.41)	0.96- 1.26( 1.14)	2.34- 3.29( 2.87)
K <sub>2</sub> O	0.07- 0.66( 0.14)	0.11- 0.16( 0.13)	0.10- 0.18( 0.14)
P <sub>2</sub> O <sub>5</sub>	0.01- 0.06( 0.02)	0.01- 0.09( 0.03)	0.09- 0.37( 0.22)
ELEMENT(ppm)			
V	61-372(208)	390-597(490)	259-293(274)
Cr	19- 60( 32)	25- 34( 20)	10- 28( 24)
Co	21- 31( 26)	34- 43( 39)	23- 31( 27)
Ni	5- 41( 20)	4- 16( 12)	12- 10( 15)
Zn	37-101( 72)	81-100( 91)	80-109( 99)
Rb	1- 7( 4)	1- 6( 3)	1- 2( 2)
Sr	277-406(372)	204-340(310)	351-359(354)
Y	N/D- 12( 5)	14- 29( 23)	10- 53( 34)
Nb	N/D- 9( 3)	1- 5( 2)	1- 3( 2)
Ba	3- 63( 22)	N/D- 96( 65)	74-150(115)

Table 3 Continued.

gradually replaced by a uniform texture, and finally by a foliated structure. The foliation is subvertical and trends E-W, and is defined by lenticular aggregates of mafic minerals.

The plagioclase occurs as a series of subhedral to euhedral interlocking crystals, up to 2 mm maximum diameter, and is unzoned. Flat stage optical determinations, and X-ray diffraction measurements, show that the composition of the plagioclase feldspars in this unit varies from  $An_{85}$  to  $An_{83}$ .

Olivine occurs as anhedral to euhedral crystals up to 2 mm in diameter, which show extensive embayment due to resorption. Some of the olivine crystals show alteration to iddingsite and magnetite.

Spinel occurs as subhedral to euhedral crystals up to 1 mm in diameter. It also occurs as vermicular grains in a reaction corona between olivine and plagioclase.

Orthopyroxene occurs as small (1 mm) interstitial crystals containing very small exsolution blebs (0.01 mm) of clinopyroxene parallel to (100).

Amphibole occurs as poikilitic crystals with green-brown to green pleochroism, and patchy color zoning. The poikilitic amphibole crystals, up to 8 mm in size, enclose plagioclase and/or olivine crystals. Some amphibole alters to a fibrous tremolitic form.

The contacts of olivine and plagioclase are characterized by reaction coronas, very similar to those of

A01N unit.

Plagioclase, olivine, and spinel are interpreted as cumulus minerals, typically making up more than 80% of the rock. The remaining 20% is made up mainly of intercumulus amphibole and opaque minerals (Table 1). Care must be exercised in placing too much reliability on this interpretation of the olivine, which is anhedral and amoeboid in form, suggesting resorption by the melt, and hence a lack of equilibrium prevailing between the two phases. However, some of this reaction has taken place during the formation of the symplectic rims.

The rocks are characterized by high CaO,  $Al_2O_3$ , and Sr, moderate  $\Sigma Fe_2O_3$ , and MgO, and low  $Na_2O$ ,  $TiO_2$ ,  $K_2O$ , and  $P_2O_5$  contents (Table 3). These features reflect the large proportion of plagioclase in the rocks. Since the rocks are cumulates large differences in composition exist in closely related rock types depending upon the relative proportions of the cumulate minerals. Such rock types cannot be used to plot smooth variation curves and their compositions do not give a direct indication of the composition of the melts from which they were derived.

### 3. Orthopyroxene-Amphibole-Olivine-Gabbro (OA01G)

The gabbro has an average grain size of less than 2 mm, and consists of up to 55 or 60% plagioclase, 15% olivine, 12% clinopyroxene, 3% orthopyroxene, less than 8% amphibole, less than 2% spinel, and 2% opaques (Table 2). It is the

finest grained main rock unit in the complex, and has a uniform texture and structure, showing no evidence of foliation or lineation.

The plagioclase occurs as a series of anhedral to subhedral interlocking crystals, less than 2 mm in diameter, and is unzoned. The flat-stage optical determinations and X-ray diffraction measurements show that the composition of the plagioclase feldspars in this unit varies from  $An_{93}$  to  $An_{80}$ . A few plagioclase crystals show spotty alteration to chlorite and calcite.

Olivine occurs as anhedral to subhedral crystals, less than 2 mm in diameter, altered to iddingsite and magnetite along internal fractures.

Clinopyroxene occurs as anhedral to subhedral crystals, less than 2 mm in diameter. It is characterized by a "sieved" texture with the "holes" filled by late-stage amphibole. The crystals aggregate together with other clinopyroxene grains, forming clots reaching a maximum 4 mm in diameter.

Orthopyroxene generally occurs as thin rims, (less than 0.5 mm), which are adjacent to the olivine in the coronas. It shows moderate pleochroism from pale pink to pale green, and has fine exsolution lamellae of clinopyroxene parallel to (100).

Spinel occurs as subhedral crystals and is generally associated with interstitial opaque grains. The subhedral opaque grains are found at olivine to olivine grain



boundaries. Individual opaque grains are also found, which are scattered through plagioclase crystals.

Poikilitic amphibole, up to 8 mm in diameter, encloses all other minerals. Individual crystals of amphibole may show patchy pleochroism in green-brown shades, and a few grains show spotty alteration to a fibrous tremolitic form.

The contact of the plagioclase and olivine is characterized by a reaction corona (Wheeler, 1979). Amphibole which occurs in the corona, shows a pleochroism from pale blue/green to green color. It is intergrown with spinel in a fibrous manner.

Wheeler (1979) interprets the plagioclase, olivine, spinel and clinopyroxenes as cumulus minerals in this rock unit. These minerals make up from 80% to 90% of the rock, the remainder comprises the intercumulus minerals orthopyroxene, amphibole, and opaques.

The  $\text{CaO}$ ,  $\text{Al}_2\text{O}_3$ ,  $\text{MgO}$ ,  $\text{Sr}$ , and  $\text{Ni}$  contents of these rocks are intermediate in value between those of the LAT and A01N (Table 3). This rock unit is the finest grained of the major rock units and lies along the boundary between the other plagioclase-olivine rocks and the plagioclase-pyroxene rocks. It may represent a more rapidly chilled zone of the plagioclase-olivine series. If this interpretation is correct then the rock unit may be considered to have a composition close to that of the melt from which the plagioclase-olivine series was formed. However, the unzoned minerals and failure to completely surround the plagioclase-

olivine rocks suggest this interpretation may not be correct.

#### 4. Amphibole-Gabbronorite (AGN)

The gabbronorite is a medium to coarse grained rock (grain size 2 to 5 mm) and consists of 60% to 65% plagioclase, 14% orthopyroxene, 10% clinopyroxene, 12% amphibole, and 5% opaque grains, (Table 2). It contains a weak foliation defined by alignment of plagioclase crystals. The foliation trends NE-SW with an average dip of  $75^{\circ}$  to the SE. In the west, amphibole exceeds orthopyroxene leading to an overall black and white weathered appearance. In the east, orthopyroxene exceeds amphibole, leading to an overall red and white weathered surface.

The plagioclase occurs as subhedral crystals up to 5 mm maximum diameter, and is unzoned. Flat stage optical determinations and X-ray diffraction measurements show that the composition of the plagioclase feldspars from this unit, varies from  $An_{90}$  to  $An_{85}$ , in the east where orthopyroxene is dominant, and from  $An_{64}$  to  $An_{53}$  in the west where hornblende is dominant.

Prismatic orthopyroxene occurs as subhedral grains, averaging 3 to 4 mm in diameter. It shows the strongest pink to green pleochroism, among the orthopyroxenes within the pluton. It also has fine exsolution lamellae of clinopyroxene parallel to (100).

Clinopyroxene occurs as anhedral crystals, up to 3 mm

in diameter. In a few samples, aggregates of these grains occur reaching a maximum diameter of 1 cm.

Anhedral opaque grains, less than 1 mm in diameter, occur associated with poikilitic amphiboles. Spinel is almost entirely absent from this rock unit, only one very small subhedral crystal having been found.

Amphibole generally occurs interstitially, but a few poikilitical crystals up to 1 cm in diameter enclosing plagioclase and orthopyroxene, have been noted.

The amphibole shows dark brown/green to light green/brown pleochroism and some color zoning. There is some alteration of the amphibole to a secondary, fibrous, tremolite form.

Plagioclase, clinopyroxene, and orthopyroxene are interpreted as cumulus minerals, and generally comprise more than 85% of the rock. The remainder is made up of intercumulus amphibole and opaque minerals. This rock unit is notably higher in  $\text{Na}_2\text{O}$ , and  $\text{K}_2\text{O}$  and V, and slightly higher in  $\text{SiO}_2$ , and lower in Ni than the rocks of the plagioclase-olivine series (Table 3). These differences are explained by the absence of olivine (Ni) and spinel (Cr) and the presence of increased amphibole ( $\text{Na}_2\text{O}$  and  $\text{K}_2\text{O}$ ) and opaques (V). The increase in amphibole and decrease in orthopyroxene from east to west may result from the presence of increasing intercumulus liquid in the system prior to solidification. It may result from differentiation within the unit with the high temperature orthopyroxenes separating

early on and modifying the composition of the melt.

## 5. Dyke Rock Units

Two sets of dykes are found in the pluton, a lighter grey, non-foliated dyke suite and a darker grey, foliated dyke suite.

The lighter grey, non-foliated (A01G) dykes average 6 to 10 cm in width, and reach a maximum of 25 cm.. They trend mostly NW-SE, dip at 70 to 75°N. They consist of 43 to 52% plagioclase, 3 to 8% olivine, 6 to 13% clinopyroxene, 3 to 9% orthopyroxene, 16 to 31% amphibole, (Table 2). Two sub-groups are recognized, one in which 15% opaque minerals occur, and a second containing 2% spinel. The opaque minerals and spinel do not occur together.

The plagioclase occurs as anhedral to euhedral crystals, and is unzoned. Flat stage optical determinations and X-ray diffraction measurements show that the composition of the plagioclase feldspars in this unit varies from An<sub>80</sub> to An<sub>75</sub>.

Rounded olivine occurs as subhedral crystals, and may be altered to iddingsite and magnetite along the fractures.

Clinopyroxene occurs as anhedral to subhedral crystals, with a sieved appearance as described previously.

Orthopyroxene occurs as subhedral crystals, up to 1 mm in diameter, and has very fine exsolution lamellae of clinopyroxene parallel to (100).

The spinel, when present, occurs as anhedral to

subhedral crystals and is found either closely associated with olivine crystals or as an interstitial phase. Opaques occur as anhedral to subhedral crystals.

Poikilitic amphibole showing moderate pleochroism from brown to light brown, encloses small, subhedral, clinopyroxene and magnetite crystals.

The contact of the plagioclase and olivine is characterized by a reaction corona of olivine  $\pm$  orthopyroxene + amphibole + plagioclase.

The mineralogy of these light grey dykes (i.e. the presence of olivine and spinel) clearly indicates their affinities to the plagioclase-olivine series but their field relationships indicate that they post-date the AGN. These contradictory characteristics are part of the evidence leading to the suggestion of multiple intrusion taking place within the complex. In this process rather similar melts are available at various times in the history of intrusion. Wheeler (1979, p. 51) has suggested that they may represent residual melts derived from the OA01G phase. They are lower in  $\text{SiO}_2$ , higher in  $\text{MgO}$  and  $\Sigma\text{Fe}_2\text{O}_3$  on average than the OA01G which makes this interpretation unlikely. Their time relationships suggest they were formed later and their chemistry may indicate that they represent crystal residue after some of the melt has been lost.

The dark grey, foliated (AG) dykes average 6 to 10 cm in width and reach a maximum of 1 m. The strike of these dykes is variable from NE-SW to NW-SE with  $70^\circ$  to  $75^\circ$  dips S.

They consist of up to 36% plagioclase crystals, 46% amphibole, and 18% opaque grains, (Table 2). The dykes have trachytoid texture resulting from a strong alignment of amphibole and plagioclase.

The plagioclase occurs as anhedral to subhedral crystals and is unzoned. Flat stage optical determinations and X-ray diffraction measurements show that the composition in this unit is  $An_{85}$ . Carlsbad-Albite twinning is dominant.

The amphibole occurs as simple-twinned subhedral crystals. It has a strong pleochroism from green/brown to lighter green.

Opaque minerals occur as anhedral to subhedral crystals, less than 1 mm in diameter.

Wheeler (1979, p.50-51) suggests that these dykes have genetic affinities to the pyroxene-plagioclase series and may represent the residual melt of the AGN unit. These rocks have lower  $SiO_2$ ,  $Na_2O$ , and higher  $\Sigma Fe_2O_3$ ,  $MgO$ , and  $CaO$  than the AGN unit. Their well developed trachytoid texture suggests that they were emplaced largely as a finely crystalline mush and it is possible that much of the melt was squeezed out from between the crystals and lost during intrusion.

## 6. Inclusions (INC) from the intrusion breccia

The inclusions are commonly rounded in outline and are fine grained (1 mm average diameter). They typically

consist of 60% plagioclase, 28% clinopyroxene, 10% opaques and about 2% amphibole, (Table 2).

These inclusions are embedded in a groundmass of AGN. They have an equigranular texture characterized by many triple junctions, and are interpreted as hornfelses.

The plagioclase occurs as anhedral crystals and shows ragged cores. Flat stage optical determinations and X-ray diffraction measurements show that the composition of the plagioclase feldspars in this unit varies from  $An_{54}$  to  $An_{51}$ . (These values have been redetermined by flat stage optical method). It encloses small crystals of opaques and clinopyroxene.

Clinopyroxene occurs as anhedral to subhedral crystals up to 1 mm in diameter and shows exsolution lamellae of clinopyroxene parallel to (001) and very fine lamellae of orthopyroxene to (110).

Opaque minerals occur as anhedral crystals, interstitial between clinopyroxene and plagioclase, and as small inclusions within the clinopyroxene.

Amphibole occurs as interstitial crystals.

The texture of the inclusions is very similar to that of the OA01G in hand sample and thin section reveals that the rock is probably hornfelsed by the AGN. A comparison of the chemistry of the inclusions with that of the OA01G reveals several notable differences. The  $SiO_2$ ,  $TiO_2$ ,  $\Sigma Fe_2O_3$ ,  $Na_2O$  and  $K_2O$  contents are very much higher in the inclusions and the  $MgO$  and  $CaO$  values are lower. These differences

suggest that metasomatism as well as metamorphism has affected these rocks. In view of their chemical alteration the minerals of these rocks cannot be used in this study.

### Summary

Wheeler (1979) pointed out that the rocks of the Mount Poser pluton are characterized by high  $Al_2O_3$ , low total alkalies,  $K_2O$ ,  $TiO_2$ , Rb, Ba, Y, and Nb contents. These are characteristic features of orogenic igneous rock suites (Green, 1980). However, since these rocks have been identified as cumulates the chemical characteristics noted are not those of the melts from which the rocks developed and hence cannot be used to identify the specific association.

Wheeler (1979) concluded that the chemical characteristics and mineral compositions suggest that the rocks of the Mount Poser complex were derived from parental melts of high alumina basalt/basaltic andesite composition. This conclusion is largely based on the comparison of the composition of the minerals from Mount Poser with those of other well described suites.



## CHAPTER IY

### EXPERIMENTAL TECHNIQUES

and

### BASIC THEORY

#### (A) Analytical Techniques

Samples for analysis were supplied by C. Wheeler (1979). Those selected show minimum weathering in hand specimen and thin section, and are typical representatives of all units mapped in the pluton. The major element and trace element (Rb, Sr, Ba, Y, Zr, Nb, Ni, Co, Cr, V, Cu) compositions of a total of 47 minerals separated from the representative rock samples, were determined. The separates include 16 samples of plagioclase; 10 samples of olivine, 6 samples of clinopyroxene; 5 samples of orthopyroxene; 10 samples of amphibole. The chemical analyses were carried out on glass discs, and rock-powder pellets, using a Philips PW1410 universal vacuum X-ray spectrometer.

#### (B) Preparation of samples for mineral separation

The method used has been described by Hutchison (1974). After all weathered portions of the samples were removed, the samples were split into small pieces. The rock chips were fed into the jaw crusher, and the crushed material was

ground in a shatter box. Each ground sample was sieved through a bank of N.S. standard sieves (A.S.T.M. E11 series) of 80, 100, 200 and 400 mesh. The coarser fractions, those remaining on the 100 sieve, were reground and sieved again.

The 100-200 and 200-400 mesh fractions were washed in water, using an ultrasonic cleaner, to remove the adhering dust particles. The final wash was done with acetone and the sample dried on a hot plate.

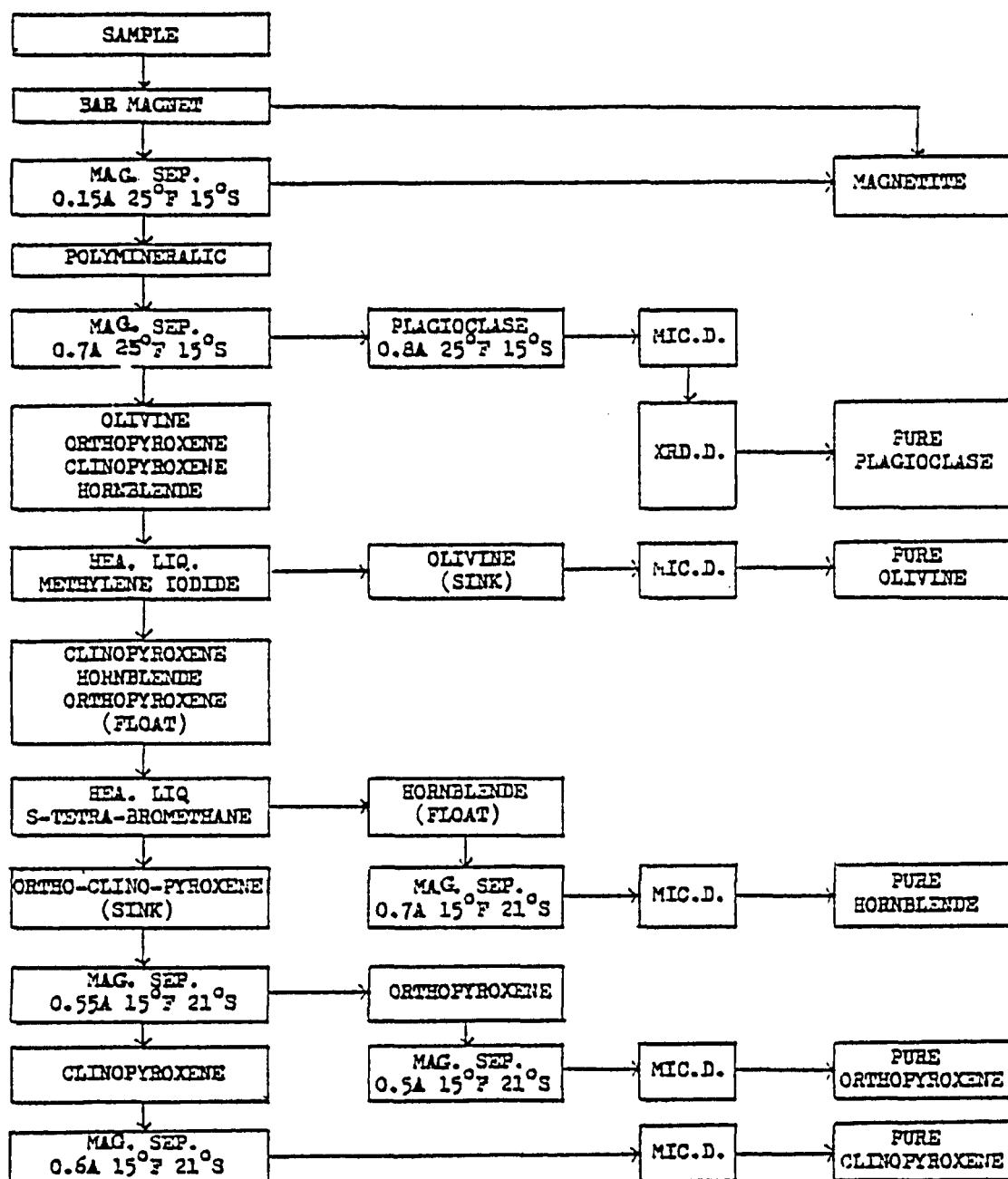
### (C) Mineral separation

The crushed samples contained various mixtures of plagioclase, olivine, orthopyroxene, clinopyroxene, amphibole, spinel, and opaque minerals. The constituent minerals of the samples were separated using magnetic and heavy liquid methods.

The Franz Isodynamic Magnetic Separator (Model L-1) was used for the magnetic separation. This method is based on the magnetic susceptibility of the mineral, i.e. minerals with high magnetic susceptibilities are removed at a low amperage, and then minerals of decreasing magnetic susceptibilities are progressively separated by increasing the amperage. The conditions used to separate each mineral are listed in Table 4.

The heavy liquids used were S-tetra bromoethane, and methylene iodide, having specific gravities of 2.955-2.965 at 25<sup>0</sup>C, and of 3.325 at 20<sup>0</sup> respectively. The separations were carried out using a 200 ml separating funnel placed in

Table 4 The procedure of the separation of minerals



MAG. SEP.	Magnetic separation
A	Amphere
F	Forward sloping
S	Side tilting
MIC.D.	Microscopic determination
XRD.D.	X-ray diffraction determination
HEA. LIQ	Heavy Liquid separation

a well ventilated fume cupboard. Mineral grains having a lower specific gravity than the liquid float, those with higher specific gravity sink.

(i) Procedure

Prior to the separation, a thin section of each sample was examined to determine the minerals present. The flow chart (Table 4) summarizes the sequential treatment of the samples and the successive separation of each of the minerals present.

The dry sieved sample was spread on a paper, and a bar magnet wrapped in a Kimwipe was used to remove the magnetite. The sample was then slowly fed through the isodynamic separator with a setting of 0.15 amp, 25° forward slope and 15° side tilt, and with medium vibration, to remove the remaining magnetite. The sample was fed through the separator again to obtain pure plagioclase feldspars in the non-magnetic fraction after a number of runs. The magnetic fraction was generally polymineralic.

Approximately 10g of the polymineralic fraction and 150 ml of heavy liquid (methylene iodide) were placed in a separating funnel, and shaken. Then the heaviest minerals (olivine) sank and were carefully drained off, collected on No. 4 Whatman filter paper, and washed with acetone. The lighter mineral grains were then drained off and washed. The float fraction was then poured into another separating funnel with S-tetra-bromoethane liquid and shaken.

Amphibole crystals floated and the residual polymineralic crystals sank and were drained off first. The amphibole separate needed purification using the isodynamic separator with a suitable setting. The residue, comprising orthopyroxene and clinopyroxene crystals, was fed into the isodynamic separator under the conditions indicated on Table 4, where orthopyroxene crystals were separated as the magnetic fraction and clinopyroxene crystals as the non-magnetic fraction. The details of each separation are described in the following passages.

(ii) Separation of plagioclase feldspars

After complete removal of the ferro-magnetic minerals the polymineralic crystals were fed through the magnetic separator at a setting of 0.7 amp (Table 4), as suggested by Hutchison (1974). The plagioclase feldspars were collected as the non-magnetic fraction. The initial separate was examined with a binocular microscope and was not pure enough. It was necessary to run it through the magnetic separator twice more, at a setting of 0.8 amp, to obtain a satisfactory separation. In the majority of samples the magnetic fraction remaining was polymineralic and was subjected to heavy liquid separation.

(iii) Separation of olivine

The initial heavy liquid separation was carried out using methylene iodide (S.G. 3.325), (Table 4). The

polymineralic sample was shaken in a separating funnel and olivine which has a S.G. greater than 3.40 allowed to settle. The olivine was then carefully drained off and caught with a filter paper. Olivine was washed several times with acetone and the wash collected and stored in a smoked glass bottle for further recovery of the heavy liquid. The olivine separate was then dried on a hot plate and examined with a binocular microscope. A second heavy liquid separation was necessary in order to produce a pure olivine separate. The lighter specific gravity fraction which remained floating on the heavy liquid was generally polymineralic. It was recovered and subjected to further heavy liquid separation.

(iv) Separation of amphibole

The polymineralic samples, recovered after the olivine separation, were added to 150 ml of S-tetra-bromethane, (S.G. 2.962), (Table 4), and shaken in the separating funnel. Although orthopyroxene, clinopyroxene and amphibole have similar specific gravity, the orthopyroxene and clinopyroxene grains sink slowly and the amphibole crystals float on the heavy liquid. The heavier minerals were run off first, collected and washed in preparation for further treatment. The floating fraction was carefully run off and collected on a filter paper, and washed with acetone. It was dried on a hot plate, and examined with a binocular microscope. Generally, the sample was insufficiently pure

and required further processing.

(v) Purification of amphibole

The amphibole separate was fed through the separator at a setting of 0.7 amp with  $15^{\circ}$  forward slope and  $21^{\circ}$  side tilt (Table 4). The amphibole crystals then collected as the non-magnetic fraction and the orthopyroxene and clinopyroxene collected as the magnetic fraction.

(vi) Separation of orthopyroxene and clinopyroxene

Orthopyroxene and clinopyroxene have very similar specific gravity and cannot be separated using heavy liquids. The bimineralline sample was fed through the isodynamic separator at a setting of 0.55 amp with  $15^{\circ}$  forward slope and  $21^{\circ}$  side tilt (Table 4). Examination with a binocular microscope showed that the more magnetic fraction contained mainly orthopyroxene with some clinopyroxene, and the less magnetic fraction contained mainly clinopyroxene with some orthopyroxene. The more magnetic fraction, (orthopyroxene dominant) was fed through the separator again, after reducing the current to 0.5 amp, in order to remove the clinopyroxene present. The less magnetic fraction, (clinopyroxene dominant) was then fed through the separator after increasing the current to 0.6 amp for final purification. The process was repeated until satisfactory purity, i.e. greater than 95% of each mineral was obtained.

(D) Preparation of samples for X-ray fluorescence analysis

(i) Preparation of mineral-powder pellets

The mineral separates were ground in a shatter box for 2-3 minutes until 99% of the ground material passed through a 200 mesh sieve. 2.5g of the ground mineral were mixed thoroughly with 4 drops of 2% polyvinyl alcohol in a plastic vial. The mixture was put in an assembled 32 mm die and formed into a disc by counter-rotation of the perspex plunger and aluminium sleeve. The plunger and sleeve were removed and about 4g of boric acid backing added. The rest of the die was assembled and the powder pressed with a hydraulic press for 15 seconds at 9 tons. The pellet was then labelled and placed face down on a "Kimwipe" for at least 24 hours to dry. The period of drying helps prevent the pellets from cracking when they are heated up by the X-rays.

(ii) Preparation of glass discs

A fusion mixture was prepared by melting 38.0g of lithium tetraborate (anhydrous), 29.6g of lithium carbonate and 13.2g of lanthanum oxide. The melt is poured onto a clean aluminum sheet, and then ground into a coarse powder when cool. The glass disc was prepared by melting 0.350g mineral powder 0.025g sodium nitrate and 1.875g fusion mixture in a platinum crucible. This was done by heating the mixture with a Meker burner for 20 minutes until all the powder was dissolved, and appeared homogeneous with no



bubbles. The melt was then poured quickly into a brass ring-former on a clean polished brass plate, held at  $500^{\circ}\text{C}$ . A firm but gentle pressure is immediately applied to the bead with a polished aluminium plunger, also heated to  $500^{\circ}\text{C}$ . If the glass disc has no bubbles and fills the brass ring, it is transferred to a second hot plate at about  $200^{\circ}\text{C}$  for annealing.

(iii) Preparation of plagioclase feldspars for X-ray diffraction analysis

The plagioclase feldspar was ground to less than 325 mesh with an agate pestle and mortar. A suspension of the powder in acetone was then smeared evenly over a glass slide, and dried for few minutes, before mounting in the goniometer.

(E) Technique of the X-ray diffraction

The composition of the plagioclase feldspars was determined by X-ray diffraction as a check on the chemical and optical analyses. A schematic diagram of the X-ray diffractometer is shown in Fig. 5. Patterns were taken with a Philips PW1050 Diffractometer using  $\text{Cu K}\alpha$  radiation and scanning from  $27^{\circ}$  to  $37^{\circ}$ . A divergence parallel slit of  $1^{\circ}$ , receiving slit of  $0.1^{\circ}$  fitted with a Ni filter, and a scatter slit of  $1^{\circ}$  were used. Scans were run at a speed of (2 $\theta$ )  $1/4^{\circ}$  per minute using a chart speed of 20 mm per minute. The intensity of the diffracted beam is recorded

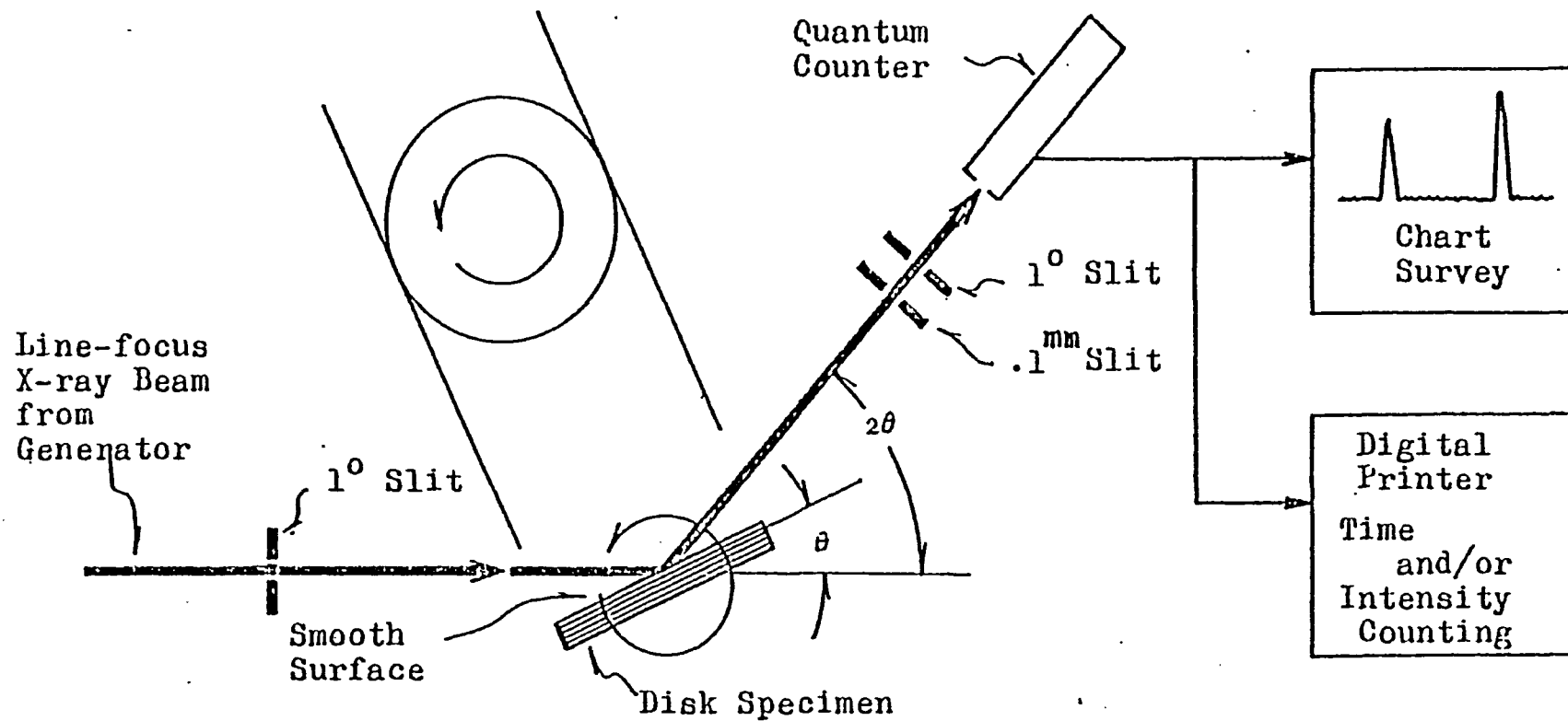


Fig. 5 Schematic view of X-ray powder diffractometer.

continuously on the chart.

The % An was determined by plotting  $2\theta(1\bar{3}1)-2\theta(131)$ , and  $2\theta(\bar{2}41)-2\theta(2\bar{4}1)$  values on diagrams provided by Bambauer et al. (1967, p.337). The results of the determinations are given in Table 5.

(F) The theory of X-ray fluorescence spectroscopy

The technique of X-ray fluorescence is based on the fact that when the X-ray photons (Fig. 6) from the X-ray tube impinge upon the sample at an average angle, secondary (fluorescent) X-rays are emitted from the sample (Norrish and Chappell, 1967). This secondary radiation is composed of various intensities of the characteristic wavelengths of each element present in the sample.

In the flat crystal system, a portion of the secondary radiation is selected by a primary collimator, and the parallel beam is allowed to fall onto the plane surface of a single crystal. The radiation is diffracted in accordance with Bragg's law, i.e.  $n\lambda = 2d \sin\theta$ , where  $\lambda$  is the wavelength of the radiation diffracted through an angle  $\theta$ , by planes in the analysing crystal of spacing  $d$ ;  $n$  is an integer. This relationship allows us to use crystals of known  $d$  spacing to select the characteristic radiation of each element, present in the rock. After diffraction, the radiation passes to the detector which is connected to the goniometer. The intensity of radiation of each wavelength is proportional to the concentration of the corresponding element. The

ROCK TYPE	SAMPLE NO.	$2\theta(\bar{1}\bar{3}1)-2\theta(131)$	An	$2\theta(\bar{2}41)-2\theta(2\bar{4}1)$	An
LAT	C-36	2.259	97	0.275	94
	MP-18	2.338	100	0.100	84
	MP-87	2.198	86	0.200	88
AOIN	MP-22	2.250	92	0.300	94
	C-16	2.244	93	0.103	83
	MP-86	2.269	94	n.s.	n.s.
OAOLG	MP-59	2.231	90	0.251	93
	C-34	2.246	93	0.238	92
AGN	C-48-B	2.231	90	0.219	90
	C-53	1.981	66	n.s.	n.s.
AG	C-57	2.248	91	n.s.	n.s.
AOLG	C-9-A	2.209	87	n.s.	n.s.
	C-44	2.231	91	0.144	86
	MP-31	2.175	82	0.218	87
INCLUSIONS	C-45	1.885	58	0.081	74
	C-39	1.809	53	0.363	59

n.s. not significant

Table 5 An % plagioclase feldspars determined by XRD

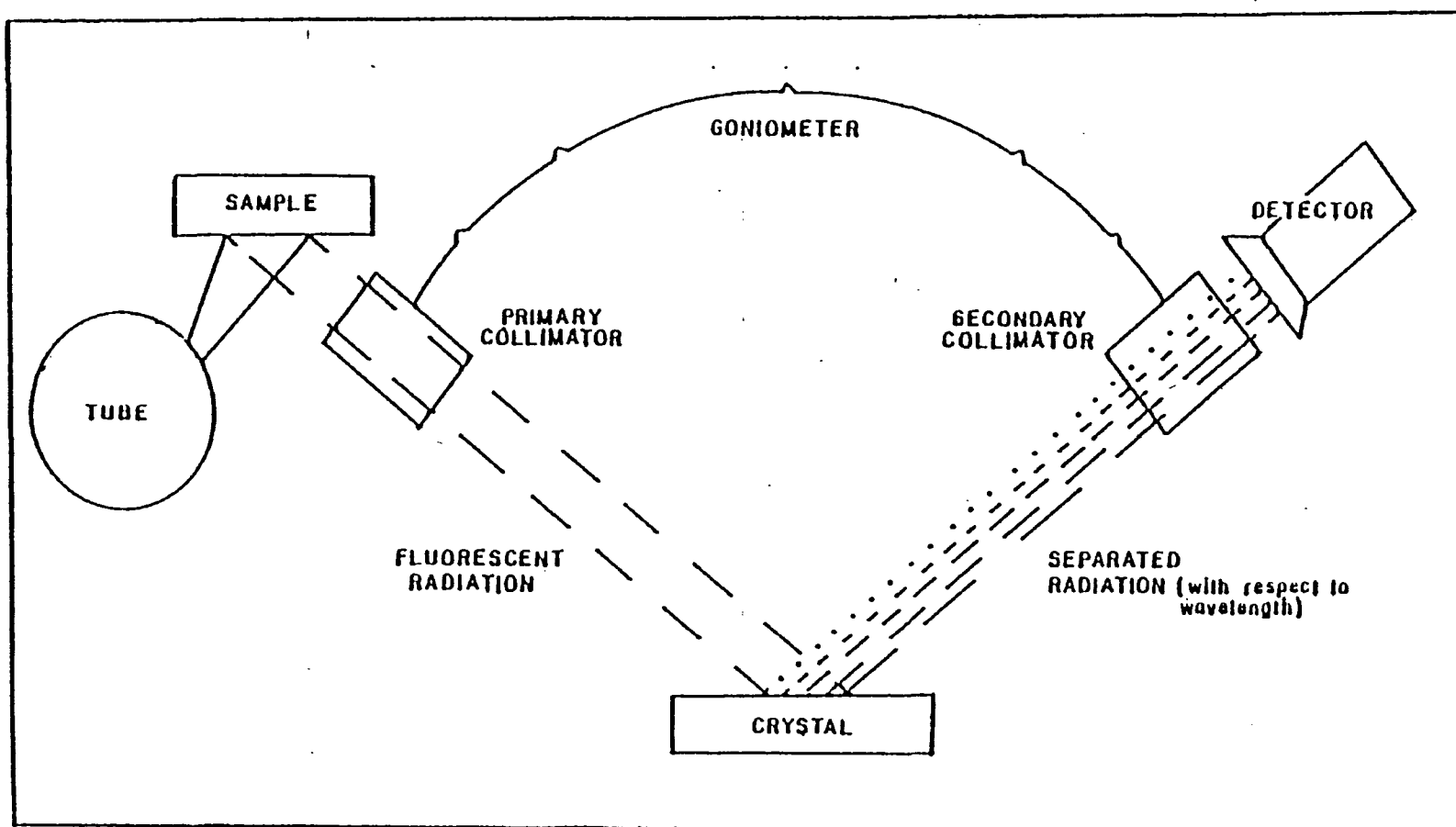


Fig.6 Schematic view of X-ray powder fluorescence

detector converts the X-rays into a form of energy which can be measured and integrated over a finite period of time. Two different types of detectors are used in these studies, the gas flow counter for light elements (atomic number less than 32) and the scintillation counter for heavy elements (atomic number greater than 32). A dead time correction has been determined for each detector (0.00000185 and 0.000002 second/count were used for scintillation and gas flow counter respectively).

The concentrations of the elements were determined by the fixed count or the fixed time method.

In the fixed count method, the peak counting rate was obtained by measuring the time in seconds required to collect a fixed number of counts. After dead time correction, the concentration of the element was calculated using (1)

$$U\% = S\% \times \frac{t_s - (N \times D)}{t_u - (N \times D)} \quad (1)$$

where       $N$  = fixed number of counts  
 $t_s$  = time for the standard sample in seconds  
 $t_u$  = time for the unknown sample in seconds  
 $D$  = dead time of counter in seconds  
 $S\%$  = the concentration of the element in standard sample  
 $U\%$  = the concentration of the element in unknown sample

In those cases where background count rates could not be ignored, the fixed time method was employed. The total counts accumulated on peak and background positions in a selected time, usually 100 seconds for the peak, 40 seconds for backgrounds were measured. Counting times were chosen to yield the required levels of precision. The concentration of the element was obtained from equation (2)

$$U\% = S\% \times \frac{P_u}{P_s} \quad (2)$$

where  $P_u$  = net Peak of unknown sample  
 $P_s$  = net Peak of standard sample

These were determined using the following equation (3)

$$P's = (CPS)_p - f[(CPS)_{b1} + (CPS)_{b2}] \quad (3)$$

where  $(CPS)'s$  = the dead time corrected counting rates

$f$  = the background curvature

$P's$  = the dead time corrected net peak counting rates

$b$  = background

The curvature of background,

$$f = \frac{(CPS)_p}{(CPS)_{b1} + (CPS)_{b2}} \quad (4)$$

was obtained by peak and background counting rates of a pure

quartz pellet.

The major elements were all analysed using the Cr target tube except for Mn where the W target tube was used. The values obtained from the analyses were then corrected for the mass absorption effects using a computer program.

In trace element analysis Compton scatter peaks were measured for each sample, for U.S.G.S. standard rock powders W-1, AGV, GSP, BCR, G-2 and for quartz on Ag, Mo, Cr and W target tubes. Mass absorption values for each sample were determined from these data. The mass absorption is inversely proportional to the intensity of the Compton scatter peak. The values derived from the measurements using the Ag target tube were used to correct the analyses of Nb, Y and Zr for mass absorption effects. Those values derived from the Mo target tube were used to correct the analyses of Rb, Sr, Ni and Cr for mass absorption effects. Using the Cr target tube, values were obtained to correct the analyses of Co, Ba, Cu and Zn for mass absorption effects. The analyses of V were corrected for mass absorption effects using data obtained with the W target tube. The precision of the analyses for the major elements determined are listed in Table 6. The analytical conditions for the major and trace elements are given in Tables 7 and 8. The theoretical precision values for Rb, Sr, Ba, Zn, Cu, Zr, Y, Nb, V and Ni analyses are  $\pm 5\%$  but Cr and Co should be within  $\pm 20\%$ . The precision of the analyses for the trace elements determined are given in Table 6.



OXIDE	2 $\sigma$ %	% OXIDE AND DEVIATION PRECISION
SiO <sub>2</sub>	0.52	50.00 $\pm$ 0.260
Al <sub>2</sub> O <sub>3</sub>	0.74	4.00 $\pm$ 0.029
TiO <sub>2</sub>	0.78	0.60 $\pm$ 0.005
Fe <sub>2</sub> O <sub>3</sub>	0.92	8.00 $\pm$ 0.074
MnO	1.98	0.30 $\pm$ 0.006
MgO	0.80	17.00 $\pm$ 0.136
CaO	1.66	20.00 $\pm$ 0.332
Na <sub>2</sub> O	8.74	0.28 $\pm$ 0.024
K <sub>2</sub> O	0.58	0.02 $\pm$ 0.0001

ELEMENT	2 $\sigma$ %	PPM ELEMENT AND DEVIATION PRECISION
Ni	9.78	5 $\pm$ 0.489
Co	16.50	90 $\pm$ 14.85
Cr	0.72	60 $\pm$ 0.432
Ba	0.70	50 $\pm$ 0.35
Zr	4.00	30 $\pm$ 1.20
Y	0.44	5 $\pm$ 0.022
Rb	0.60	25 $\pm$ 0.15
Sr	1.34	30 $\pm$ 4.02
Nb	1.86	30 $\pm$ 0.558
V	2.00	200 $\pm$ 4.000

Table 6 Precision of XRF Analyses

Table 7 Analytical conditions for determination of major elements

OXIDE	TUBE	kV	mA	CRYSTAL	COLLIMATOR	LL	W	ATT'N	PEAK	COUNTS or TIME	BKGD	TIME	COUNTER/ HELIPOT SETTING
SiO <sub>2</sub>	Cr	50	40	TLAP	Fine	100	190	3	32.05	4x10 <sup>5</sup>	-	-	FC500
Al <sub>2</sub> O <sub>3</sub>	Cr	50	40	TLAP	Fine	150	250	2	37.70	100s	36.73 39.00	40s	FC490
TiO <sub>2</sub>	Cr	50	40	LiF200	Fine	150	180	3	86.18	100s	85.20 87.00	40s	FC488
Fe <sub>2</sub> O <sub>3</sub>	Cr	50	40	LiF200	Fine	150	200	3	57.53	1x10 <sup>6</sup> * 4x10 <sup>5</sup>	-	-	FC470
MnO	W	50	40	LiF200	Coarse	300	260	3	62.97	100s	62.15 63.48	40s	FC500
MgO	Cr	60	45	ADP	Fine	120	350	2	136.57	100s	136.05 138.70	40s	FC501
CaO	Cr	50	40	LiF200	Fine	250	230	3	113.14	1x10 <sup>6</sup>	-	-	FC510
Na <sub>2</sub> O	Cr	60	50	TLAP	Coarse	190	300	2	54.89	100s	53.00 55.40	40s	FC526
K <sub>2</sub> O	Cr	50	40	TLAP	Fine	250	300	3	16.61	100s	15.95 18.00	40s	FC516
P <sub>2</sub> O <sub>5</sub>	Cr	50	40	Germ	Coarse	250	250	2	141.00	100s	143.00	40s	FC492

\* 1x10<sup>6</sup> counts for olivine and orthopyroxene  
 4x10<sup>5</sup> for clinopyroxene and hornblende

Explanation of symbols : LL lower level  
 W window  
 ATT'N Attenuation

BKGD background  
 FC flow counter  
 S seconds

Table 8 Analytical conditions for determination of trace elements

ELEMENT	TUBE	kV	mA	CRYSTAL	COLLIMATOR	LL	W	ATT'N	PEAK	TIME	BKGD	TIME	COUNTER/ HELIPOT SETTING
V	W	60	50	LiF220	Fine	400	300	3	123.37	100s	121.00 126.80	40s	FC510
Cr	Mo	55	25	LiF200	Coarse	100	300	3	69.36	100s	68.60 70.80	40s	FC480
Co	Cr	55	40	LiF220	Coarse	110	200	3	77.78	100s	77.30 80.50	40s	FC466
Ni	Mo	60	25	LiF220	Coarse	240	270	3	71.14	100s	70.00 73.00	40s	FC488
Rb	Mo	60	30	LiF220	Fine	200	400	3	37.99	100s	37.00 41.10	40s	SC250
Sr	Mo	60	30	LiF220	Fine	200	400	3	35.85	100s	35.10 37.00	40s	SC250
Y	Ag	50	40	LiF220	Fine	160	340	3	33.88	100s	33.20 35.00	40s	SC240
Zr	Ag	50	40	LiF220	Fine	160	340	3	32.07	100s	29.70 33.20	40s	SC240
Nb	Ag	60	40	LiF220	Fine	170	350	3	30.44	100s	29.90 33.20	40s	SC230
Ba	Cr	60	40	LiF200	Fine	150	250	3	87.32	100s	70.60 90.00	40s	FC488
Cu	Cr	50	40	LiF200	Coarse	100	200	3	45.00	100s	44.00 46.00	40s	SC260
Zn	Cr	50	40	LiF220	Fine	210	330	3	60.64	100s	60.00 61.50	40s	SC280

Explanation of symbols: Sc Scintillation Counter  
other symbols as in previous Table.

CHAPTER V

THE  
GEOCHEMISTRY OF MINERALS  
OF THE  
MOUNT POSER GABBROIC PLUTON

A. Introduction

Miller (1938), Larsen (1948), Larsen and Draisin (1950), Nockolds and Allen (1953), Sen et al. (1959), Simon and Rollinson (1976), and Nishimori (1976) have reported data for the major and trace element concentrations of the minerals present in the igneous rocks of the Peninsular Ranges batholith. These reports include data for the minerals of the gabbroic rocks (Appendices I to V). In these studies, minerals have been analyzed from a variety of rock types without having established the relationships of the rocks to each other. Nishimori (1976), in a study which was more detailed than the others, analyzed minerals from two separate gabbroic plutons. However, he did not establish the relationships within, or between the plutons. His work failed to reveal the multiple intrusive nature of the majority of the gabbroic plutons in the Peninsular Ranges batholith, or the existence of two distinct rock series, the olivine-pyroxene gabbro-norite series, and the amphibole gabbro series (Walawender and Smith, 1980).

This work seeks to follow up these studies in more detail using samples from a complex in which the relationships of the rocks present are known. The olivine-pyroxene gabbro-norite series can be divided into two subseries -- the olivine-clinopyroxene subseries and the amphibole-orthopyroxene subseries. The former series is defined by the presence of olivine and/or interstitial orthopyroxene and opaques whereas the latter series is characterized by the absence of olivine and the presence of prismatic orthopyroxene and opaques. The A01N, LAT, OA01G, A01G rock units of the Mount Poser gabbroic pluton correspond to the olivine-clinopyroxene subseries and AGN and AG units correspond to the amphibole-orthopyroxene subseries.

The major minerals were separated from each of the rock types as described in Chapter IV. Plagioclase has been separated from 16 rock samples representing all the rock units described in the complex. Olivine, clinopyroxene, orthopyroxene, and amphibole have been separated from 10, 5, 5, and 10 rock samples respectively. The number of each mineral species separated from each rock unit is shown on the following chart (Table 9). Samples localities are shown on Fig. 7.

The full mineral analyses of the plagioclase olivine group and the plagioclase pyroxene group, are presented in tabular form and their more important features are commented on in the text.

Table 9 Number of mineral samples separated from each rock unit.

	AO1N	LAT	OA01G	AO1G	AGN	AG	INC
Plagioclase	3	3	2	3	2	1	2
Olivine	3	2	2	3	-	-	-
Clinopyroxene	1	-	1	2	1	-	-
Orthopyroxene	-	1	-	2	2	-	-
Hornblende	3	3	-	2	1	1	-

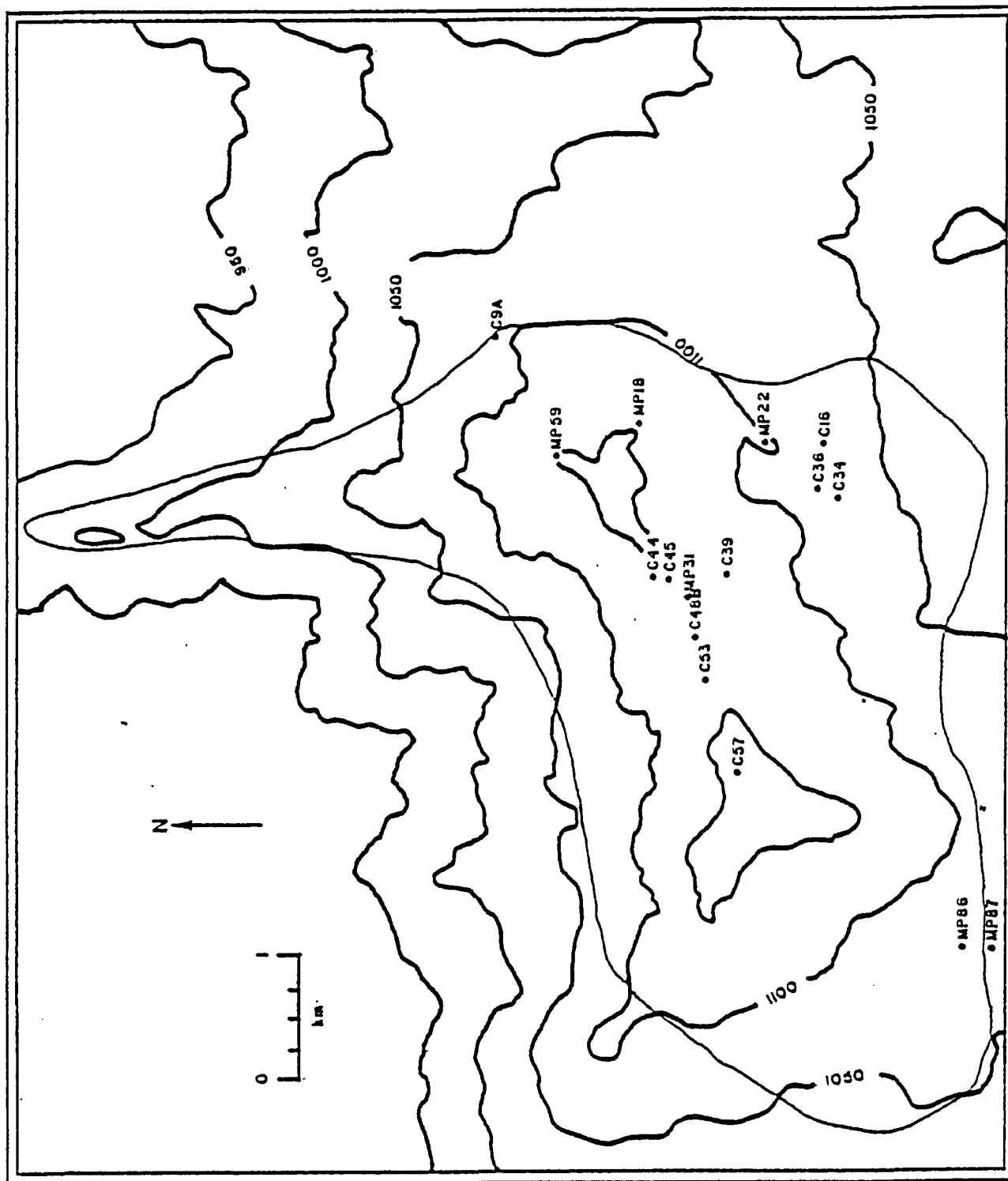


FIG. 7 LOCATION OF SAMPLES USED IN THE GEOCHEMICAL ANALYSIS. OUTLINE AREA REPRESENTS THE MARGIN OF THE MOUNT POSER PLUTON.

The chemical compositions of the minerals are used as indicators of the parental magma or magmas of the Mount Poser gabbroic pluton. An attempt is made to identify chemical differences between the minerals of the various units mapped within the pluton which support the suggestion that the complex was formed by multiple intrusion. Chemical trends are sought within the minerals of the individual rock units, and between the minerals of separate units, which are indicative of differentiation in situ.

A careful comparison of the compositions of the cumulate mineral assemblages of the Mount Poser gabbroic pluton, with the compositions of the cumulate minerals of well described mafic intrusive complexes, and with the compositions of cumulate minerals of volcanic blocks and phenocrysts in lava flows, has been made. The purpose of this comparison is to establish the compositional affinities of the gabbros, and to try to identify the parent magma type or types from which they formed.

Calculations, using the trace element compositions of the minerals, and well established partition coefficients, were carried out to determine the trace element contents of the melts from which the cumulate rocks were derived. This information is used to confirm the composition of the parental magma type, and to follow the differentiation trends of the melt fractions.



## B. Geochemistry of Minerals

### 1) Plagioclase

Pure plagioclase separates for analysis, have been obtained from 3 samples of the A01N unit; 3 of the LAT unit; 2 of the OA01G unit; 3 of the A01G unit; 2 of the AGN unit; 1 of the AG unit; and 2 of the INC unit. Major element analyses and structural formulae are presented in Table 10. In the structural formulae all iron has been arbitrarily assigned to the Si, Al, Ti,  $\text{Fe}^{3+}$  group, since most of the iron in feldspars is  $\text{Fe}^{3+}$  and substitutes for Al (Deer et al., 1963). Minor differences between the optically and chemically determined plagioclase compositions result from the difficulty in obtaining precise results optically. The trace element contents of the plagioclases are listed in Table 11.

The majority of the plagioclases analysed have a very high anorthite content (Table 10). In the plagioclase-olivine group, plagioclase ranges in composition from  $\text{An}_{97.5}$  (A01N) to  $\text{An}_{86.6}$  (A01G). In the plagioclase-pyroxene group the feldspars range in composition from  $\text{An}_{85.3}$  to  $\text{An}_{64.5}$  (both in AGN). In the inclusions the anorthite content of the plagioclases ranges from  $\text{An}_{54.5}$  to  $\text{An}_{51.5}$ .

The plagioclase compositions in the main outcrops of A01N (average  $\text{An}_{95.3}$ ) and LAT (average  $\text{An}_{92.2}$ ), with an average modal abundance of 34% and 64%, differ notably from those of the small outcrops of A01N (MP-86,  $\text{An}_{90.5}$ ) and LAT

	A01N			LAT		
	MP-22	C-16	MP-86	C-36	MP-18	MP-87
SiO <sub>2</sub>	45.03	45.16	45.96	45.95	43.75	44.98
Al <sub>2</sub> O <sub>3</sub>	33.89	34.59	35.34	35.16	35.82	34.84
TiO <sub>2</sub>	-	0.01	-	-	-	-
Fe <sub>2</sub> O <sub>3</sub>	0.46	0.75	0.58	0.58	0.46	0.48
MnO	0.02	0.02	0.02	0.01	0.01	0.01
MgO	-	0.72	-	-	-	-
CaO	18.35	18.12	17.97	18.06	18.28	17.65
Na <sub>2</sub> O	0.14	0.62	0.93	0.72	0.76	1.28
K <sub>2</sub> O	0.18	0.19	0.17	0.17	0.17	0.19
P <sub>2</sub> O <sub>5</sub>	-	0.03	0.01	-	-	0.01

Numbers of ions on the basis of 32(O)

Si	8.455	16.02	8.324	15.94	8.388	16.07	8.408	16.07	8.150	16.08	8.350	16.04
Al	7.501		7.514		7.600		7.582		7.864		7.621	
Ti	-		0.001		-		-		-		-	
Fe <sup>3+</sup>	0.065		0.105		0.080		0.080		0.065		0.067	
Mn	0.002		0.003		0.002		0.001		0.001		0.002	
Mg	-		0.197		-		-		-		-	
Ca	3.692	3.79	3.578	4.05	3.513	3.89	3.541	3.84	3.649	3.96	3.510	4.02
Na	0.052		0.222		0.329		0.256		0.273		0.461	
K	0.042		0.044		0.041		0.040		0.041		0.044	
P	-		0.005		0.001		-		-		-	
An	97.53		93.08		90.49		92.28		92.09		87.42	
Name	Anorthite		Anorthite		Anorthite		Anorthite		Anorthite		Bytownite	

Table 10 Major elements(wt%) compositions of plagioclase feldspars  
from the different rock types in the pluton

	OA01G		A01G		
	C-34	MP-59	MP-31	C-44	C-9-A
SiO <sub>2</sub>	44.12	46.50	42.30	46.40	46.41
Al <sub>2</sub> O <sub>3</sub>	33.65	29.85	31.21	34.63	34.73
TiO <sub>2</sub>	-	-	0.01	0.02	-
Fe <sub>2</sub> O <sub>3</sub>	0.60	0.60	0.66	0.80	0.80
MnO	0.01	0.01	0.01	0.02	0.02
MgO	-	-	0.43	-	-
CaO	18.02	18.06	17.18	16.87	18.04
Na <sub>2</sub> O	0.81	0.84	1.25	1.30	0.76
K <sub>2</sub> O	0.18	0.17	0.17	0.17	0.17
P <sub>2</sub> O <sub>5</sub>	-	-	-	-	-
Numbers of ions on the basis of 32 (O)					
Si	8.373	8.924	8.412	8.514	8.471
Al	7.525	6.752	7.315	7.489	7.472
Ti	-	-	0.001	0.002	-
Fe <sup>3+</sup>	0.086	0.087	0.098	0.110	0.110
Mn	0.002	0.002	0.002	0.003	0.003
Mg	-	-	0.127	-	-
Ca	3.665	3.713	3.660	3.36	3.528
Na	0.297	0.311	0.482	0.464	0.269
K	0.043	0.042	0.043	0.039	0.041
P	-	-	-	-	-
An	91.50	91.31	87.45	86.83	91.93
Name	Anorthite	Anorthite	Bytownite	Bytownite	Bytownite

Table 10 continued

	AGN		AG	INCLUSIONS	
	C-48	C-53	C-57	C-39	C-45
SiO <sub>2</sub>	46.69	50.36	44.24	54.08	52.93
Al <sub>2</sub> O <sub>3</sub>	32.91	30.86	33.87	28.34	28.41
TiO <sub>2</sub>	-	0.01	0.01	0.01	0.02
Fe <sub>2</sub> O <sub>3</sub>	0.64	0.61	0.59	0.47	0.60
MnO	0.02	0.01	0.01	0.01	0.01
MgO	-	-	0.20	0.12	-
CaO	16.91	13.24	17.11	10.80	11.50
Na <sub>2</sub> O	1.49	3.89	1.48	5.4	5.04
K <sub>2</sub> O	0.18	0.22	0.18	0.34	0.49
P <sub>2</sub> O <sub>5</sub>	-	-	-	0.09	0.05

Numbers of ions on the basis of 32(O)

Si	8.688	16.00	9.257	16.04	8.366	16.00	9.822	15.95	9.710	15.94
Al	7.218		6.685		7.548		6.066		6.144	
Ti	-		0.002		0.001		0.002		0.002	
Fe <sup>3+</sup>	0.089		0.084		0.085		0.064		0.083	
Mn	0.003		0.001		0.002		0.002		0.002	
Mg	-		-		0.056		0.032		-	
Ca	3.371	3.95	2.608	4.05	3.466	4.11	2.101	4.13	2.261	4.18
Na	0.538		1.386		0.544		1.901		1.793	
K	0.042		0.051		0.043		0.078		0.114	
P	-		-		-		0.013		0.008	

An	85.32	64.48	85.52	51.50	54.25
Name	Bytownite	Labradorite	Bytownite	Labradorite	Labradorite

Table 10 continued

	A01N			LAT			OA01G	
	MP-22	C-16	MP-86	C-36	MP-18	MP-87	C-34	MP-59
Rb	2	2	1	1	-	2	1	-
Sr	487	669	554	487	468	546	474	490
Ba	15	25	24	12	11	34	15	12
I	-	-	-	-	-	-	-	-
Zr	-	-	-	-	-	-	-	-
Nb	-	2	4	1	1	1	1	1
Cu	20	28	19	32	30	24	33	31
Ni	-	-	-	-	-	-	-	-
Co	2	7	4	-	3	2	-	2
Cr	-	-	-	-	-	-	-	-
V	-	-	-	-	2	-	1	2

	A01G			AGN		AG	INCLUSIONS	
	MP-31	C-44	C-9-A	C-53	C-48	C-57	C-39	C-45
Rb	1	1	1	-	-	1	2	1
Sr	553	552	546	734	660	695	489	549
Ba	8	8	11	50	23	22	23	85
I	-	-	-	-	-	-	4	-
Zr	-	-	-	-	-	-	30	-
Nb	-	-	-	3	2	-	2	-
Cu	50	27	31	27	36	54	33	25
Ni	-	-	-	-	-	-	-	-
Co	4	3	4	4	5	3	3	4
Cr	-	-	-	-	-	-	-	-
V	3	4	3	2	3	5	1	3

Table 11 Trace elements (ppm) compositions of plagioclases  
from the different rock types of the pluton

(MP-87,  $An_{87.4}$ ), with an average modal abundance of 50% and 50% respectively, exposed along the southwest margin of the complex (Fig. 7). Differences are also noted in the major elements. The  $CaO$ ,  $Na_2O$ ,  $Al_2O_3$ , and  $SiO_2$  contents of the plagioclases vary in the same manner as their  $An$  contents.  $K_2O$  content of plagioclases in A01N is higher in the main outcrops (average 0.19%) than in the southwestern outcrop (0.17%), where as  $K_2O$  content of plagioclases in LAT is lower in the main outcrops (average 0.17%) than in the small outcrop (0.19%). The  $Na/Ca$  ratios of the A01N and LAT are 0.022 and 0.042 in the main outcrops, and 0.054 and 0.075 in the southwestern outcrops respectively. Differences are also noted in the  $Sr$  content of the plagioclases. They average 578 ppm and 477 ppm in the main outcrops, and 554 ppm and 546 ppm in the southwestern units, of the A01N and LAT respectively. The  $Ba$  content of plagioclases only show differences between the main outcrops (12 ppm) and in the western outcrops (34 ppm) of the LAT unit. The average  $Rb$  content is 1 ppm, and shows no significant difference from unit to unit. There is no clinopyroxene in the mode of any of the samples of the main unit of A01N but this mineral occurs in the small southwestern outcrop of A01N.

It has been suggested (P.25) that the OA01G unit may represent a chilled margin around the A01N and LAT units. The plagioclases analyzed from the OA01G unit have an average composition of  $An_{91.4}$  and a  $Sr$ ,  $Rb$ ,  $Ba$  content of 488 ppm, 13 ppm, and 1 ppm respectively, and show little

variation. The average concentration of  $\text{SiO}_2$ ,  $\text{Al}_2\text{O}_3$ ,  $\text{CaO}$ ,  $\text{Na}_2\text{O}$  and  $\text{K}_2\text{O}$  are 45.31%, 31.75%, 18.04%, 0.83% and 0.18% respectively. The average Na/Ca ratio is 0.048.

The plagioclase composition in the A01G dykes ranges from  $\text{An}_{91.9}$  to  $\text{An}_{86.8}$ . The modal data (Table 2) shows that the more calcic plagioclase ( $\text{An}_{91.9}$ ) occurs in a spinel-bearing dyke with a 52% modal abundance of plagioclase and the less calcic plagioclases (average  $\text{An}_{87.2}$ ) are found in dykes lacking spinel with lower modal plagioclase abundance (44%). The  $\text{CaO}$  and  $\text{Na}_2\text{O}$  contents of the plagioclases vary in the same manners as their An contents. The average concentration of  $\text{SiO}_2$ ,  $\text{Al}_2\text{O}_3$ , and  $\text{K}_2\text{O}$  are 45.04%, 33.52% and 0.17% respectively. The Na/Ca ratios in the dykes near eastern margin (0.044) are lower than those from the central pluton (average 0.078). The Ba content of the plagioclases in dykes near the eastern margin (11 ppm) is slightly different from those of the central pluton (8 ppm).

In the AGN unit of the plagioclase-pyroxene group, the feldspar ranges in composition from  $\text{An}_{85}$ , with 660 ppm Sr, and 23 ppm Ba, where orthopyroxene is the dominant mafic mineral, to  $\text{An}_{64}$  with 734 ppm Sr and 50 ppm Ba, where amphibole is the dominant mafic mineral. Plagioclase in the orthopyroxene-dominant rock of this unit are characterized by lower contents of  $\text{SiO}_2$  (46.69%),  $\text{Na}_2\text{O}$  (1.49%) and  $\text{K}_2\text{O}$  (0.18%), and higher contents of  $\text{Al}_2\text{O}_3$  (32.91%) and  $\text{CaO}$  (16.91%) than those of the amphibole-dominant rocks of this

unit. The Na/Ca ratio of plagioclase in orthopyroxene-dominant rock is much lower (0.091) than the amphibole-dominant rock (0.305).

The composition of the plagioclase determined from the AG unit is  $An_{85.5}$  with 695 ppm Sr, 22 ppm Ba and 1 ppm Rb. The plagioclase of this unit has lower content of  $SiO_2$  (44.24%) and higher contents of  $Al_2O_3$  (33.87%), and CaO (17.11%), than the AGN unit. The Na/Ca ratio of plagioclase in this unit is 0.09.

In the inclusions, the composition of the plagioclases ranges from  $An_{54.3}$  to  $An_{51.5}$ , and the Sr content ranges from 489 ppm to 549 ppm and the Ba content (C-45, 85 ppm) is the highest among other units. The feldspars in the inclusions are characterized by the highest average concentration of  $SiO_2$  (53.51%),  $Na_2O$  (5.22%), and  $K_2O$  (0.42%), and Na/Ca ratio (0.0437), and with lowest  $Al_2O_3$  (28.38%) and CaO (11.15%) in the pluton.

## 2) Olivine

10 samples of olivine were separated out from the plagioclase-olivine series, 3 from the A01N unit; 2 from the LAT unit; 2 from the OA01G unit and 3 from the A01G unit. No olivine occurs in the plagioclase-pyroxene series. The major element and trace element contents of the olivines are presented in Tables 12 and 13 respectively. Olivines average from  $Fo_{77.9}$  in the A01N unit,  $Fo_{75.6}$  in the LAT unit,  $Fo_{73.7}$  in the OA01G unit, to  $Fo_{73.0}$  in the A01G unit.



	A01N			LAT	
	MP-22	C-16	MP-86	C-36	MP-18
SiO <sub>2</sub>	37.13	37.76	41.24	38.61	36.90
Al <sub>2</sub> O <sub>3</sub>	1.61	2.92	1.30	1.74	0.98
TiO <sub>2</sub>	0.03	0.03	0.07	0.04	0.03
Fe <sub>2</sub> O <sub>3</sub>	21.70	21.67	22.54	22.76	24.18
MnO	0.27	0.26	0.31	0.30	0.29
MgO	39.28	37.61	34.21	36.51	36.95
CaO	0.32	0.42	1.88	0.52	0.46

Numbers of ions on the basis of 4(O)

Si	0.924	0.933	1.008	0.958	0.930
Al	0.047	0.085	0.037	0.051	0.029
Ti	0.001	0.001	0.001	0.001	-
Fe <sup>3+</sup>	0.406	0.403	0.414	0.425	0.459
Mn	0.006	0.005	0.006	0.006	0.006
Mg	1.457	1.385	1.247	1.350	1.308
Ca	0.008	0.011	0.049	0.014	0.013

Atomic ratios

Mg	78.2	77.5	75.0	76.1	75.2
Fe	21.8	22.5	25.0	23.9	24.8

$\frac{100 \times \text{Mg}}{(\text{Mg} + \text{Fe}^{3+} + \text{Mn})}$					
(Mg+Fe <sup>3+</sup> +Mn)	61.6	60.7	57.4	58.7	57.6
Name	Chrysolite	Chrysolite	Chrysolite	Chrysolite	Chrysolite

Table 12 Major elements (wt%) compositions of olivines from the different rock types in the pluton.

	0A01G		A01G		
	MP-59	C-34	C-9-A	C-44	MP-31
SiO <sub>2</sub>	37.85	38.82	37.80	39.51	40.32
Al <sub>2</sub> O <sub>3</sub>	1.61	0.51	0.92	1.93	1.80
TiO <sub>2</sub>	0.04	0.07	0.03	0.10	2.03
Fe <sub>2</sub> O <sub>3</sub>	24.51	23.15	25.99	22.96	22.26
MnO	0.32	0.33	0.37	0.33	0.57
MgO	33.72	33.61	34.62	31.13	30.31
CaO	1.33	3.01	1.20	4.29	3.49

Numbers of ions on the basis of 4(0)

Si	0.956	0.981	0.946	0.989	0.999
Al	0.048	0.015	0.027	0.057	0.053
Ti	0.001	0.001	0.001	0.002	0.038
Fe <sup>3+</sup>	0.446	0.440	0.490	0.433	0.415
Mn	0.007	0.007	0.008	0.007	0.012
Mg	1.271	1.265	1.292	1.162	1.120
Ca	0.036	0.081	0.032	0.115	0.093

Atomic ratios

Mg	73.2	74.2	72.5	72.9	73.0
Fe	26.8	25.8	24.5	27.1	27.0

<u>100 x Mg</u>					
(Mg+Fe <sup>3+</sup> +Mn)	55.0	56.3	54.1	57.9	54.4
Name	Chrysolite	Chrysolite	Chrysolite	Chrysolite	Chrysolite

Table 12 continued

	A01N			LAT		
	MP-22	C-16	MP-86	C-36	MP-18	MP-87
Rb	3	2	4	3	7	3
Sr	-	-	-	-	1	2
Ba	-	-	-	-	-	8
I	-	-	-	-	-	-
Zr	-	-	-	-	-	2
Nb	4	4	5	6	6	5
Ni	369	504	301	229	163	112
Co	94	95	87	91	90	63
Cr	73	93	151	42	63	55
V	8	17	51	15	9	72

	OA01G		A01G		
	*C-34	MP-59	*MP-31	C-44	C-9-A
Rb	2	4	3	2	-
Sr	-	-	12	-	7
Ba	3	-	67	-	-
I	-	-	-	-	-
Zr	-	-	-	-	-
Nb	5	6	4	6	3
Ni	92	193	23	195	104
Co	197	90	145	82	211
Cr	110	106	8	356	34
V	41	22	61	82	14

Table 13 Trace elements (ppm) compositions of olivines from the different rock types of the pluton (\*pure quartz added to the sample)

Olivine is only present in specimens where the plagioclase composition is more calcic than  $An_{86}$ . The modal abundances of olivines are different in each of the rock units. The main outcrops of A01N and LAT contain 40% and 13% respectively, and the small outcrops of these rock types in the southwest contain 32% and 5% respectively. The average modal abundance in the OA01G units is 15%. In the A01G unit, olivine is more abundant modally (14%) in spinel-bearing dykes and is less abundant (6%) in the non-spinel bearing dykes.

In the main outcrops of the A01N and LAT units the forsterite content of the olivines averages  $Fo_{77.9}$  and  $Fo_{75.6}$ , and has Mg numbers\* of 61.2 and 58.2 respectively. The concentrations of the major elements  $SiO_2$ ,  $CaO$ ,  $MgO$ ,  $Fe_2O_3$ , and  $Al_2O_3$  vary in the same manner as the Fo content and Mg numbers. The olivines have an average of 437 ppm Ni and 95 ppm Co in the A01N unit, and an average of 196 ppm Ni and 91 ppm Co in the LAT unit.

No olivine could be separated for major element analysis from the small outcrop of the LAT unit exposed in the southwest of the complex. Olivines from the southwest exposure of A01N have a composition of  $Fo_{75.0}$  (MP-86), and an Mg number of 57.4. The olivines from these outcrops contain 301 ppm Ni and 87 ppm Co in the A01N unit and 112 ppm Ni and 63 ppm Co in the LAT unit. Thus the Fo content, Mg number,

---

\*Mg Number:  $100 \times Mg / (Mg + Fe + Mn)$ .

and Ni and Co contents of these exposures of A01N and LAT differ significantly from the olivines in the main outcrops of these rock types.

In the OA01G unit, the olivine has an average composition of  $\text{Fo}_{73.7}$  and has an average Mg number of 55.7. The average  $\text{SiO}_2$ ,  $\text{Al}_2\text{O}_3$ ,  $\text{MgO}$ ,  $\text{Fe}_2\text{O}_3$  and  $\text{CaO}$  contents are 38.34%, 1.06%, 33.67%, 23.83% and 2.17% respectively. The average concentrations of Ni and Co are 143 ppm and 144 ppm respectively.

In the A01G unit, olivine ranges in composition from  $\text{Fo}_{73}$  with a Mg number of 56.2, where spinel is present in the dykes, to  $\text{Fo}_{72.5}$  with a Mg number of 54.1, where spinel is absent from the dykes. Differences are also noted in major elements ( $\text{SiO}_2$ ,  $\text{Al}_2\text{O}_3$ ,  $\text{TiO}_2$ ,  $\text{CaO}$ ,  $\text{Fe}_2\text{O}_3$  and  $\text{MgO}$ ), which vary in the same manner as their Fo contents. The Co content of the olivines range in composition from an average of 114 ppm in the non-spinel dykes, to an average of 104 ppm in the spinel-bearing dykes. The Ni and Sr contents of these olivines are 107 ppm and 6 ppm respectively.

The mean MgO content of olivines decreases from 38.45% in the A01N unit, 36.73% in the LAT unit, 33.67% in the OA01G unit, to 30.72% in the A01G unit with increasing iron content from 21.69% in the A01N unit, 23.47% in the LAT unit, to 23.83% in the OA01G unit, except in the A01G unit (22.61%). The average Ni content decreases from 437 ppm in the A01N unit, 196 ppm in the LAT unit, 143 ppm in the OA01G unit, to 109 ppm in the A01G unit with decreasing Mg

number from 61.2 in the A01N unit, 58.2 in the LAT unit, to 55.7 in the OA01G unit, except in the A01G unit(56.2).

### 3) Clinopyroxene

There are 6 clinopyroxene samples separated from 4 rock units; 1 from the A01N unit; 1 from the OA01G unit; 3 from the A01G unit; 1 from the AGN unit.

Major element analyses and structural formulae, of the clinopyroxenes are presented in Table 14 and are illustrated in Fig. 8. The trace element contents of the clinopyroxenes are presented in Table 15.

All of the clinopyroxenes analyzed fall within the calcic augite compositional field (Fig. 8), having Mg number in the range 72.8 to 80.5, (Fe/Mg ratios range from 0.54 to 0.83). In the plagioclase-olivine series, the composition of clinopyroxenes range from  $\text{Ca}_{41.3}\text{Mg}_{45.6}\text{Fe}_{13.2}$  in the OA01G unit to an average of  $\text{Ca}_{40.1}\text{Mg}_{48.6}\text{Fe}_{11.4}$  in the A01G unit and Mg numbers increase from 77.6 to 80.4 (Fe/Mg ratios ranges from 0.64 to 0.54). Clinopyroxene does not occur in the main outcrops of the A01N and LAT units, or in the rocks of the southwest outcrop of the LAT unit. Only one sample (MP-86) of the A01N unit from the small southwest outcrop, contains this mineral.

In the A01N unit, the composition of the clinopyroxene is  $\text{Ca}_{40.2}\text{Mg}_{48.4}\text{Fe}_{11.4}$  having a Mg number of 80.5 (Fe/Mg ratio 0.54). The concentrations of  $\text{SiO}_2$ ,  $\text{Al}_2\text{O}_3$  and  $\text{TiO}_2$  in clinopyroxene are 50.71%, 4.30% and 0.45% respectively and

	<u>A01N</u>	<u>0A01G</u>	<u>A01G</u>			<u>AGN</u>
	Mp-86	C-34	Mp-31	C-44	C-9-A	C-53
SiO <sub>2</sub>	50.71	53.12	51.35	51.39	46.47	50.87
Al <sub>2</sub> O <sub>3</sub>	4.30	4.24	4.34	4.17	6.79	2.98
TiO <sub>2</sub>	0.45	0.40	0.62	0.59	0.38	0.52
Fe <sub>2</sub> O <sub>3</sub>	8.09	9.36	8.05	8.56	8.25	10.62
MnO	0.17	0.18	0.29	0.31	0.14	0.32
MgO	17.26	16.78	17.21	18.55	15.46	14.31
CaO	19.97	21.08	20.53	20.47	16.37	19.42
Na <sub>2</sub> O	-	0.18	0.28	-	-	0.53
K <sub>2</sub> O	-	-	0.02	-	-	-

Numbers of ions on the basis of 6(0)

Si	1.832	2.00	1.844	2.00	1.828	2.00	1.808	1.98	1.793	2.01	1.868	2.00
Al(IV)	0.168		0.156		0.172		0.173		0.207		0.128	
Al(VI)	0.015		0.018		0.010		-		0.102		-	
Ti	0.012		0.011		0.016		0.016		0.011		0.014	
Fe <sup>3+</sup>	0.220		0.245		0.216		0.227		0.239		0.293	
Mn	0.005		0.005		0.009		0.009		0.005		0.010	
Mg	0.929	1.95	0.868	1.94	0.913	1.97	0.973	2.00	0.889	1.92	0.811	1.93
Ca	0.773		0.784		0.783		0.772		0.677		0.764	
Na	-		0.012		0.020		-		-		0.038	
K	-		-		0.001		-		-		-	
Mg	48.35		45.76		47.76		48.55		49.25		43.40	
Fe	11.44		12.90		11.28		11.52		13.27		15.70	
Ca	40.21		41.34		40.96		39.14		37.48		40.90	

100 x Mg

(Mg+Fe <sup>3+</sup> +Mn)	80.50	77.64	80.23	80.48	75.65	72.80
Name	Augite	Augite	Augite	Augite	Augite	Augite

Table 14 Major elements(wt%) compositions of clinopyroxenes  
from the different rock types in the pluton

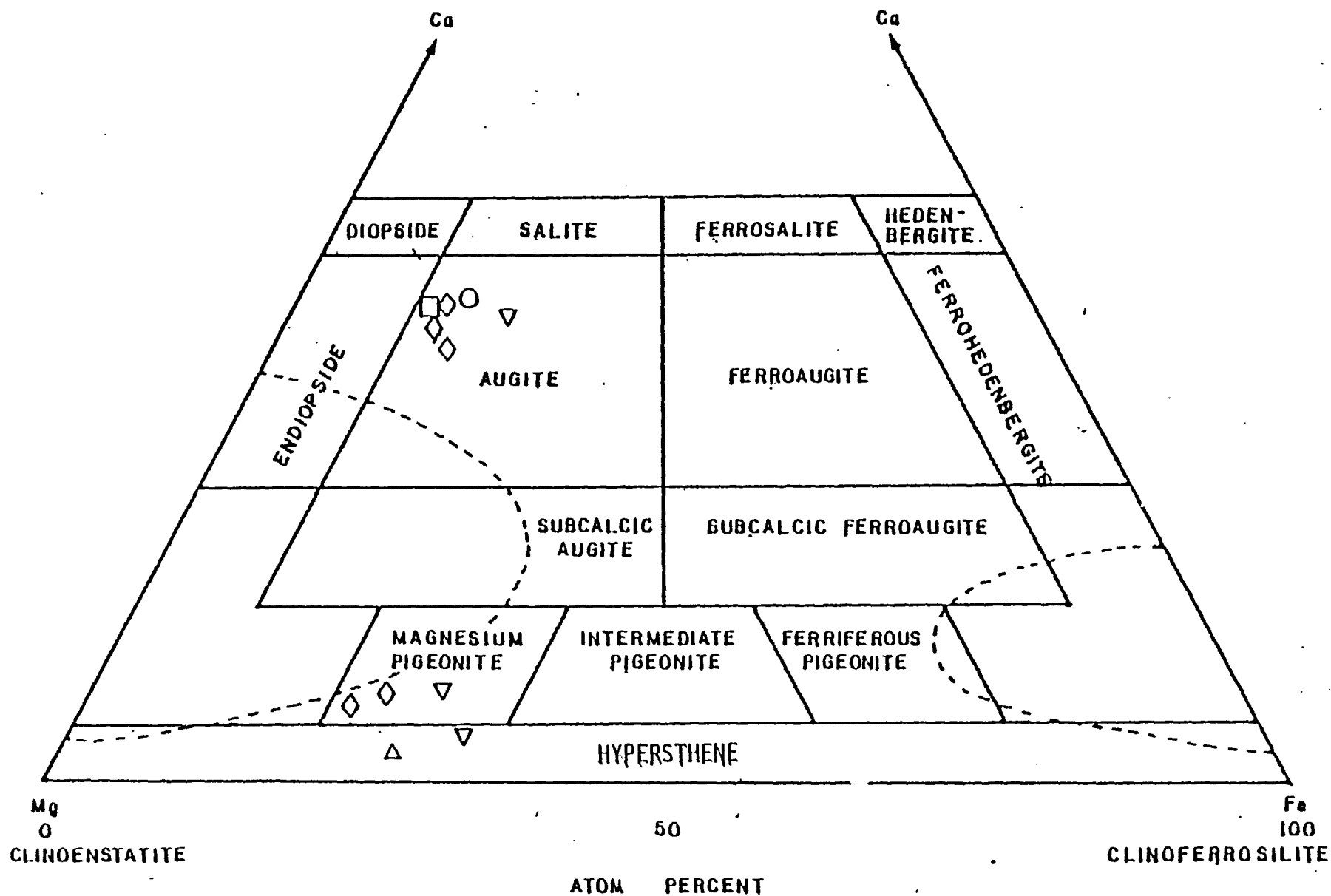


Fig. 8 Variation in composition for clinopyroxene and orthopyroxene.  
 Symbols used as follow: □ AOlN, Δ LAT, ○ OAolG, ◇ AolG, ▽ AGN.



	<u>OA01G</u>	<u>A01G</u>			<u>AGN</u>
	C-34	MP-31	C-44	C-9-A	*C-53
Rb	5	5	3	6	5
Sr	29	102	71	116	73
Ba	39	65	49	34	69
Y	12	31	72	9	11
Zr	11	-	29	5	-
Nb	4	6	2	4	-
Ni	72	14	32	87	23
Co	30	31	22	31	54
Cr	1478	16	41	905	29
V	279	208	203	279	202

Table 15 Trace elements (ppm) compositions of clinopyroxenes from the different rock types of the pluton.  
(\*pure quartz added to the sample)

have an Al(IV) value of 0.168. It was not possible to separate enough clinopyroxene for any sample of the A01N unit for trace element determinations.

Clinopyroxene was successfully separated for analyses from only one sample of 0A1G (C-34). Its composition is  $\text{Ca}_{41.3}\text{Mg}_{45.8}\text{Fe}_{12.9}$  with Mg number of 77.64, (Fe/Mg ratio 0.64). It is characterized by the highest content of  $\text{SiO}_2$  (53.12%) and has the lowest  $\text{TiO}_2$  (0.40%) and  $\text{Al}_2\text{O}_3$  (4.24%) among all clinopyroxenes. The value of Al(IV) in this clinopyroxene is 0.156. The concentrations of Rb, Sr, Ba, Co, V, Cr, and Ni are 5 ppm, 29 ppm, 39 ppm, 30 ppm, 279 ppm, 1478 ppm and 279 ppm respectively.

The clinopyroxenes of the A01G dykes are generally more Mg rich, and Fe and Ca poor, than the clinopyroxenes from the other units. The composition of clinopyroxenes from the central outcrops and the eastern margin of A01G are,  $\text{Ca}_{40.1}\text{Mg}_{48.6}\text{Fe}_{11.4}$  (average) and  $\text{Ca}_{37.5}\text{Mg}_{49.3}\text{Fe}_{13.3}$ , and have Mg numbers of 80.4 and 75.6, (Fe/Mg ratios 0.54 and 0.62) respectively. The clinopyroxene separated from the eastern most dyke (C-9-A) of this unit is exceptionally high in  $\text{Al}_2\text{O}_3$  (6.79%), Cr (905 ppm), Ni (87 ppm) and V (279 ppm) contents as compared to those from the centre of the pluton (MP-31 and C-44). Dykes from the central area average 4.23%  $\text{Al}_2\text{O}_3$ , 29 ppm Cr, 23 ppm Ni and 206 ppm V. The clinopyroxene of sample (C-9-A) also has the lowest content of  $\text{SiO}_2$  (46.47%),  $\text{TiO}_2$  (0.38%), MnO (0.14%) and CaO (16.37%). The tetrahedral value of Al in clinopyroxene of the eastern dyke (0.207) is

higher than the value (Al<sub>IV</sub>) in clinopyroxene from dykes in the central outcrops (average 0.173). The concentrations of Rb, Sr, Ba, Y and Co of the clinopyroxenes in the central outcrops and the eastern margin, are 4 ppm and 6 ppm, 87 ppm and 116 ppm, 57 ppm and 34 ppm, 52 ppm and 9 ppm, and 27 ppm and 31 ppm respectively.

The only clinopyroxene, analyzed from the plagioclase-pyroxene series, comes from the AGN unit (C-53). It has the composition of Ca<sub>40.7</sub>Mg<sub>43.2</sub>Fe<sub>16.1</sub> and Mg number of 72.80, (Fe/Mg ratio of 0.83). It contains the least Al<sub>2</sub>O<sub>3</sub> (2.98%), and the most Fe<sub>2</sub>O<sub>3</sub> (10.62%), and a moderate contents of TiO<sub>2</sub> (0.52%) and SiO<sub>2</sub> (50.37%). It has the lowest Al(IV) value (0.168) in clinopyroxene of all the other units. The concentrations of Rb, Sr, Ba, Ni, V, Co and Cr are 5 ppm, 73 ppm, 69 ppm, 23 ppm, 202 ppm, 54 ppm and 29 ppm respectively.

#### 4) Orthopyroxene

5 samples of orthopyroxene were separated out from 3 rock units, 1 from the LAT unit, 2 from the A01G unit, and 2 from the AGN unit. The orthopyroxene occurs as interstitial crystals and reaction rims in the A01N, LAT and OA01G unit, as subhedral prismatic crystals in the A01G and AGN unit. No orthopyroxene is present in the AG unit. It was not possible to separate sufficient orthopyroxene for analysis from any sample of the A01N, OA01G, or the main outcrops in the LAT unit. Subhedral orthopyroxene only occurs in rock

types where the olivine has Fo<sub>71</sub> and the plagioclase lies in the compositional range An<sub>83-65</sub>.

Major element analyses and structural formulae of the orthopyroxenes are presented in Table 16 and shown on Fig.8. Trace element compositions of the orthopyroxenes are presented in Table 17. Modal abundance of orthopyroxene ranges from 1% to 14%. It tends to increase with decreasing bulk Mg number of the assemblage.

The orthopyroxene from the LAT unit is much less calcic than any of the others and falls in the compositional field of hypersthene (Ca<sub>2.0</sub>Mg<sub>71.5</sub>Fe<sub>26.7</sub>) and has Mg number of 72.4, (Fe/Mg ratio of 0.85). In the LAT, the orthopyroxene contents of K<sub>2</sub>O, Al<sub>2</sub>O<sub>3</sub> and TiO<sub>2</sub> is 0.01%, 2.47% and 0.13% respectively. The Al value in the Z site is 0.105. There was insufficient material in the separate for trace element analysis.

The low Ca-pyroxene from the other two units is classified as inverted pigeonite. The recognition of the presence of the inverted pigeonite is supported by the existence of fine exsolution lamellae of clinopyroxenes. The average compositions of inverted pigeonites from the A01G and AGN units, are Ca<sub>7.0</sub>Mg<sub>71.4</sub>Fe<sub>21.4</sub> and Ca<sub>6.1</sub>Mg<sub>64.4</sub>Fe<sub>29.5</sub>. They have average Mg numbers of 75.8 and 67.9, (Fe/Mg ratios 0.71 and 1.05) respectively.

The inverted pigeonites from the A01N unit are rich in Al<sub>2</sub>O<sub>3</sub> (3.18% to 2.06%), CaO (3.7% to 2.98%), V (118 ppm to 96 ppm), Ni (22 ppm to 8 ppm) and Sr (15 ppm to 7 ppm), and

	LAT	A01G			AGN					
	MP-87	C-44	MP-31	C-53	C-48					
SiO <sub>2</sub>	49.37	50.43	51.78	51.34	50.46					
Al <sub>2</sub> O <sub>3</sub>	2.47	3.23	3.13	1.55	2.56					
TiO <sub>2</sub>	0.13	0.32	0.37	0.25	1.31					
Fe <sub>2</sub> O <sub>3</sub>	19.60	16.44	16.39	20.93	20.17					
MnO	0.36	0.55	0.52	0.62	0.57					
MgO	26.43	25.02	29.15	22.59	22.66					
CaO	1.03	3.58	3.82	2.28	3.67					
Na <sub>2</sub> O	-	0.10	0.05	-	-					
K <sub>2</sub> O	0.01	-	0.02	-	-					
Number of ions on the basis of 6(O)										
Si	1.782	1.89	1.808	1.95	1.763	1.89	1.855	1.92	1.798	1.91
Al	0.105		0.137		0.126		0.066		0.108	
Ti	0.004		0.009		0.009		0.007		0.035	
Fe	0.532		0.444		0.420		0.569		0.541	
Mn	0.011		0.017		0.015		0.019		0.017	
Mg	1.422	2.01	1.338	1.95	1.480	2.07	1.216	1.90	1.203	1.94
Ca	0.040		0.138		0.139		0.088		0.140	
Na	-		0.007		0.003		-		-	
K	0.001		-		0.001		-		-	
Mg		71.3		69.71		72.56		64.92		63.86
Fe		26.7		23.12		20.60		30.36		28.70
Ca		2.0		7.17		6.84		4.72		7.44
100 x Mg										
(Mg+Fe <sup>3+</sup> +Mn)		72.4		74.39		77.27		67.42		68.32
En		71		70		73		63		64
Name	hypersthene	inverted pigeonite		inverted pigeonite		inverted pigeonite		inverted pigeonite		

Table 16 Major elements (wt%) compositions of orthopyroxenes  
from the different rock types in the pluton

	A01G		AGN	
	*MP-31	*C-44	C-53	C-48
Rb	1	2	4	3
Sr	14	16	9	4
Ba	33	24	26	30
Y	-	-	1	1
Zr	-	-	-	3
Nb	3	-	4	1
Ni	19	24	16	1
Co	76	96	46	45
Cr	17	17	51	44
V	102	89	105	130

Table 17 Trace elements (ppm) compositions of orthopyroxenes from the different rock types of the pluton.  
(\*pure quartz added to the sample)

poorer in  $\text{TiO}_2$  (0.35% to 0.78%),  $\text{MnO}$  (0.54% to 0.60%) and Cr (17 ppm to 48 ppm) than those from the AGN unit. The Al values in the Z sites of the A01G and AGN are 0.132 and 0.087 respectively.

## 5) Amphibole

10 samples of amphibole were separated out from the two main rock series; 3 from the A01N unit; 3 from the LAT unit; 2 from the A01G unit; 1 from the AGN unit and 1 from the AE unit. No amphibole was successfully separated out from the OA01G unit. Only the amphibole separated from the AG unit was prismatic in form. All other amphiboles occurred either interstitially or as poikilitic crystals and are regarded as intercumulus in origin. Major element analyses, structural formulae and trace element analyses of the amphiboles are presented in Table 18 and Table 19 respectively. All of the amphiboles are classified according to the system recommended by Leake (1978).

In the plagioclase-olivine series, all of the amphiboles separated from the main units of A01N and LAT fall in the compositional field of tschermakite. Magnesio-taramite occurs in the small LAT outcrop in the southwest. There is a high modal abundance of amphibole (35%) in the southwest outcrops, whereas only 6% of amphibole occurs in the main outcrop of the LAT. The calculated Mg numbers for the main outcrops of the A01N (average 79.3) and the LAT (74.2) differ notably from those

	A01N			LAT		
	MP-22	C-16	MP-36	C-36	MP-18	MP-87
SiO <sub>2</sub>	43.87	43.25	44.00	41.13	41.37	42.62
Al <sub>2</sub> O <sub>3</sub>	14.51	13.78	11.11	17.88	19.78	15.66
TiO <sub>2</sub>	0.13	0.45	0.73	0.28	0.09	1.20
Fe <sub>2</sub> O <sub>3</sub>	9.12	8.94	12.71	10.29	10.46	11.43
MnO	0.15	0.15	0.17	0.14	0.14	0.16
MgO	17.16	18.47	18.49	14.97	15.59	14.41
CaO	10.94	10.51	10.72	10.93	10.46	11.07
Na <sub>2</sub> O	1.08	1.74	0.82	0.98	1.78	3.30
K <sub>2</sub> O	0.11	0.12	0.21	0.12	0.06	0.35

Numbers of ions on the basis of 23(O)

Si	6.211	8.00	6.130	8.00	6.201	8.00	5.874	8.00	5.732	8.00	5.958	8.00
Al	1.789		1.870		1.799		2.126		2.268		2.042	
Al	0.633		0.431		0.046		0.883		0.962		0.534	
Ti	0.015		0.048		0.077		0.030		0.009		0.126	
Fe <sup>3+</sup>	0.972	5.26	0.954	5.35	1.348	5.38	1.105	5.22	1.091	5.30	1.202	4.88
Mn	0.017		0.017		0.020		0.017		0.017		0.018	
Mg	3.621		3.901		3.884		3.187		3.221		3.004	
Ca	1.660		1.595		1.618		1.672		1.553		1.659	
Na	0.298	1.98	0.478	2.10	0.224	1.88	0.270	1.96	0.477	2.04	0.893	2.61
K	0.020		0.022		0.037		0.021		0.010		0.062	

100 x Mg						
(Mg+Fe <sup>3+</sup> +Mn)	78.54	80.07	73.96	73.95	74.41	71.11

Name	Tschemakite	Tschemakite	Tschemakite	Tschemakite	Magnesian Taramite
------	-------------	-------------	-------------	-------------	-----------------------

Table 18 Major elements (wt%) compositions of amphiboles from the different rock types in the pluton



	A01G		AGN	AG
	C-44	MP-31	C-18	C-57
SiO <sub>2</sub>	43.73	40.21	48.36	43.39
Al <sub>2</sub> O <sub>3</sub>	13.38	13.17	10.94	12.71
TiO <sub>2</sub>	2.21	2.25	0.89	1.97
Fe <sub>2</sub> O <sub>3</sub>	11.36	10.80	10.54	13.98
MnO	0.22	0.20	0.23	0.21
MgO	15.26	15.24	13.95	12.91
CaO	12.10	12.16	13.94	11.55
Na <sub>2</sub> O	2.04	1.87	1.01	1.86
K <sub>2</sub> O	0.13	0.14	0.05	0.16
Si	6.087] 8.00	5.887] 8.00	6.691] 8.00	6.171] 8.00
Al	1.913]	2.113]	1.309]	1.829]
Al	0.283]	0.159]	0.476]	0.303]
Ti	0.232]	0.248]	0.093]	0.211]
Fe <sup>3+</sup>	1.190] 4.90	1.190] 4.95	1.098] 4.57	1.497] 4.77
Mn	0.025]	0.025]	0.027]	0.025]
Mg	3.167]	3.325]	2.877]	2.737]
Ca	1.805]	1.908]	2.067]	1.760]
Na	0.551] 2.38	0.532] 2.47	0.270] 2.35	0.514] 2.30
K	0.023]	0.026]	0.008]	0.028]
<u>100 x Mg</u>				
(Mg+Fe <sup>3+</sup> +Mn)	72.26	73.23	71.90	64.27
Name	Pargasite	Pargasite	Magnesian Hornblende	Ferroan Pargasite

Table 18 continued

	A01N		LAT	
	C-16	MP-86	*MP-18	MP-87
Rb	4	8	1	5
Sr	86	70	114	72
Ba	53	83	12	141
I	21	24	-	67
Zr	31	32	-	66
Nb	10	4	-	6
Ni	170	142	34	101
Co	29	41	74	37
Cr	144	378	44	106
V	121	262	31	291

	A01G		AGN	AG
	MP-31	C-44	*C-48	C-57
Rb	4	4	5	6
Sr	129	130	107	107
Ba	168	154	181	167
I	128	121	25	64
Zr	12	11	-	28
Nb	5	5	5	4
Ni	18	23	12	9
Co	29	28	60	35
Cr	59	59	25	62
V	414	374	482	481

Table 19 Trace elements (ppm) compositions of amphiboles from the different rock types of the pluton  
(\*pure quartz added to the sample)

of the small outcrops of A01N (74.0) and LAT (71.1) exposed along the southwestern corner of the complex.

The Al(IV) and  $(\text{Fe}^{3+} + \text{Ti}^{2+})$  contents and  $\text{Al}^{3+}/\text{Si}^{4+}$  ratios of amphiboles of the A01N in the main outcrops (1.830, 6.50 and 0.38) differ from those in the southwestern outcrop (1.799, 9.33 and 0.29) respectively. The amphiboles of the LAT units show the same variation. They range from 2.197, 7.37 and 0.52 in the main outcrops, to 2.042, 8.71 and 0.42 in the southwestern outcrops respectively. Differences are also noted in the major elements and trace elements. The composition of amphibole of  $\text{Fe}_2\text{O}_3$  and  $\text{K}_2\text{O}$  are 9.03% and 0.12% in the main outcrops, and 12.71% and 0.21% in the small outcrops respectively. Amphiboles from the A01N unit in the main outcrops are richer in Sr (86 ppm to 70 ppm) and Ni (170 ppm to 142 ppm), and poorer in Rb (4 ppm to 8 ppm), V (121 ppm to 62 ppm), Ba (53 ppm to 83 ppm) and Cr (144 ppm to 378 ppm) than those from the southwestern outcrop. In the LAT unit, similar variations are also noted. The amphibole of LAT in the small southwestern outcrop is characterized by lower contents of MgO (14.41% to 15.28%) and Sr (72 ppm to 114 ppm), and higher  $\text{K}_2\text{O}$  (0.35% to 0.09%),  $\text{Na}_2\text{O}$  (3.30% to 1.38%), Rb (5 ppm to 1 ppm), Ba (141 ppm to 12 ppm), Ni (101 ppm to 34 ppm) and Cr (106 ppm to 44 ppm) than those from the main outcrop.

The A01G unit is characterized by pargasite, an amphibole containing high CaO (12.13%),  $\text{Na}_2\text{O}$  (1.96%),  $\text{K}_2\text{O}$  (0.14%) and low Ni (21 ppm), as compared to the

tschermakites in the main outcrops of the A01N and LAT unit. The Mg number averages 72.75, (Fe/Mg ratios 0.84). The amounts of Al in the Z site, and (Fe<sup>3+</sup> + Ti<sup>2+</sup>), and the Al<sup>3+</sup>/Si<sup>4+</sup> ratios of the amphiboles in this unit are 2.013, 9.09 and 0.36 respectively.

In the plagioclase-pyroxene series, the AGN unit contains magnesio-hornblende and the AG dykes contain ferroan-pargasite, with Mg numbers of 71.9 and 64.27, (Fe/Mg ratios 0.88 and 1.26) respectively. The magnesio-hornblende is low in K<sub>2</sub>O (0.05%), Al(IV) (1.309), Al<sup>3+</sup>/Si<sup>4+</sup> ratio (0.26), Ni (12 ppm) and Cr (25 ppm) and high in SiO<sub>2</sub> (48.36%), CaO (13.94%), (Fe<sup>3+</sup> + Ti<sup>2+</sup>) (7.90%), and Ba (181 ppm) as compared to the tschermakites in the main outcrops of the A01N and LAT unit. The ferroan-pargasite, which is the only prismatic amphibole, is low in MgO (12.91%) and Ni (9 ppm) and high in Na<sub>2</sub>O (1.86%) and K<sub>2</sub>O (0.16%) as compared to the tschermakites of the A01N and LAT unit. It has an Al(IV) value of 1.829 and a Al<sup>3+</sup>/Si<sup>4+</sup> ratio of 0.33.

The Mg number shows a clear trend from 79.3 in the A01N, 74.2 in the LAT, 72.8 in the A01G, 71.9 in the AGN and 64.3 in the AG, with decreasing Ni content from 170 ppm, 14 ppm, 21 ppm, 12 ppm to 9 ppm respectively.

### C. Multiple intrusion and in situ fractionation

Two rock series are represented in the Mount Poser batholith, the plagioclase-olivine series and the plagioclase-pyroxene series. These two rock series are

separated by a sharp contact, and occur principally at the east and west end of the complex respectively. Hornfelsed fragments of the olivine bearing series occur in the plagioclase-pyroxene series. This evidence indicates that they were intruded separately, with the plagioclase-olivine series emplaced first, and the plagioclase-pyroxene series emplaced later. The absence of olivine from the plagioclase-pyroxene series, and the lower An and Sr contents of the plagioclase, as compared to those of the plagioclase-olivine series, suggest that it was derived from a more differentiated magma.

There is a small outcrop, containing rocks of the A01N and LAT units of the plagioclase-olivine series, exposed near the southwest margin of the pluton and surrounded by the rocks of the pyroxene bearing series. The mineralogy of these rocks is very similar to that of the main outcrops of the units, except that clinopyroxene occurs in the southwestern outcrop (MP-86), but not in any of the other areas. Plagioclase feldspars, and olivines occurring in these southwest outcrops differ both in their major and trace element chemistry from the compositions of the same minerals in the main outcrops. The An and Sr contents of the plagioclases in the main outcrops are higher than those of the southwest outcrops. Similarly the Fo, Ni, and Co contents, and the Mg numbers are higher in the olivines of the rocks in the main outcrops than are those of the southwest outcrops. No overlap exists between the chemical

ranges shown the minerals in the main and southwest outcrops of these units, (see pages 59 and 70). This evidence strongly suggests that these two separate areas of similar rock types crystallized from different batches of magma, and that the southwest rocks were derived from a more differentiated magma than that from which the main outcrops formed.

It has been noted that the dykes of the plagioclase-olivine series may be divided into two separate groups, one in which spinel is present and one in which it is absent. There are differences in the chemistry of the principle minerals of these two types of dykes, e.g. anorthite contents. In addition, the olivine-bearing dykes penetrate all of the major rock units in the batholith, i.e. they post-date the main units of the plagioclase-pyroxene series. The AG dykes penetrate the olivine-bearing dykes.

All of this evidence points to the conclusion that the Mount Poser Pluton was formed by multiple intrusion of mafic magmas. These magmas were all similar in their general composition in that highly calcic anorthite, clinopyroxene and amphibole crystallized from them. Differences in the mineral parageneses and in the chemistry of the minerals formed suggest that there were differences in the compositions of these magmas. These differences may have been the result of different degrees of partial melting of the source material, differences in the composition of the source material, or perhaps differences in the degree of

differentiation of the individual batches of magma after they were formed.

The minerals of each individual rock unit all show a range of composition which may be explained by differentiation in situ (see pages 60 and 67). For example, in the plagioclases and olivines of the A01N, An ranges from 97.5 to 93.1, and Fo ranges from 78.2 to 77.5, similar ranges are noted in the LAT unit. Similarly the differences in plagioclase and olivine of A01N and LAT may be explained in terms of the LAT unit having formed from a somewhat more differentiated magma than the A01N unit. The A01N and LAT grade into each other by change in mineral proportions. It is suggested that the plagioclase and olivine of the A01N unit settled from the magma first with olivine settling more rapidly and being more abundant modally. Then as the composition of the magma became more felsic and of lower viscosity, the olivine became less abundant and plagioclase settled more rapidly and their modal proportions changed. The most prominent evidence of differentiation in situ is found in the AGN unit. There is a change in the mineralogy of this unit from east to west. In the east prismatic orthopyroxene is abundant and the plagioclase is calcium rich, ( $An_{85.3}$ ). In the west orthopyroxene is almost absent and the plagioclase is much more sodic ( $An_{64.5}$ ). These changes are best explained in terms of in situ differentiation, calcic plagioclase and orthopyroxene crystallizing from the more primitive magma,

and less calcic plagioclase and amphibole from a more differentiated magma. Whole rock compositions of these rocks are very mafic and suggest that the residual melt from which these rocks formed has been lost from the system.

#### D. Parent magma type

The chemistry, mineralogy and structures of all of the rock units on Mount Poser indicate that they were formed from mafic magmas, commonly by a process of accumulation. None of these units is considered to have the composition of the original magma and hence it is necessary to identify this parent magma type indirectly. This has commonly been done by comparing the compositions of the minerals in the cumulate rocks with the compositions of the cumulate minerals of other well described plutonic suites. Alternatively the mineral compositions can be compared with the chemistry of the cumulate minerals present in volcanic blocks and with the chemistry of the phenocrysts in associated lava flows, which belong to well known volcanic suites.

This has been done in Table 20, and it should be noted that it is best to make comparisons of the whole mineral assemblages rather than individual minerals. The most characteristic features of the suites are the extremely calcic nature of the plagioclases and the common presence of amphiboles, both features suggesting that the rocks were formed from a hydrous mafic magma. Examination of Table 20



Minerals	1	2	3	4	5	6	7	8
Plagioclase	An <sub>57-67</sub> <sup>a</sup> An <sub>45-65</sub> <sup>b</sup>	An <sub>50-60</sub>	An <sub>57-64</sub>	An <sub>62-71</sub>	An <sub>50-75</sub>	An <sub>45-70</sub>	An <sub>77</sub>	An <sub>60</sub>
Olivine	For <sub>70-73</sub>	For <sub>79-70</sub>	For <sub>79-70</sub>	For <sub>63-70</sub>	For <sub>60-76</sub>	For <sub>74</sub>	For <sub>81</sub>	For <sub>74</sub>
Clinopyroxene	Ca <sub>33</sub> Mg <sub>48</sub> Fe <sub>13</sub> <sup>a</sup> Ca <sub>41</sub> Mg <sub>43</sub> Fe <sub>16</sub> <sup>b</sup>	Ca <sub>45</sub> Mg <sub>45</sub> Fe <sub>10</sub>	Ca <sub>39-45</sub> Mg <sub>43-48</sub> Fe <sub>10-16</sub>	Ca <sub>43</sub> Mg <sub>45</sub> Fe <sub>12</sub>	Augite Pigeonite	0.72 0.16 ( $\frac{Fe}{Mg}$ ) Mg 0.78	Ca <sub>42</sub> Mg <sub>48</sub> Fe <sub>10</sub> Ca <sub>40</sub> Mg <sub>43</sub> Fe <sub>17</sub>	
Orthopyroxene	Ca <sub>2</sub> Mg <sub>71</sub> Fe <sub>27</sub> <sup>a</sup> Ca <sub>7</sub> Mg <sub>62</sub> Fe <sub>30</sub> <sup>b</sup>	Ca <sub>2</sub> Mg <sub>61</sub> Fe <sub>37</sub>	-	Ca <sub>3</sub> Mg <sub>69</sub> Fe <sub>28</sub>	Hypersthene		Ca <sub>4</sub> Mg <sub>77</sub> Fe <sub>19</sub>	-
(En)	En <sub>71-62</sub>	En <sub>61</sub>	En <sub>71-62</sub>	En <sub>71</sub>	En <sub>73-75</sub>	En <sub>62</sub>	En <sub>80</sub>	En <sub>72-68</sub>
Amphibole	0.65 - 0.84 <sup>a</sup>	0.44 - 1.16	0.44 - 1.26	1.04 - 2.68	-	0.56 - 1.99	-	-
( $\frac{Fe}{Mg}$ )	Tschermakite to Pargasite	Pargasitic hornblende to Fe-pargasite	Pargasitic hornblende to Fe-pargasite	Pargasitic hornblende to Fe-pargasite	Hornblende	Pargasite to Tschermakitic hornblende		
Parent magma	High-Al basalt	Calc-alkali	-	Calc-alkali	Calc-alkali	High-Al basalt	Olivine- tholeiitic basalt	-

Table 20 A comparison of the compositions of the cumulate mineral assemblages of the Mount Posar gabbroic pluton and some well described complexes.

- (1) Mount Posar (this paper)  
 (2) Penninsular Ranges (Nishiyama, 1976)  
 (3) Penninsular Ranges (include Larsen and Dralun, 1950, and San et al., 1959)  
 (4) Guadalupe, California (Best and Muey, 1967)  
 (5) Virgin Islands (Longshore, 1966)  
 (6) Northwest Japan (Tanaka, 1980)  
 (7) Sharyard Intrusion (Wager and Brown, 1968)  
 (8) Miskat Intrusion (Irvine, 1970)

a. Olivine series  
 b. Pyroxene series

	1	2	3	4	5	6	7
Minerals							
Plagioclase	An <sub>97-64</sub>	An <sub>100-90</sub>	An <sub>93-90</sub>	An <sub>73-60</sub>	An <sub>91-40</sub>	An <sub>98-95</sub>	An <sub>95-93</sub>
Olivine	Fo <sub>79-70</sub>	Fo <sub>79-65</sub>	Fo <sub>80-70</sub>	Fo <sub>85-78</sub>	Fo <sub>86-70</sub>	Fo <sub>80-53</sub>	-
Clinopyroxene	Ca <sub>39-45</sub> Mg <sub>48-43</sub> Fe <sub>10-16</sub>	Ca <sub>46</sub> Mg <sub>42</sub> Fe <sub>12</sub>	$\beta = 1.697 \pm 0.02$ $2v = \pm 56^\circ$ (approximately 46 34 20)	-	Ca <sub>42</sub> Mg <sub>47</sub> Fe <sub>11</sub> <sup>a</sup> Ca <sub>45</sub> Mg <sub>42</sub> Fe <sub>13</sub> <sup>b</sup>	Ca <sub>50</sub> Mg <sub>41</sub> Fe <sub>9</sub>	Ca <sub>46</sub> Mg <sub>42</sub> Fe <sub>12</sub>
Orthopyroxene	Ca <sub>2-6</sub> Mg <sub>71-65</sub> Fe <sub>27-30</sub>	-	$\gamma = 1.711 \pm 0.02$ $2v = 59-62$ (approximately En <sub>60</sub> )	-	Ca <sub>9</sub> Mg <sub>61</sub> Fe <sub>30</sub> <sup>a</sup> Ca <sub>2</sub> Mg <sub>70</sub> Fe <sub>28</sub> <sup>b</sup>	Ca <sub>3</sub> Mg <sub>61</sub> Fe <sub>36</sub>	-
(En)	En <sub>71-62</sub>	-	-	-	En <sub>72-67</sub>	En <sub>63</sub>	-
Amphibole	0.44 - 1.26	0.89	-	1.01	1.05 - 1.41	-	0.93 - 1.25
( $\frac{Fe}{Mg}$ )	Pargasitic hornblende to Fe-pargasite	Tschermakite	Hornblende	Tschermakite	Ferroan <sup>a</sup> Pargasite to Magnesio Taramite	Hornblende	Tschermakite to Ferroan Pargasite
Parent Magma	-	Calc-alkali	Calc-alkali	High-Al Olivine Tholeiite	High-Al basalt	Olivine- basalt	Not definite

Table 20 continued

- (1) Pennisular Ranges (Include Larsen and Draisin, 1950, and Sen et al., 1959)
- (2) Saint Vincent, West Indies (Lewis, 1973)
- (3) Mount Misery, West Indies (Baker, 1968)
- (4) Southern Cascades, California (Hertzman, 1978)
- (5) Cyclades, Greece (Nicholls, 1971)
- (6) Hakone, Japan (Kuno, 1950)
- (7) Inclusions in calc-alkaline rocks (Yamazaki et al., 1966)

- a. Basalt
- b. Xenolith

shows that the rocks of the Mount Poser Pluton contain minerals similar in composition to a number of plutonic and volcanic suites occurring in orogenic areas. The areas include Peninsular Ranges (Larsen and Draisin, 1950; Sen et al., 1959 and Nishimori, 1976), Guadalupe, California (Best and Mercy, 1967), Virgin Islands (Longshore, 1966), Northeast Japan (Tanaka, 1980), Skaergaard Intrusion (Wager and Brown, 1968), Muskox Intrusion (Irvine, 1970), Saint Vincent, West Indies (Lewis, 1973), Mount Misery, West Indies (Baker, 1968), Southern Cascades, California (Mertzman, 1978), Cyclades, Greece (Nicholls, 1971), Hakone, Japan (Kuno, 1950), and inclusions in calc-alkaline rocks (Yamazaki et al., 1966). The original magma has been identified to a lesser or greater degree of precision in each of these other areas by the various workers involved, and the consensus suggests that it was probably a high  $\text{Al}_2\text{O}_3$  (olivine). tholeiite. This implies that the Mount Poser pluton was also formed from magmas related to high  $\text{Al}_2\text{O}_3$  tholeiite.

Wheeler (1979) has also summarized the arguments which suggest that the parental melt was similar to high-alumina basalt in composition. The most convincing evidence is that the compositions of the cumulate minerals of the gabbros, are very similar to the compositions of phenocrysts occurring in calc-alkaline lavas and volcanic blocks. Probably the best documented evidence which may be used to indicate the original magma type relates to a series of

volcanic blocks, erupted from Soufriere volcano, Saint Vincent, West Indies. Lewis (1973) has described these cumulate plutonic blocks in which the petrography, geochemistry, and mineralogy, are very similar to those in the troctolitic rocks of the Peninsular Ranges Gabbros. In some of the Soufriere blocks the crystals are coated with interstitial scoria, which has the composition of a saturated subalkaline, aluminous basalt. Lewis (1973) suggests that the scoria represents the liquid phase with which the minerals were in equilibrium at depth.

#### E. Calculated Composition of the Residual Melts

Since the majority of the rocks of Mount Poser are interpreted as cumulates and the complex has a multiple intrusive nature, it is quite probable that the residual melts present at any given stage have been swept from the intrusion by the emplacement of the next batch of magma. Evidence supporting this conclusion is formed in the development of comb layered structures, indicating gas streaming, in the Los Pinos Pluton (Walawender, 1976). These melts may erupt at the surface to form volcanic rock. Hence, none of the rocks present in the pluton represent either the original magma or the residual melt.

However, the minerals of many of the rocks have the characteristics of having crystallized in equilibrium with a melt, i.e. they lack zoning and have cumulate textures. Knowing the trace element contents of these minerals and

having well established crystal/melt distribution coefficients, it is possible to calculate the trace element contents of the residual melts, (Table 21 to 25).

For example, the trace element contents of the melt can be obtained by the following equation,

$$\text{Conc. in liquid} = \frac{\text{Conc. in mineral}}{K_D}$$

whereas  $K_D$  is the distribution coefficient.

This provides an additional check on the conclusions drawn concerning the parental magma type, using the major element chemistry of the minerals. By using minerals from successively more differentiated units in the pluton it is possible to follow the general evolution of the residual melts. The calculated compositions of the melts were compared with known composition of various volcanic rock suites (Table 21 to 25). The comparisons suggest that the rock units in the plagioclase-olivine series were derived from the melt of island arc tholeiitic olivine basalt and the plagioclase-pyroxene series were derived from the melt of more silicic or island arc tholeiitic andesite.

Table 21. Calculation of liquid composition using analyzed plagioclase results from the AOIN, LAT, OAOIG AND AQN unit and reported coefficients.  
(Data for  $K_p^{S/L}$  from Philpotts and Schnetzler, 1970). STDA - Island arc tholeiitic basalt. STDB - Island arc tholeiitic andesite to dacite.

An %	Unit	Mean Concentration (ppm)				Crystal/liquid distribution Coefficients				Concentration (ppm) in melt			
		K	Ba	Sr	Rb	K	Ba	Sr	Rb	K	Ba	Sr	Rb
	STDA									4400	75	200	5
93	AOIN	0.18	21	570	2	0.361	0.231	2.75	0.188	4140	91	207	11
90.6	LAT	0.18	19	500	2	0.361	0.231	2.75	0.188	4140	82	182	11
91.4	OAOIG	0.18	14	482	1	0.361	0.231	2.75	0.188	4140	61	175	5
	STDB									4300 to 15800	100 to 175	200 to 90	-
85.32	AQN	0.18	23	660	-	0.361	0.263	2.75	-	4140	87	240	-
64.48	AQN	0.22	50	734	-	0.361	0.285	3.30	-	5059	175	222	-

Table 22. Calculation of liquid composition using analyzed olivine results from the AOIN, LAT and OAOLG and reported coefficients.  
(Data for  $K_D^{S/L}$  : a - Philpotts and Schnetzler, 1970. b : Interpretation of Igneous Rock, Cox et al, 1979).

Unit	Mean Concentration (ppm)			Crystal/liquid distribution Coefficients			Concentration (ppm) in melt		
	Sr	Ni	Co	Sr	Ni	Co	Sr	Ni	Co
STDA							200	15-30	17-28
AOIN	-	391	92	-	$10^b$	$4.44^a$	-	39.1	20
LAT	2	160	81	$0.0093^a$	$10^b$	$4.44^a$	215	16.8	18
OAOLG	-	142	144	-	$10^b$	$4.44^a$	-	14.2	32

Table 23. Calculation of liquid composition using analyzed clinopyroxene results from the OA01G and AGN unit and reported coefficients.  
(Data for  $K_D^{S/L}$  a ; Philpotts and Schnetzler, 1970 ., b : Dale and Henderson, 1972, c : Wager and Mitchell, 1951., d : Hakli and Wright, 1967., e : Cox et al 1979).

Unit	Mean Concentration (ppm)						Crystal/liquid distribution Coefficients						Concentration (ppm) in melt					
	Rb	Sr	Ba	Co	Cr	Ni	Rb	Sr	Ba	Co	Cr	Ni	Rb	Sr	Ba	Co	Cr	Ni
STDA													5-12	200	103	17-28	50	30
OA01G	5	70	36	30	1176	67	0.284 <sup>a</sup>	0.43 <sup>a</sup>	0.388 <sup>a</sup>	1.22 <sup>b</sup>	18 <sup>c</sup>	2 <sup>e</sup>	18	163	93	24	65	34
STDB													15	220	175	20	4	20
AGN	5	73	69	54	29	23	0.284 <sup>a</sup>	0.43 <sup>a</sup>	0.388 <sup>a</sup>	1.22 <sup>b</sup>	6 <sup>d</sup>	2 <sup>e</sup>	17	170	178	44	5	12



Table 24. Calculation of liquid composition using analyzed orthopyroxene results from the LAT and AGN unit and reported coefficients.

(Data for  $K_D^{S/L}$  : a - Philpotts and Schnetzler, 1970. b : Interpretation of Igneous Rock, Cox et al, 1979).

Unit	Mean Concentration (ppm)			Crystal/liquid distribution Coefficients			Concentration (ppm) in melt		
	K	Sr	Ni	K	Sr	Ni	K	Sr	Ni
STDA							4400	-	-
LAT	0.01	-	-	0.02 <sup>a</sup>	-	-	4151	-	-
STDB							-	200-90	20-1
AGN	-	7	9	-	0.04 <sup>a</sup>	4 <sup>b</sup>	-	175	2

Table 25. Calculation of liquid composition using analyzed amphibole results from the AGN unit and reported coefficients.

(Data for  $K_D^{s/l}$  are from Philpotts and Schnetzler, 1970).

Unit	Mean Concentration (ppm)					Crystal/liquid distribution Coefficients					Concentration (ppm) in melt				
	Rb	Sr	Ba	Cr	Ni	Rb	Sr	Ba	Cr	Ni	Rb	Sr	Ba	Cr	Ni
STDB											5-12	200	103-175	15-4	20-1
AG N	5	107	181	25	12	0.5	0.5	0.8	12	0.8333	10	214	226	2	14

CHAPTER VI

PETROGENESIS OF THE GABBROS  
AND  
THEIR RELATIONSHIPS TO THE GRANITOIDS  
OF THE PENINSULAR RANGES BATHOLITH

A more detailed discussion is carried out in the following paragraphs in order to identify the parental rock type of the cumulate gabbros and to define the relationship between gabbros and the granitoid rocks of the Peninsular Ranges batholith.

LITERATURE REVIEW

There are several models concerning the origin of the Peninsular Ranges batholith. These models, which are representative of current interpretations of batholiths in general, seek to explain the genesis and relationships of the various intrusive rocks of the batholith, which range from gabbroic to granitic in composition. Such studies also bear on the controversy as to the crustal or mantle origin of granitoid magmas (Leake et al., 1980).

Larsen (1948) proposed that the batholith was derived from a single gabbroic magma that differentiated at depth. He suggested that the differentiation products, which range in composition from gabbro to granite, were systematically emplaced into the upper crust. If this model is correct, it

illustrates Bowen's (1928) scheme of fractional crystallization and also implies that the magmas from which the Peninsular Ranges batholith formed, were derived from the mantle.

Nishimori (1974, 1976) provided some support for this hypothesis. He studied the crystallization sequences, and mineral chemistry, of two gabbroic plutons from the Peninsular Ranges batholith. He concluded that the gabbros represent refractory residua, or crystal cumulates, formed by the fractional crystallization of a high-alumina basalt/basaltic-andesite melt. He suggests that the fractional crystallization took place under elevated  $P_{H_2O}$  at crustal depths, and may have led to the formation of either the granitoid rocks of the batholith, or of sialic volcanic rocks which have subsequently been eroded away. He noted that subtraction of the compositions of these gabbros from the proposed parental magmas would produce both the major and trace element variations observed in some calc-alkaline rock sequences.

Nishimori's work (1974, 1976) can be criticized on several grounds. He analyzed the minerals from only eleven rocks collected from only two, out of more than forty gabbroic plutons, exposed in the batholith. He acknowledged that both plutons were formed by multiple intrusion but did not describe the evolution of either. He failed to note that there are two distinct suites of gabbros present (Walawender and Smith, 1980) characterized by different

mineral parageneses. Under such circumstances, it seems unlikely that Nishimori's study would lead to comprehensive conclusions.

Erikson (1977), in a study of the Mount Stuart batholith of Washington State, suggested that it originated by the fractionation of a gabbroic melt. The Mount Stuart batholith comprises similar rock types in similar proportions, to the Peninsular Ranges batholith and Erikson's interpretation is identical in essence to that of Larsen. In his discussion, and mathematical analysis of the data, Erikson (1977) points out that the fractionation process should yield 80% gabbroic, and 20% intermediate to granitic rocks. The observed abundances of the different rock types, exposed at the surface in the Mount Stuart batholith, are 90% intermediate to granitic, and only 10% gabbroic, rock. Similar rock proportions occur in the Peninsular Ranges batholith. These mass balance calculations, show that serious discrepancies exist between the observed and predicted percentages of the various rock types, and must be explained. Thus the model of the evolution of the Peninsular Ranges batholith, proposed by Larsen (1948) and Nishimori (1974, 1976), may be legitimately rejected unless some satisfactory explanation for the observed proportions of rock types can be found.

This model derives from Bowen's proposition (1928) that fractional crystallization of a basaltic magma can account for the diversity in composition of igneous rocks. In his

discussion on the course of fractional crystallization of basaltic magma Bowen (1928, pp. 79-80) emphasised the enrichment of the residual liquid in silica and alkali feldspar components but did not consider the enrichment in iron or ferriferous pyroxene component to be significant. On the other hand, Fenner (1929) emphasized the enrichment of the residual liquid in iron rather than silica, during crystallization. Bowen's argument is valid for the chemical trends produced by fractional crystallization of calc-alkaline magmas, but as noted in the studies above (Larsen, 1948; Nishimori, 1974, 1976; Erikson, 1977), calculations show that the rock proportions produced are not the same as those occurring in natural associations.

The discrepancy between the calculated and observed proportions of the various rock types in proposed fractionated rock sequences has been known for many years. Studies of mafic igneous intrusions, such as the Skaergaard Intrusion, (Wager and Deer, 1939) show that only a fraction of a percent of the magma crystallizes as a granitic rock. This would imply that tremendous volumes of mafic melt had differentiated to yield the volume of granitic rocks present in the typical batholith. Morse (1976), and Wager and Deer (1939) concluded that granitic rocks found in orogenic zones are not produced by fractional crystallization from a basaltic parent.

Alternatively Erikson (1977) suggested that a large body of gabbroic rocks must lie at depth beneath the Mount

Stuart batholith. However, a wide variety of evidence suggests that this cannot be so. For instance Bott and Smithson (1967) stated "Granite magma may also originate by differentiation within a chamber of mafic magma in the crust, or by fusion of crustal material by a mafic intrusion." In this case, the granite pluton would be expected to occupy a much smaller volume than the parent mafic igneous pluton, giving rise to a dominantly positive gravity anomaly, with a relatively small negative residual anomaly over the granite itself. Walcott (1967) showed that there is a negative anomaly along the Central Pacific seaboard which suggests that the earth's crust is predominantly of granitic composition in this area. These observations make it unlikely that there are vast quantities of gabbro at depth.

Oliver (1977) has proposed a gravity model for the Sierra Nevada batholith, which is associated with a negative Bouguer anomaly, and requires the existence of a mafic layer at depths of 30 km. This hypothesis cannot satisfactorily explain the formation of the gabbros of the Peninsular Ranges batholith, since they have mineralogies consistent with crystallization at pressures of less than 5 kbar (15 km) and there is no evidence of significant differentiation at greater depth (Walawender, 1976). Berggreen and Walawender (1977) have demonstrated that the regional metamorphism of the Morena Reservoir roof pendant (Julian Schists), which is spatially associated with the Corte Madera Gabbroic Pluton,

took place at about 2.0 - 2.5 mpa pressure and 600°C. These relationships confirm that the gabbros were emplaced, and differentiated, at relatively high levels in the crust, and they do not suggest the presence of a mafic layer at 30 km.

An alternative escape from the volume argument may be to follow Hamilton and Myers (1967) and assume that batholiths are thin tabular bodies that extend only to very shallow depths. In this model the volume of granitic rocks would be comparatively small and Bowen's suggestion (1928, pp. 87-88), that the middle and lower parts of the crust beneath a batholith are gabbroic, would be reasonable. However, if the granitic rocks formed by fractional crystallization from such a lower crust, any water present in the system would concentrate in the upward moving granitic liquids. The nearly anhydrous residual material would form eclogite or garnet granulite (Ringwood and D.H. Green, 1966; Ito and Kennedy, 1971; D.H. Green and Ringwood, 1972) and would have a P-wave velocity much greater than is observed, for instance, beneath the Sierra Nevada batholith (Bateman and Eaton, 1967). Thus the middle and lower crust beneath batholiths cannot have a basaltic composition resulting from fractional crystallization that produced granitic rocks emplaced at upper crustal levels.

Albarede (1976), in his study of the Peninsular Ranges batholith, suggested that it was formed by differentiation of a tonalite parental magma. He suggests that the gabbros are cumulate rocks formed by separation of the early



crystallizing minerals and that the granodiorites were derived from a residual magma. The arguments presented above indicate that the gabbros are cumulative rocks formed at pressures of less than 5 mpa. The liquidus minerals present in a tonalitic melt, at pressures less than 5 mpa, are plagioclase, hornblende, and biotite (Piwinskii and Wyllie, 1968). The gabbroic rocks, which comprise mixtures of cumulate crystals of plagioclase, olivine, clinopyroxene, and orthopyroxene, could not have formed from a tonalite magma.

In a series of studies (of the gabbroic rocks of the Peninsular Ranges batholith (Walwender, 1976; Walawender et al., 1977, 1979; Lillis et al., 1979,; Wheeler, 1979 and Walawender and Smith, 1980) presented arguments to demonstrate that the gabbros are not cogenetic with the granitic rocks of the batholith. These studies include petrographic, geochemical, and structural observations on the gabbroic rocks, and their field relationships with the metamorphic host rocks, and the associated granitic rocks of the batholith. These authors suggest that, in general, there is a wide compositional gap between the gabbroic rocks and the granitoids, which cannot be explained by the fractionation trends shown by either group. Trace element distributions suggest that the dioritic rocks associated with the gabbros, and having major element compositions intermediate between the gabbros and the granitic rocks, were formed by contamination of a mafic melt. These trace

element distributions also preclude the origin of the granitic components of the batholith by fractional crystallization of a parental gabbroic melt.

A summary paper (Walawender and Smith, 1980) demonstrates that the basic plutons of the Peninsular Ranges batholith are multiple intrusive complexes, in which cumulate rocks of two series, the olivine-pyroxene series, and the amphibole-gabbro series, occur. It is suggested that these are formed by differentiation of a parental high-alumina basalt melt at pressures of less than 5 mpa. The data presented above suggest that the gabbros evolved from high  $Al_2O_3$  melts of tholeiitic affinities. Whole rock trace element studies (Lillis et al., 1979; Walawender et al., 1979; 1978; and Walawender and Smith, 1980) have shown that it is unlikely that the granitoid and gabbroic rocks of the Peninsular Ranges batholith evolved from the same magma.

The mineral parageneses of the two rock series in the Mount Poser Pluton may be used as further support for this conclusion. The cumulate minerals of the plagioclase-olivine series are plagioclase and olivine and they occur in a modal ratio of 50:25. The original melt contains approximately 51.6%  $SiO_2$  and a typical granitoid rock contains 70%  $SiO_2$ . Calculation shows that it requires the crystallization of 75% of the crystal mixture having an average  $SiO_2$  content of 70% noted above, in order to produce this change by fractional crystallization. The

plagioclase-pyroxene series contains cumulate plagioclase, orthopyroxene, and clinopyroxene, in modal proportions of 60:10:10 and an average  $\text{SiO}_2$  content of 50%. These rocks probably formed from a basaltic-andesite melt having approximately 57.4%  $\text{SiO}_2$ . Calculation shows that the residual melt would have a content of 71%  $\text{SiO}_2$  after crystallization of 65% of the melt.

Both calculations indicate that most of the magma must crystallize before the residual melt has a sufficient  $\text{SiO}_2$  content to form a granitoid rock. The lack of any evidence indicating the presence of a very large volume of the mafic cumulates associated with the batholith suggests that the granitoid rocks are not co-genetic with the gabbros, and reinforces the arguments presented above.

Some evidence exists, in the cumulates at Los Pinos (Walawender, 1976), of the venting of gases to the surface, and by implication of associated volcanic activity. Nishimori (1974, 1976) suggested that sialic volcanic rocks of the calc-alkali series may have been formed by the fractional crystallization processes which led to the formation of the cumulate gabbros. The trace element calculations reported above, however, indicate that the residual melts probably belonged to the island arc tholeiite series and not the calc-alkali series. The comparatively small concentration of  $\text{SiO}_2$  in the melt during fractionation supports this conclusion.

## CONCLUSIONS

Previous work has indicated that the gabbros of the Peninsular Ranges batholith are made up of cumulate rocks formed from multiple intrusions of mafic magma (Walawender and Smith, 1980). This study of the major and trace element chemistry of the minerals of the gabbroic rocks of the Mount Poser Pluton confirms these suggestions. Evidence is presented to show that there are repeated intrusions of mafic magma with generally similar characteristics but which were evolved to a greater or lesser degree at the time of intrusion. Two series of rocks are recognized, a plagioclase-olivine series produced from a less differentiated melt, and a plagioclase-pyroxene series produced from a more differentiated melt.

The differences in the magmas at the time of intrusion, may be the result of different degrees of partial melting of the same source material, partial melting of source materials with somewhat different chemistries, or differences in the amount of differentiation taking place in the magma as it rises through the mantle to be emplaced in the crust. There is no systematic trend from less differentiated to more differentiated magmas as they are emplaced, and the differences in their chemistries are small. The situation is further complicated by the fact that each batch of melt emplaced has differentiated in situ. It has not proved possible to decide on an explanation for

these differences.

The chemistry of the cumulate minerals suggests that the magma from which they formed was a high  $\text{Al}_2\text{O}_3$  (Olivine) tholeiitic basalt. The presence of highly anorthitic plagioclase and of amphiboles in these gabbros, indicates that the magmas contained more water than typical continental and oceanic tholeiitic magmas. The hydrous nature and high  $\text{Al}_2\text{O}_3$  content of the parent magmas is typical of magmas presently erupting in orogenic areas (Green, 1980), and the water content plays a critical role in controlling differentiation patterns.

The trace element contents of the cumulate minerals, and known distribution coefficients, were used to calculate the trace element chemistry of the melts from which the minerals crystallized. These calculated trace element contents were compared with the established values for the various melts which erupt in active orogenic areas. The comparison shows that the cumulate minerals of the plagioclase-olivine series were in equilibrium with a melt having a trace element composition very similar to that of an island arc tholeiitic basalt. The minerals of the plagioclase-pyroxene series crystallized in equilibrium with a melt having the composition of an island arc tholeiitic andesite. Those calculations confirm the general conclusions derived from a study of the major element chemistry of the minerals.

Simple calculations show that about 70% and 65%, of the

basaltic and andesitic magmas respectively, have to crystallize, with the typical modal proportions of the cumulate minerals, in order to produce a residual melt having an  $\text{SiO}_2$  content of 70% (typical of the granitoids of the batholith). Thus the differentiation of the mafic magmas, which is actually seen to take place, would produce a rock sequence containing less than 30% granitoid rocks. The batholith contains more than 80% granitoids, therefore confirming that they could not have been formed by fractionation of the mafic magmas from which the gabbros were formed. The gabbros and granitoid rocks of the Peninsular Ranges batholith are not co-genetic.

There is evidence in the Los Pinos Pluton of volcanic activity associated with the gabbros. It is suggested that the residual melts formed within the gabbroic plutons were repeatedly swept from the chamber during multiple intrusion. These melts erupted at the surface to form a sequence of volcanic rocks having compositions similar to those of the island arc tholeiitic sequence.

## Appendix I

## Plagioclase Analyses

Sample No	GU10	NP9	GU13	MP6	T740	58245	58212	58240	58243	58241
SiO <sub>2</sub>	44.74	45.50	45.94	47.05	45.13	43.86	50.92	46.85	53.70	52.84
Al <sub>2</sub> O <sub>3</sub>	34.87	34.52	34.25	33.35	34.92	36.28	31.55	34.20	29.67	29.48
Fe <sub>2</sub> O <sub>3</sub> <sup>a</sup>	0.39	0.24	0.51	0.81	0.32	-	-	-	-	0.86
MnO	-	-	-	-	-	-	-	-	-	-
MgO	-	-	-	-	-	-	-	-	-	-
CaO	18.92	18.19	17.88	16.53	19.40	18.75	13.99	17.21	11.75	12.59
Na <sub>2</sub> O	1.11	1.42	1.80	2.21	0.57	0.67	3.37	1.62	4.85	4.04
K <sub>2</sub> O	0.01	0.02	0.03	0.06	0.01	0.10	-	-	-	0.30
An	90.15	87.16	83.92	79.76	94.98	93	70	86	59	64

GU10, Anorthite, Olivine Gabbro, PRG (Nishimori, 1976).  
 NP9, Bytownite, Hypersthene Olivine Gabbro, PRG (Nishimori, 1976).  
 GU13, Bytownite, Amphibole Gabbro (layered), PRG, (Nishimori, 1976).  
 MP6, Bytownite, Anorthositic Amphibole, PRG (Nishimori, 1976).  
 T740, Anorthite, interstitial scoria., PRG (Lewis, 1973).  
 58245, Anorthite, Olivine norite (Olivine-hornblende-troctolite and calcic gabbro) S. California, (Sen et al, 1959).  
 58212, Anorthite, Noritic hornblende gabbro S. California, (Sen et al, 1959).  
 58240, Bytownite, calcic hornblende gabbro, S. California, (Sen et al, 1959).  
 58243, Labradorite, Norite (rich in iron ore), S. California, (Sen et al, 1959).  
 58241, Labradorite, typical norite, S. California, (Sen et al, 1959).  
 Fe<sub>2</sub>O<sub>3</sub><sup>a</sup>, as total Fe.

## Appendix I contd.

## Plagioclase Analyses

Sample No	SLR354	SLM334	P	334	335	P <sub>5</sub>	P <sub>4</sub>	520	301	P <sub>2</sub>	N-40-1
SiO <sub>2</sub>	43.77	52.97	45.93	46.14	46.30	45.30	46.13	44.93	45.17	44.94	43.4
Al <sub>2</sub> O <sub>3</sub>	36.11	29.41	33.69	34.08	33.54	34.44	33.41	34.96	34.43	36.50	35.9
Fe <sub>2</sub> O <sub>3</sub>	0.09	0.76	0.44	0.35	1.25	0.35	1.15	0.80	0.39	0.14	1.2
MnO	-	-	0.01	0.03	0.02	0.01	0.03	0.01	0.01	0.03	0.01
MgO	0.07	-	-	-	-	-	-	-	-	-	0.17
CaO	18.73	12.59	17.97	18.32	18.31	18.54	18.53	18.70	19.00	19.33	18.2
Na <sub>2</sub> O	0.67	3.97	1.38	1.00	0.97	0.94	0.88	0.74	0.64	0.57	0.77
K <sub>2</sub> O	0.11	0.26	0.01	0.04	0.04	0.03	0.03	0.04	0.03	0.01	0.07
An	93.6	63.5	87.90	90.70	91.04	91.40	91.93	93.17	94.09	94.89	92.5

SLR354, Anorthite, SLR354 calcic gabbro, S. California (Larsen & Dralain, 1950)  
 SLM334, Labradorite, SLM334 typical norite of San Marcos gabbro, S. California (Larsen & Dralain, 1950)  
 P, Dytonite in Gabbro, Thessaloniki (Sapountzis, 1979)  
 334, Anorthite in Gabbro, Thessaloniki (Sapountzis, 1979)  
 335, Anorthite in Gabbro, Thessaloniki (Sapountzis, 1979)  
 P<sub>5</sub>, Anorthite in Gabbro, Thessaloniki (Sapountzis, 1979)  
 P<sub>4</sub>, Anorthite in Gabbro, Thessaloniki (Sapountzis, 1979)  
 520, Anorthite in Olivine gabbro, Thessaloniki (Sapountzis, 1979)  
 301, Anorthite in Gabbro, Thessaloniki (Sapountzis, 1979)  
 P<sub>2</sub>, Anorthite in hornblende anorthite pegmatite, Duke Island, Alaska (Irvine, 1974)  
 N-40-1, Anorthite in hornblende anorthite pegmatite, Duke Island, Alaska (Irvine, 1974)



Appendix I contd.  
Plagioclase Analyses

Sample No'	EB18	ED38	EB43	ED41	7510
SiO <sub>2</sub>	46.34	47.67	49.19	52.95	49.06
Al <sub>2</sub> O <sub>3</sub>	33.36	33.46	31.82	29.48	32.14
Fe <sub>2</sub> O <sub>3</sub>	0.54	-	0.55	0.56	0.27
MnO	-	-	-	-	-
MgO	0.38	0.35	0.41	0.10	0.20
CaO	17.31	16.23	14.95	12.70	15.38
Na <sub>2</sub> O	1.55	2.19	2.78	4.12	2.57
K <sub>2</sub> O	0.55	0.07	0.09	0.13	0.17
An	86.0	80.2	74.4	62.9	76.0
EB18,	Bytownite, norite, Stillwater Intrusion, U.S.A. (Hager and Brown, 1967)				
ED38,	Bytownite, lower Gabbro, Stillwater Intrusion, U.S.A. (Hager and Brown, 1967)				
ED43,	Bytownite, upper Gabbro, Stillwater Intrusion, U.S.A. (Hager and Brown, 1967)				
ED41,	Labradorite, upper Gabbro, Stillwater Intrusion, U.S.A. (Hager and Brown, 1967)				
7510,	Bytownite, Gabbro, Bushveld Intrusion, south Africa (Hess, 1960)				

# Appendix II

## Olivine Analyses

Sample No	520	301	P <sub>5</sub>	335	337	D <sub>6</sub>	344	10	I-40-2
SiO <sub>2</sub>	40.24	40.27	39.28	40.32	39.87	39.83	38.18	39.92	37.1
Al <sub>2</sub> O <sub>3</sub>	0.04	-	-	0.03	-	0.03	0.05	-	0.2
Fe <sub>2</sub> O <sub>3</sub>	17.75	18.46	19.04	19.21	20.18	21.17	24.23	16.52	17.5
TiO <sub>2</sub>	-	-	-	0.08	-	0.05	0.30	-	-
MnO	0.18	0.31	0.22	0.24	0.21	0.16	0.17	-	0.1
MgO	42.73	42.95	42.37	41.05	40.26	39.72	38.59	43.90	44.2
CaO	0.03	0.01	0.01	0.01	0.01	0.02	0.02	0.17	-
Fe	81.3	80.3	79.6	78.1	77.8	76.8	73.8	83.0	81.9

520, Olivine in gabbro, Thessaloniki (Sapountzis, 1979)

301, Olivine in olivine gabbro, Thessaloniki (Sapountzis, 1979)

P<sub>5</sub>, Olivine in gabbro, Thessaloniki (Sapountzis, 1979)

335, Olivine in olivine gabbro, Thessaloniki (Sapountzis, 1979)

337, Olivine in olivine gabbro, Thessaloniki (Sapountzis, 1979)

D<sub>6</sub>, Olivine in gabbro, Thessaloniki (Sapountzis, 1979)

344, Olivine in gabbro, Thessaloniki (Sapountzis, 1979)

10, Olivine syokilitically enclosing amphibole at Little Mount Hoffman California, (Olivine basalt, Mertzman, 1978)

I-40-2, Olivine in Dunite, Duke Island, Alaska (Irvine, 1974)

## Appendix II contd.

Sample No	Olivine Analyses							
	NP4	NP3	NP9	GU10	GU16	GU18	Q4C	T770
SiO <sub>2</sub>	39.36	38.42	38.49	39.24	39.60	39.19	37.57	38.38
Al <sub>2</sub> O <sub>3</sub>	0.19	0.55	0.06	0.03	0.11	0.33	-	-
Fe <sub>2</sub> O <sub>3</sub>	19.36	25.50	24.18	23.41	21.34	26.45	26.71	0.06
MnO	0.31	0.32	0.33	0.37	0.40	0.45	0.23	0.34
MgO	40.64	36.31	37.40	37.67	39.55	35.68	34.71	40.01
CaO	0.09	0.07	0.02	0.07	0.04	-	-	0.06
Fe	78.9	71.7	73.4	74.2	76.8	71.2	69.8	64.97

NP4, Olivine in plagioclase peridotite, PRG (Nishimori, 1976)  
 NP3, Olivine in olivine gabbro, PRG (Nishimori, 1976)  
 NP9, Olivine in hypersthene olivine gabbro, PRG (Nishimori, 1976)  
 GU10, Olivine in olivine gabbro, PRG (Nishimori, 1976)  
 GU16, Olivine in gabbro, PRG (Nishimori, 1976)  
 GU18, Olivine in olivine gabbro, PRG (Nishimori, 1976)  
 Q4C, Olivine in olivine gabbro, PRG (Nishimori, 1976)  
 T770, Olivine in interstitial scoria Soufriere, Mont Indies (Lewis, 1973)

Appendix III  
Clinopyroxene Analyses

Sample No	140	128	132	153	Sg-2	lhg-2	T770	37541	37571
SiO <sub>2</sub>	52.32	52.51	52.03	51.20	49.77	48.17	48.73	53.40	53.50
TiO <sub>2</sub>	0.59	0.37	0.34	0.27	0.90	0.89	0.81	0.13	0.21
Al <sub>2</sub> O <sub>3</sub>	1.97	2.11	2.15	0.80	4.83	6.70	5.98	0.75	0.83
Fe <sub>2</sub> O <sub>3</sub>	7.56	9.06	10.17	16.39	7.29	8.27	7.43	6.85	10.00
MnO	0.17	0.20	0.24	0.36	0.15	0.17	0.15	0.47	-
MgO	15.75	14.23	13.69	10.27	13.80	13.01	14.43	15.50	14.10
CaO	21.26	21.58	21.23	20.37	21.47	22.23	22.49	22.50	21.50
Na <sub>2</sub> O	0.31	0.28	0.33	0.32	0.91	0.37	0.26	0.25	0.30
K <sub>2</sub> O	0.04	0.04	0.02	0.06	0.14	0.04	0.0008	-	-
Mg	44.6	40.8	39.4	30.0	41.74	38.99	41.60	43.65	40.09
Ca	43.3	44.5	44.0	42.8	46.40	47.62	46.57	45.54	43.94
Fe	12.1	14.7	16.6	27.2	11.86	13.39	11.63	10.81	15.96

140, Augite in Fe-poor gabbroic rock, Guadalupe (Best and Mercy, 1967)

128, Augite in middle gabbroic rock, Guadalupe (Best and Mercy, 1967)

132, Augite in middle gabbroic rock, Guadalupe (Best and Mercy, 1967)

153, Augite in Fe-rich gabbroic rock, Guadalupe (Best and Mercy, 1967)

Sg-2, Salite in clinopyroxene bearing hornblende gabbroic inclusion from Shigurami, Nagano Prefecture, Central Japan (Yamazaki, et al 1966)

lhg-2, Salite in clinopyroxene hornblende gabbroic inclusion from Ichinomegata, Akita Prefecture, Central Japan (Yamazaki, et al 1966)

T770, Salite in interstitial scoria, Soufriere, West Indian (Lewin, 1973)

37541, Salite in norite, New Zealand, (Price & Sinton, 1978)

37571, Augite in gabbro, New Zealand, (Price & Sinton, 1978)

Appendix III contd.  
Clinopyroxene Analyses

Sample No	P <sub>2</sub>	335	301	520	P <sub>5</sub>	344	P <sub>3</sub>	D6	337	334
SiO <sub>2</sub>	52.71	52.67	52.69	52.00	51.71	51.97	52.62	52.54	51.36	51.86
TiO <sub>2</sub>	0.18	0.30	0.14	0.09	0.13	0.42	0.37	0.28	0.45	0.47
Al <sub>2</sub> O <sub>3</sub>	2.22	1.91	1.97	2.08	2.24	2.49	2.15	2.04	2.18	2.29
Fe <sub>2</sub> O <sub>3</sub>	4.90	5.23	4.62	4.89	5.04	5.22	6.23	6.65	7.43	7.46
MnO	=	0.21	0.18	0.12	0.12	0.24	0.18	0.20	0.25	0.29
MgO	17.56	16.90	16.52	16.97	16.29	16.68	17.12	17.02	15.02	14.92
CaO	23.49	22.23	21.67	22.25	22.66	22.57	21.31	21.73	22.04	22.24
Na <sub>2</sub> O	0.12	0.09	0.13	-	-	-	0.12	0.16	0.17	-
Mg	45.85	47.56	47.47	47.43	45.92	46.37	48.12	47.40	42.70	42.31
Ca	47.17	44.97	44.78	44.71	45.92	45.11	43.06	43.50	45.05	45.35
Fe	6.98	7.47	7.75	7.86	8.16	8.52	8.82	8.82	12.25	12.34

P<sub>2</sub>, Augite in gabbro, Thessaloniki (Sapountzis, 1979)  
 335, Augite in gabbro, Thessaloniki. (Sapountzis, 1979)  
 301, Augite in olivine gabbro, Thessaloniki (Sapountzis, 1979)  
 520, Augite in gabbro, Thessaloniki (Sapountzis, 1979)  
 P<sub>5</sub>, Augite in gabbro, Thessaloniki (Sapountzis, 1979)  
 344, Augite in gabbro, Thessaloniki (Sapountzis, 1979)  
 P<sub>3</sub>, Augite in gabbro, Thessaloniki (Sapountzis, 1979)  
 D6, Augite in gabbro, Thessaloniki (Sapountzis, 1979)  
 337, Augite in olivine gabbro, Thessaloniki (Sapountzis, 1979)  
 334, Augite in gabbro, Thessaloniki (Sapountzis, 1979)

Appendix III contd.  
Clinopyroxene Analyses

Sample No	NP4	GU10	NP9	GU18	GU16	GU13	MP6	I-40-2	I-37-2	R-38-2	II-19-3
SiO <sub>2</sub>	50.67	51.16	50.52	41.11	50.83	51.99	52.03	50.80	51.50	49.75	48.42
TiO <sub>2</sub>	0.58	0.68	0.50	0.50	0.51	0.57	0.20	0.36	0.32	0.56	0.68
Al <sub>2</sub> O <sub>3</sub>	4.45	3.73	2.84	3.81	4.07	2.93	1.58	4.04	4.31	3.58	6.38
Fe <sub>2</sub> O <sub>3</sub>	5.54	5.62	6.69	6.69	7.55	8.21	9.94	5.92	5.53	5.29	6.14
MnO	0.19	0.27	0.28	0.28	0.29	0.34	0.51	0.10	0.06	0.05	0.08
MgO	15.81	14.20	15.34	14.23	14.03	13.68	13.27	14.79	15.20	15.96	14.33
CaO	22.00	21.51	22.98	23.05	20.43	22.40	22.45	23.26	22.42	23.98	22.86
Na <sub>2</sub> O	0.15	0.18	0.28	0.20	0.29	0.38	0.22	0.37	0.47	0.61	0.66
K <sub>2</sub> O	-	-	-	-	-	-	-	0.03	0.04	0.09	0.09
Mg	45.5	45.4	42.9	41.2	42.3	40.4	37.9	42.5	44.2	44.2	42.0
Ca	45.5	45.4	46.5	47.9	44.6	46.6	46.2	48.0	46.9	47.7	48.2
Fe	9.0	9.3	10.6	10.9	13.0	13.0	15.9	9.5	8.9	8.0	9.8

NP4, Clinopyroxene in plagioclase peridotite, PQG (Nishimori, 1976)  
 GU10, Clinopyroxene in olivine gabbro, PQG (Nishimori, 1976)  
 NP9, Clinopyroxene in hypersthene olivine gabbro, PQG (Nishimori, 1976)  
 GU18, Clinopyroxene in olivine gabbro, PQG (Nishimori, 1976)  
 GU16, Clinopyroxene in gabbro, PQG (Nishimori, 1976)  
 GU13, Clinopyroxene in amphibole gabbro, PQG (Nishimori, 1976)  
 MP6, Clinopyroxene in norite, PQG (Nishimori, 1976)  
 I-40-2, Salite in a coarse pyroxene vein in peridotite, Duke Island, Alaska (Irvine, 1974)  
 I-37-2, Salite in olivine clinopyroxenite, Duke Island, Alaska (Irvine, 1974)  
 R-38-2, Salite in olivine clinopyroxenite, Duke Island, Alaska (Irvine, 1974)  
 II-19-3, Salite in hornblende-magnetite clinopyroxenite, Duke Island, Alaska (Irvine, 1974)

Appendix III contd.

Glinopyroxene Analyses

Sample No	ED175	ED43	ED41	3A660
SiO <sub>2</sub>	52.61	51.83	51.86	52.90
TiO <sub>2</sub>	0.44	0.49	0.55	0.37
Al <sub>2</sub> O <sub>3</sub>	2.72	3.07	2.33	2.41
Fe <sub>2</sub> O <sub>3</sub>	7.21	8.59	11.05	6.13
MnO	0.18	0.17	0.24	0.16
MgO	15.97	16.00	14.50	16.18
CuO	20.50	19.21	18.92	21.46
Na <sub>2</sub> O	0.28	0.27	0.23	0.34
K <sub>2</sub> O	0.02	0.02	-	0.02
Hg	46.0	45.0	42.5	46.1
Ca	42.3	41.0	39.5	44.0
Fe	11.7	14.0	18.0	9.9

ED175, Augite in lower gabbro, Stillwater Intrusion, U.S.A. (Wager and Brown, 1967)  
 ED43, Augite in upper gabbro, Stillwater Intrusion, U.S.A. (Wager and Brown, 1967)  
 ED41, Augite in upper gabbro, Stillwater Intrusion, U.S.A. (Wager and Brown, 1967)  
 3A660, Diopsidic augite in gabbro, Eastern Bushveld (Wager and Brown, 1967)

Appendix IV  
Orthopyroxene Analyses

Sample No	58241	335	301	520	P <sub>5</sub>	P <sub>2</sub>	344	P <sub>3</sub>	D6	334	P
SiO <sub>2</sub>	52.01	54.62	55.89	54.32	54.46	55.34	54.93	54.27	54.47	53.79	53.28
TiO <sub>2</sub>	0.35	0.17	0.06	0.03	0.03	0.23	0.23	0.10	0.13	0.24	0.20
Al <sub>2</sub> O <sub>3</sub>	1.92	1.51	1.58	1.49	1.52	1.47	1.42	1.67	1.48	1.34	0.83
Fe <sub>2</sub> O <sub>3</sub>	21.77	12.66	11.50	11.59	11.95	12.28	13.12	13.79	14.25	18.46	23.79
MnO	-	0.28	0.28	0.19	0.22	0.47	0.51	0.41	0.35	0.46	0.50
MgO	20.92	29.84	30.54	30.18	30.05	30.22	29.80	28.75	28.51	25.12	20.99
CaO	2.78	1.42	1.01	1.08	1.30	0.75	0.72	1.34	1.36	1.00	0.89
Na <sub>2</sub> O	0.11	0.16	-	-	-	-	-	0.06	0.12	-	0.22
Mg	65.18	79.42	80.62	80.33	79.45	79.70	78.49	77.34	76.95	68.90	65.19
Ca	4.9	2.72	1.92	2.07	2.47	1.42	1.36	2.59	2.64	1.97	1.75
Fe	29.91	17.87	17.46	17.60	18.06	18.08	20.15	20.07	20.41	29.13	33.06
En	68.55	81.63	82.21	82.03	81.45	80.85	79.67	79.40	79.04	70.29	66.34

58241, Hypersthene in typical norite in S. California (Larsen & Drasin, 1950)  
335, Bronzite, in gabbro, Thessaloniki (Sapountzis, 1979)  
301, Bronzite, in olivine gabbro, Thessaloniki (Sapountzis, 1979)  
520, Bronzite, in gabbro, Thessaloniki (Sapountzis, 1979)  
P<sub>5</sub>, Bronzite, in gabbro, Thessaloniki (Sapountzis, 1979)  
P<sub>2</sub>, Bronzite, in gabbro, Thessaloniki (Sapountzis, 1979)  
344, Hypersthene, in gabbro, Thessaloniki (Sapountzis, 1979)  
P<sub>3</sub>, Hypersthene, in gabbro, Thessaloniki (Sapountzis, 1979)  
D6, Hypersthene, in gabbro, Thessaloniki (Sapountzis, 1979)  
334, Hypersthene, in gabbro, Thessaloniki (Sapountzis, 1979)  
P, Hypersthene, in gabbro, Thessaloniki (Sapountzis, 1979)



Appendix IV contd.  
Orthopyroxene Analyses

Sample No	140	128	132	153	106	37541	37511	N25-1	EB130	EB41
SiO <sub>2</sub>	53.64	52.77	51.81	49.27	50.00	54.40	52.30	49.80	53.67	52.81
TiO <sub>2</sub>	0.42	0.33	0.40	0.43	0.49	0.14	0.33	0.12	0.29	0.37
Al <sub>2</sub> O <sub>3</sub>	1.47	1.12	1.26	0.94	0.47	0.86	0.92	4.14	1.65	1.65
Fe <sub>2</sub> O <sub>3</sub>	17.91	13.29	25.31	34.96	34.39	17.20	23.90	20.87	16.44	19.26
MnO	0.40	0.52	0.64	0.87	0.84	0.70	-	0.37	0.33	0.38
MgO	24.72	21.06	19.39	12.43	11.51	26.10	21.40	21.28	25.37	19.81
CaO	1.62	1.15	1.28	1.38	1.74	1.00	1.19	2.80	1.81	5.13
Na <sub>2</sub> O	0.03	0.04	0.06	0.04	0.20	-	-	0.36	-	0.05
K <sub>2</sub> O	0.02	0.02	0.04	0.04	0.05	-	-	0.08	-	-
Mg	68.8	60.0	56.0	37.3	35.4	58.92	46.03	60.60	73.1	58.0
Ca	3.2	2.4	2.7	3.0	3.8	2.26	2.56	5.70	3.6	10.0
Fe	28.0	37.6	41.3	59.7	60.8	38.83	51.41	33.70	23.3	32.0
En	71.07	61.48	57.55	38.45	36.80	60.28	47.24	64.70	75.8	64.4

140, Hypersthene in Fe-poor gabbroic rock, Guadalupe (Best and Mercy, 1967)  
 128, Hypersthene in middle gabbroic rock, Guadalupe (Best and Mercy, 1967)  
 132, Hypersthene in middle gabbroic rock, Guadalupe (Best and Mercy, 1967)  
 153, Ferohypersthene in Fe-rich gabbroic rock, Guadalupe (Best and Mercy, 1967)  
 106, Ferohypersthene in gabbro, Guadalupe (Best and Mercy, 1967)  
 37541, Hypersthene in norite, New Zealand (Price & Sinton, 1978)  
 37511, Ferohypersthene in norite, New Zealand (Price & Sinton, 1978)  
 N25-1, Hypersthene in rhythmically layered norite, Duke Island, Alaska (Irvine, 1974)  
 EB130, Bronzite in upper gabbro, Stillwater Intrusion, U.S.A. (Hager and Brown, 1967)  
 EB41, Inverted pigeonite in upper gabbro, Stillwater Intrusion, U.S.A. (Hager and Brown, 1967)

Appendix IV contd.  
Orthopyroxene Analyses

Sample No	GU10	NP9	GU18	GU16	GU13	MP1	MP6	CG11	O4G	SA660
SiO <sub>2</sub>	53.86	53.38	53.57	53.83	53.26	52.69	52.05	50.79	52.81	54.32
TiO <sub>2</sub>	0.12	0.22	0.27	0.19	0.21	0.29	0.11	0.27	0.45	0.25
Al <sub>2</sub> O <sub>3</sub>	1.82	2.21	2.30	1.93	1.22	1.53	1.00	1.05	0.50	1.83
FeO*	14.45	14.91	14.84	15.15	19.05	23.46	24.10	29.25	17.65	14.72
MnO	0.43	0.37	0.38	0.45	0.62	0.54	0.98	0.81	nd	0.29
MgO	28.00	27.65	27.44	27.58	24.97	21.65	20.90	16.64	26.83	27.56
CaO	1.36	1.09	1.38	1.35	1.17	0.89	1.11	1.12	1.52	1.18
Na <sub>2</sub> O	nd	0.33	0.04	0.07	0.02	0.07	0.05	0.13	0.01	0.05
Mg	75.9	74.7	74.6	73.9	68.5	61.1	59.4	49.2	71.0	75.0
Cu	2.1	2.6	2.7	2.6	2.3	1.8	2.2	2.3	2.9	2.3
Fe	22.0	22.7	22.7	23.5	29.2	37.1	38.4	48.5	26.1	22.7
En	77.53	76.69	76.67	75.81	70.11	62.22	60.74	50.36	73.12	76.76

GU10, Hypersthene in olivine gabbro, PRQ (Nishimori, 1976)  
NP9, Hypersthene in hypersthene olivine gabbro, PRQ (Nishimori, 1976)  
GU18, Hypersthene in olivine gabbro, PRQ (Nishimori, 1976)  
GU16, Hypersthene in gabbro, PRQ (Nishimori, 1976)  
GU13, Hypersthene in amphibole gabbro, PRQ (Nishimori, 1976)  
MP1, Hypersthene in norite, PRQ (Nishimori, 1976)  
MP6, Hypersthene in norite, PRQ (Nishimori, 1976)  
CG11, Hypersthene in amphibole gabbro, PRQ (Nishimori, 1976)  
O4G, Hypersthene in olivine gabbro, PRQ (Nishimori, 1976)  
SA660, Bronzite in gabbro, Eastern Bushveld (Hager and Brown, 1967)

Appendix V  
Amphibole Analyses

Sample No	1	2	3	4	5	Sg-1	Sg-2	Kj-1	Iht-1	Ihg-1
SiO <sub>2</sub>	40.87	42.05	43.3	42.6	40.6	40.42	40.45	41.27	40.29	39.75
TiO <sub>2</sub>	1.82	2.46	2.9	2.9	5.5	2.23	2.59	2.06	2.43	1.90
Al <sub>2</sub> O <sub>3</sub>	16.25	14.27	11.5	13.4	14.5	15.12	15.03	13.96	16.99	17.36
Fe <sub>2</sub> O <sub>3</sub>	12.22	9.25	12.2	14.3	13.4	11.64	11.38	12.11	11.99	11.90
MnO	-	0.26	-	-	-	0.21	0.19	0.18	0.18	0.17
MgO	13.93	14.52	13.2	11.7	12.0	13.46	13.49	13.88	12.03	11.85
CaO	10.87	11.98	10.8	10.9	9.6	12.13	11.96	11.81	12.04	11.76
Na <sub>2</sub> O	2.54	2.45	2.4	1.6	2.1	1.89	1.91	1.72	1.44	1.49
K <sub>2</sub> O	0.13	0.53	0.3	0.4	0.5	0.78	0.79	0.98	0.33	0.97

- 1, Amphibole from LMH in California (Mertzman, 1978)
- 2, Amphibole from Kick'em Jenny high-alumina olivine tholeiite, (Mertzman, 1977)  
Lesser Antilles island arc (Sigurdsson & Shepherd, 1974)
- 3, Hornblende (Holloway & Burnham, 1972, Table 4, no. 20, Table 5, no. 2)
- 4, Tschermakite hornblende in California (Holloway & Burnham, 1972, Table 4 & 5, no. 3)
- 5, Kaersutite in California (Holloway & Burnham, 1972, Table 4, no. 7, Table 5, no. 4)
- Sg-1, Hornblende in hornblende gabbroic inclusion from Shigarami, Nagano Prefecture, Central Japan (Yamazaki, et al, 1966)
- Sg-2, Hornblende in clinopyroxene bearing hornblende gabbroic inclusion from Shigarami, Nagano Prefecture, Central Japan (Yamazaki, et al, 1966)
- Kj-1, Hornblende in hornblende gabbroic inclusion from Kujiranami, Niigata Prefecture, Central Japan (Yamazaki, et al, 1966)
- Iht-1, Hornblende in hornblendite inclusion from Ichinomegata, Akita Prefecture, Central Japan (Onuki, 1965)
- Ihg-1, Hornblende in hornblende gabbroic inclusion from Ichinomegata, Akita Prefecture, Central Japan (Onuki, 1965)

## Appendix V contd.

Sample No.	Amphibole Analysis						MP6	violet C4C	T896
	MP4	QU10	MP9	brown GU13A	rim on brown GU13B	green GU13C			
SiO <sub>2</sub>	44.08	43.94	43.73	43.22	49.18	52.43	45.11	41.67	40.88
TiO <sub>2</sub>	1.02	1.38	1.11	2.83	.79	1.11	1.53	1.96	2.54
Al <sub>2</sub> O <sub>3</sub>	11.59	12.65	11.96	10.95	6.13	6.94	8.94	13.00	14.23
Fe <sub>2</sub> O <sub>3</sub>	6.70	9.35	10.75	13.18	13.03	8.16	15.89	11.76	11.38
MnO	.11	.10	.13	.15	.19	.15	.18	.07	0.09
MgO	16.43	15.03	13.87	13.17	15.16	13.75	12.49	13.93	14.74
CaO	13.75	13.05	13.27	12.22	12.69	12.92	11.78	11.75	11.59
Na <sub>2</sub> O	1.84	1.92	1.74	1.90	.93	1.10	1.02	2.02	2.45
K <sub>2</sub> O	.43	.16	.27	.42	.36	.40	.42	.40	0.28

MP4, Pargasitic hornblende in plagioclase peridotite, PRG (Nishimori, 1976)  
 QU1B, Pargasitic hornblende in olivine gabbro, PRG (Nishimori, 1976)  
 MP9, Ferroan pargasitic hornblende in hypersthene olivine gabbro, PRG (Nishimori, 1976)  
 GU13A, Ferroan pargasitic hornblende in amphibole gabbro, PRG (Nishimori, 1976)  
 GU13B, Magnesian hornblende in amphibole gabbro, PRG (Nishimori, 1976)  
 GU13C, Actinolitic hornblende in amphibole gabbro, PRG (Nishimori, 1976)  
 MP6, Magnesian hornblende in norite, PRG (Nishimori, 1976)  
 G4C, Ferroan Pargasite in olivine gabbro, PRG (Nishimori, 1976)  
 T896, Tacheraukite in interstitial scoria, Soufriere, West Indies, (Lewis, 1973)

Appendix V contd.  
Amphibole Analyses

Sample No	128	132	153	37267	37262	37541
SiO <sub>2</sub>	46.12	43.64	44.48	42.70	41.60	42.10
TiO <sub>2</sub>	2.38	2.67	1.69	1.48	3.08	3.05
Al <sub>2</sub> O <sub>3</sub>	9.27	9.80	7.47	12.50	13.00	11.80
Fe <sub>2</sub> O <sub>3</sub>	12.51	15.07	21.61	10.10	10.70	11.90
MnO	0.11	0.15	0.26	-	-	-
MgO	13.95	12.28	9.34	15.50	14.00	13.90
CaO	11.62	11.75	10.72	11.90	11.90	11.60
Na <sub>2</sub> O	1.55	1.73	1.46	2.40	2.60	2.53
K <sub>2</sub> O	0.54	0.69	0.97	0.49	0.38	0.35

- 128, Ferroan pargasitic hornblende in middle gabbroic rock, Guadalupe (Best & Mercy, 1967)  
132, Ferroan pargasitic hornblende in middle gabbroic rock, Guadalupe (Best & Mercy, 1967)  
153, Ferroan edenite in Fe-rich gabbroic rock, Guadalupe (Best & Mercy, 1967)  
37267, Magnesio-taramite in hornblende gabbro, New Zealand (Price & Sinton, 1978)  
37262, Magnesio-taramite in hornblende gabbro, New Zealand (Price & Sinton, 1978)  
37541, Magnesio-taramite in gabbro, New Zealand (Price & Sinton, 1978)

Appendix V contd.  
Amphibole Analyses

Sample No	Ilg-2	SLRM354	SLRM30	SLRM108	SLRM53	SLRM229B	I-31-4	I-27-1
SiO <sub>2</sub>	41.18	44.71	48.55	45.19	48.17	47.81	41.20	42.48
TiO <sub>2</sub>	1.62	0.63	0.97	2.06	0.57	1.26	1.42	1.38
Al <sub>2</sub> O <sub>3</sub>	16.55	16.76	8.57	13.42	11.18	7.96	16.16	14.56
Fe <sub>2</sub> O <sub>3</sub>	10.08	8.94	11.75	11.20	11.94	15.95	11.16	13.43
MnO	0.22	0.11	0.09	0.09	0.08	0.08	0.04	0.33
MgO	13.51	15.30	14.81	13.72	13.37	12.65	13.96	11.63
CuO	12.28	10.39	12.59	11.17	11.69	11.40	12.63	12.26
Na <sub>2</sub> O	1.80	1.72	0.99	1.55	0.91	1.16	2.27	2.53
K <sub>2</sub> O	0.31	0.11	0.16	0.21	0.14	0.71	0.62	0.41

- Ilg-2, Hornblende in clinopyroxene hornblende gabbroic inclusion from Ichinomegata, Akita Prefecture, Central Japan (Yamazaki, et al, 1966)
- SLRM354, Hornblende, Troctolite, S. California (Larsen & Draisin, 1950)
- SLRM30, Hornblende, Calcic hornblende-gabbro, S. California (Larsen & Draisin, 1950)
- SLRM108, Hornblende, Calcic hornblende-gabbro, S. California (Larsen & Draisin, 1950)
- SLRM53, Hornblende, Calcic hornblende-gabbro, S. California (Larsen & Draisin, 1950)
- SLRM229B, Hornblende, Norite Nodule, S. California (Larsen & Draisin, 1950)
- I-31-4, Pargasite in pegmatitic hornblendite, Duke Island, Alaska (Irvine, 1974)
- I-27-1, Magnesio-taramite in hornblende-anorthite pegmatite, Duke Island, Alaska (Irvine, 1974)

## REFERENCES

- Albarede, F., 1976, Some Trace Element Relationships among Liquid and Solid Phases in the Course of the Fractional Crystallization of Magmas: *Geochim. et. Cosmochim. Acta*, v. 40, pp. 667-673.
- Baird, A.K., Baird, K.W., & Welday, E.E., 1974, Chemical Trends across Cretaceous Batholithic Rocks of Southern California: *Geology*, v. 2, no. 10, pp. 493-495.
- Baker, P.E., 1968, Petrology of Mt. Misery Volcano, St. Kitt, West Indies: *Lithos*, v. 1, pp. 124-150.
- Bambauer, H.U., Corlett, M., Eberhard, E., and Viswanathan, K., 1967, Diagrams for the Determination of Plagioclases Using X-ray Powder Methods: *Schweiz. Mineral. Petrog. Mitt.*, v. 47, pp. 333-349.
- Bateman, P.C. and Dodge, F.C.W., 1970, Variations of Major Chemical Constituents across the Central Sierra Nevada Batholiths, *Geol. Soc. Amer. Bull.*, v. 81, pp. 409-420.
- Bateman, P.C. and Eaton, J.P., 1967, Sierra Nevada Batholith: *Science*, v. 158, no. 3807, pp. 1407-1417.
- Berggreen, R.G. and Walawender, M.J., 1977, Petrology and Metamorphism of the Morena Reservoir Roof Pendant, Southern California: *Calif. Div. of Mines Geol.*, pp. 61-65.
- Best, M.G. and Mercy, E.L.P., 1967, Composition and Crystallization of Mafic Minerals in the Guadalupe Igneous Complex, California: *Amer. Miner.*, v. 52, pp. 436-474.
- Bott, M.H.P. and Smithson, S.B., 1967, Gravity Investigations of Subsurface Shape and Mass Distribution of Granite Batholiths: *Geol. Soc. Amer. Bull.*, v. 78, pp. 859-878.
- Bowen, W.L., 1928, *The Evolution of the Igneous Rocks*, Princeton University Press, Princeton
- Cobbing, E.J., and Pitcher, W.S., 1972, The Coastal Batholith of Central Peru, *J. Geol. Soc. London*, v. 128, pp. 42-460.
- Cox, K.G., Bell, J.D., and Pankhurst, R.J., 1979, *The Interpretation of Igneous Rocks*, George Allen and Unwin Press.
- Dale, I.M., and Henderson, P., 1972, The Partition of Tran-

- sition Elements in Phenocryst--Bearing Basalts and the Implication about Melt Structure, Inter. Geol. Congress. 24th, Section 10, pp. 105-111.
- Deer, W.A., Howie, R.A., and Zussman, J., 1963, Rock Forming Minerals: 6 volumes, Longmans Ltd., London.
- Erikson, E.H., 1977, Petrology and Petrogenesis of the Mount Stuart Batholith--Plutonic Equivalent of the High Alumina Basalt Association: Contr. Mineral. Petrol., v. 60, pp. 183-207.
- Everhart, D.L., 1951, Geology of the Cuyamaca Peak Quadrangle San Diego County, California: California Division of Mines. Bull., v. 159, pp. 51-115.
- Fenner, C.N., 1929, The crystallization of Basalts, Amer. J. Sci., 5th ser., v. 18, pp. 225-253.
- Gastil, R.G., 1975, Plutonic Zones in the Peninsular Ranges of Southern California and Northern Baja California, Geology, v. 3, pp. 361-363.
- Gastil, R.G., Krummenacher, D., Doupont, J., and Bushee, J., 1974, The Batholith Belt of Southern California and Western Mexico: Pacific Geology, v. 8, pp. 73-78.
- Green, D.H., and Ringwood, A.E., 1972, A Comparison of Recent Experimental Data on the Gabbro-garnet Granulite, Eclogite Transition, J. Geol., v. 80, pp. 277-288.
- Green, T.H., 1980, Island Arc and Continent-building Magmatism--A Review of Petrogenetic Models Based on Experimental Petrology and Geochemistry, Tectonophysics, (in press).
- Hakli, T.A. and Wright, L.A., 1967, The Fractionation of Nickel between Olivine and Augite as a Geothermometer: Geochim. et. Cosmochim. Acta, v. 31, pp. 877-884.
- Hamilton, W., and Myers, W.B., 1967, The Nature of Batholiths, Prof. Pap. U.S. Geol. Surv., v. 554-C, pp. 30.
- Hess, H.H., 1960, Stillwater Igneous Complex, Montana: A Quantitative Mineralogical Study, Mem. Geol. Soc. Amer., v. 80, pp. 230.
- Holloway, J.B., and Burnham, C.W., 1972, Melting Relations of Basalt with Equilibrium Water Pressure Less Than Total Pressure: J. Petrol., v. 13, pp. 1-29.
- Hudson, F.S., 1922, Geology of the Cuyamaca Region of California with Special Reference to the Origin of the



- Nickeliferous Pyrrholite, *Bull. Geol. Sciences, U. of Calif., Berkeley*, v. 13, no. 6, pp. 175-252.
- Hutchison, C.S., 1974, *Laboratory Handbook of Petrographic Techniques*, Wiley and Sons, New York.
- Irvine, T.N., 1970, Crystallization Sequences in the Muskox Intrusion and Other Layered Intrusions, 1. Olivine-Pyroxene-Plagioclase Relations, *The Geol. Soc. South Africa, Special Publication 1, Symposium on the Bushveld Igneous Complex and Other Layered Intrusions*.
- Irvine, T.N., 1974, Petrology of the Duke Island Ultramafic Complex Southeastern Alaska, *Geological Society of America*, pp. 240.
- Ito, K., and Kennedy, G.C., 1971, An Experiment Study of the Basalt--Garnet Granulite-eclogite Transition, in the Structure and Physical Properties of the Earth's Crust, *Amer. Geoph. Union Geoph. Mon.*, v. 14, pp. 303-314.
- Krummenacher, D., Gastil, R.G., Bushee, J., and Doupont, J., 1975, K-Ar Apparent Ages, Peninsular Ranges Batholith, Southern California and Baja California: *Geol. Soc. Amer. Bull.*, v. 86, pp. 760-768. 5 Figs., June.
- Kuno, H., 1950, Petrology of Hakone Volcano and the Adjacent Areas, Japan: *Geol. Soc. Amer. Bull.*, v. 61, pp. 957-1020.
- Larsen, E.S., 1948, Crystalline Rocks of Corona, Elsinore, and San Luis Rey Quadrangles, Southern California: *Geol. Soc. Amer. Memoir* 29.
- Larsen, E.S., and Draisin, W.M., 1950, Composition of the Minerals in the Southern California Batholith: *Internat. Geol. Cong. 18th, 1948, Part II, Proc. Sect. A*, pp. 66-79.
- Leake, B.E., 1978, Nomenclature of Amphiboles: v. 42, pp. 533-563. *Mineralogical Magazine*.
- Leake, B.E., Brown, G.C., and Halliday, A.N., 1980, The Origin of Granite Magmas: A Discussion. *J. Geol. Soc. London*, v. 137, pp. 93-97.
- Lewis, J.F., 1973, Petrology of the Ejected Plutonic Blocks of the Soufriere Volcano, St. Vincent, West Indies: *J. Petrol.*, v. 14, part 1, pp. 81-112.
- Lillis, P.G., 1978, Petrology, Geochemistry, and Structure of the Corte Madera Pluton, San Diego County, California: unpubl. M.S. Thesis, San Diego State University.

- Lillis, P.G., Walawender, M.J., Smith, T.E., and Wilson, J., 1979, Petrology and Emplacement of the Corte Madera Gabbro Pluton, Southern California, in Abbott, P. L., and Todd, V.R., eds., Mesozoic Crystalline Rocks: Guidebook for the 92nd Annual Meeting of the Geological Society of America, in Press.
- Longshore, J.D., 1966, Chemical and Mineralogical Variations in the Virgin Islands Batholith and its Associated Wall Rocks: Ph.D. Thesis. Rice University, pp. 94.
- Mertzman, S.A., 1977, The Petrology and Geochemistry of the Medicine Lake Volcano, California: Contr. Mineral. Petrol., v. 62, pp. 221-247.
- Mertzman, S.A., 1978, A Tschermakite--Bearing High-Alumina Olivine Tholeiite from the Southern Cascades, California: Contr. Mineral. Petrol. v. 67, pp. 261-265.
- Miller, F.S., 1937, Petrology of the San Marcos Gabbro, Southern California: Geol. Soc. Amer. Bull., v. 48, pp. 1397-1426.
- Miller, W.J., 1935, A Geologic Cross Section Across the Southern Peninsular Range of California: Calif. Journ. Mines Geol., State Mineral Rent., v. 31, pp. 115-141.
- Miller, W.J., 1946, Crystalline Rocks of Southern California, Geol. Soc. Amer. Bull., v. 57, pp. 485-486.
- Morse, S.A., 1976, The Level Rule with Fractional Crystallization and Fusion, Amer. J. Sci. v. 276, pp. 330-346.
- Nicholls, I.A., 1971, Petrology of Santorini Volcano, Cyclades, Greece: J. Petrol., v. 12, pp. 67-119.
- Nishimori, R.K., 1974, Cumulate Anorthositic Gabbros and Periodotites and their Relation to the Origin of the Calc-alkaline Trend of the Peninsular Ranges Batholith, Cord. Sect. Geol. Soc. Amer. Abs. with program, v. 6, no. 3, pp. 229-239.
- Nishimori, R.K., 1974, The Petrology and Geochemistry of Gabbros from the Peninsular Ranges Batholith, California and a Model for their Origin, Unpublished Ph. D. Thesis, U. of California, California. pp. 234.
- Nockolds, S.R., and Allen, R., 1953, The Geochemistry of some Igneous Rock Series: Geochim. et. Cosmochim. Acta, v. , pp. 105-142.
- Norrish, K., and Chappell, B., 1967, X-ray Fluorescence Spectrography Physical Methods in Determination

- Mineralogy, ed. J. Kussman, Academic Press, London, pp. 161-214.
- Oliver, H.W., 1977, Gravity and Magnetic Investigations of the Sierra Nevada Batholith, California, Geol. Soc. Amer. Bull., v. 88, pp. 445-461.
- Onuki, H., 1965, Petrochemical Research on the Horoman and Miyamori Ultramafic Intrusives, Northern Japan: Scien. Rep. Tohoku Univer., Ser. 111, v. 9, pp. 217-276.
- Philpotts, J.A., and Schnetzler, C.C., 1970, Phenocryst-matrix Partition Coefficients for K, Rb, Sr and Ba, with Applications to anorthosite and basalt genesis: Geochim. et. Cosmochim. Acta, v. 34, pp. 307-322.
- Piwinski, A.J., and Wyllie, P.J., 1968, Experimental Studies of Igneous Rock Series: A Zoned Pluton in Wallowa Batholith, Oregon, J. Geol., v. 76, pp. 205-214.
- Price, R.C., and Sinton, J.M., 1978, Geochemistry of Granitoids and Gabbros from Southland, New Zealand: Contr. Mineral. Petrol., v. 67, pp. 267-278.
- Ringwood, A.E., and Green, D.H., 1966, An Experimental Investigation of the Gabbro-eclogite Transformation and some Geophysical Implications: Tectonophysics, v. 3(5), pp. 383-427.
- Sapountzis, E.S., 1979, The Thessaloniki Gabbros: J. Petrol., v. 20, part 1, pp. 37-70.
- Schwarz, H.P., 1969, Pre-Cretaceous Sedimentation and Metamorphism in the Winchester Area, Northern Peninsular Ranges, California: Geol. Soc. Amer. Spec. Pap. 100, 63 p.
- Sen, N., Nockolds, S.R., and Allen, R., 1959, Trace Elements in Minerals from the Rocks of the Southern California Batholith: Geochim. et. Cosmochim. Acta, v. 16, pp. 58-78.
- Sigurdsson, H., and Shepherd, J.B., 1974, Amphibole-Bearing Basalts from the Submarine Volcano Kick'em-Jenny in the Lesser Antilles Island Arc: Bull. Volcanol., v. 38, pp. 3891-3910.
- Silver, L.T., Early, T.O., and Anderson, T.H., 1975, Petrological, Geochemical, and Geochronological Asymmetries of the Peninsular Ranges Batholith: Abs. Cordilleran Section GSA, v. 7, pp. 375-376.

- Simon, F.O., and Rollinson, C.L., 1976, Chromium in Rocks and Minerals from the Southern California Batholith: *Chemical Geology*, v. 17, pp. 73-88.
- Smith, T.E., Riddle, C., and Jackson, T.A., 1979, Chemical Variation within the Coast Plutonic Complex of British Columbia between lat. 53 and 55 N, *Geol. Soc. Amer. Bull.*, v.90, part 1, pp. 346-356.
- State Mineralogist, 1890, Goodyear, W.A., San Diego County, California, *Min. Bur. Rept.*, v. 9, pp. 516-528.
- Streckeisen, A.L., 1973, Plutonic Rocks--Classification and Nomenclature, *Geotimes*, v. 18, pp. 26-30.
- Tanaka, H., 1980, Gabbroic Rocks from the Northern Abukuma Mountains, Northeast Japan, *Bull. Yama. Univ., Nat. Sci.*, v. 10, no. 1, pp. 127-142.
- Wager, L.R., and Brown, G.M., 1967, *Layered Igneous Rocks*: London, Oliver and Boyd.
- Wager, L.R., and Deer, W.A., 1939, (re-issued in 1962), *Geological Investigations in East Greenland*, part 3, The Petrology of the Skaergaard Intrusion, Kangerdlugssuag, East Greenland, *Medd. om. Gronland*, 105, no. 4, pp. 1-352.
- Wager, L.R., and Mitchell, R.L., 1951, The Distribution of Trace Elements During Strong Fractionation of Basic Magma--A Further Study of the Skaergaard Intrusion, East Greenland: *Geochim. et. Cosmochim. Acta*, v. 1, pp. 129-208.
- Walawender, M.J., 1976, Petrology and Emplacement of the Los Pinos Pluton: Southern California, *Can. J. Earth Sci.*, v. 13, part 9, pp. 1288-1300.
- Walawender, M.J., Hoppder, H., Smith, T.E., and Riddle, C., 1977, Trace Element Variation in a Gabbro-norite-quartz Diorite Sequence and the Implications on the Genesis of the Peninsular Ranges Batholith of Southern California, in *International Geological Correlation Program. Circum-Pacific Plutonism Project. Plutonism in Relation to Volcanism and Metamorphism*, pp. 49-61. Papers presented at the 7th CPPP Meeting, editor N. Yamada.
- Walawender, M.J., Smith, T.E., Hoppler, H., and Riddle, C., 1979, Trace Element Evidence for Contamination in a Gabbro-norite-quartz Diorite Sequence in the Peninsular Ranges Batholith: *J. Geol.*, v. 87, pp. 87-97.
- Walawender, M.J., and Smith, T.E., 1980, Geochemical and

Petrologic Evolution of the Basic Plutons of the Peninsular Ranges Batholith, Southern California: J. Geol., v. 88, pp. 232-242.

Walcott, R.I., 1967, Bouger Anomaly Map of Southwestern British Columbia: U. of Br. Columb. Earth Sci. Rept., v. 15, pp. 74.

Wheeler, C.F.R., 1979, The Mineralogy, Petrology, Geochemistry and Petrogenesis of the Mount Poser Gabbroic Pluton: Southern California, University of Windsor, unpublished: M. Sc. Thesis.

Wilson, J., 1978, The Geochemistry and Petrogenesis of the Corte Modera Pluton, Southern California, Unpublished: B. Sc. Thesis, University of Windsor, pp. 56.

Yamazaki, T., Onuki, H., and Tiba, T., 1966, Significance of Hornblende Gabbroic Inclusions in Calc-alkaline Rocks: J. Min. Pet. & Econo. Geol., v. 55, part 3, pp. 87-103

## VITA AUCTORIS

Name: Paul Chi Tak Cheung

Place & date

of birth: Hong Kong, March 30, 1955

Education: Lutheran Middle School, completed in 1972

Chu Hai College, Hong Kong, completed preliminary university in 1973

National Taiwan University, Taipei, Republic of China Awarded B. Sc. in Geology, in 1977

University of Windsor, Windsor, Canada, 1977-1981, present program

Experience: Teaching Assistant, (Engineering Geology, Mineralogy and Petrology) at the University of Windsor, 1977-1980

Summer of 1979; Research Assistant at the University of Windsor, Geology Dept.

Duties: Included crushing of the core sample for Los Angeles Abrasion test;

Petrographic study of sedimentary rocks